David Taylor

HYDRODYNAMIC DESIGN OF SEAPLANES

S.I.T. GRADUATE SCHOOL COURSE F. D. 215
(UNEDITED CLASS NOTES)

by

B. V. Korvin-Kroukovsky

TABLE OF CONTENTS

1. General Description and Terminology

2. Buoyancy and Static Stability

- 2.1 Submerged Displacement, Normal Flotation and the Center of Buoyancy
- 2.2 Static Stability - Metacentric Height - Application to Twin-Float Seaplanes
- 2.3 Lateral Stability of Flying Boats and of Single Float Seaplanes

3. Planing, Resistance and Take-Off

- 3.1 General Considerations
- 3.2 General Expression of Hydrodynamic Force
- 3.3 The Lift Force
- 3.4 Resistance of Prismatic Planing Surfaces
- 3.5 Ratio of Resistance to Lift
- 3.6 The Attitude and Balance of the Planing Seaplane Hull in Two-Step Planing
- 3.7 Towing Tank Data - Specific Test
  - 3.71 The "Specific Test"
  - 3.72 General Tank Test
  - 3.73 Stevens Collapsed Data Test
- 3.8 Turbulence Control and Correction of Frictional Drag for Changes in Reynolds Number
- 3.9 Take-off Calculations

4. Dynamic Stability - Porpoising and Skipping

- 4.1 Definition, Physical Nature and the Theory
- 4.2 Porpoising in Two-Step Planing at High Speed
- 4.3 Experimental Technique
- 4.4 Landing and Skipping

5. Directional Stability and Control

6. Spray

7. Impact

- 7.1 Introduction, Statement of the Problem
- 7.2 Theory and Tests Pertaining to the Impact in Smooth Water

TABLE OF CONTENTS (cont'd)

7.3 Three-Dimensional Case of Oblique Impact
7.4 Impact Basin
7.5 Landing on Waves
7.6 Pressures Acting on the Hull Bottom
7.7 Effect of the Elasticity of Supporting Structure
7.8 Waves

HYDRODYNAMIC DESIGN OF SEAPLANES

(S.I.T. Graduate School Course F.D. 215)

B. V. Korvin-Kroukovsky

1. General Description and Terminology.

The term "Seaplane" defines any type of an airplane capable of resting on, taking off from, and alighting on the surface of water. In the "float seaplane" this ability is obtained by the use of floats, the sole function of which is to provide the flotation and the planing area. In the "flying boat" the body provides the flotation and the planing area, and is used also as an integral part of the air frame, supporting the wings and the tail surfaces, and as a housing for the crew, the equipment, and the useful load. The "amphibian" is a flying boat or a float seaplane equipped with wheels in addition to the flotation and planing body, making it capable of alighting on either land or water. Most of the material in this course will apply equally to all types of seaplane, and only occasionally it will be necessary to discuss the features specific to a float seaplane, or to a flying boat. The term "planing" signifies the motion on the water surface with such a speed, and in such an attitude, that the weight of the aircraft is supported primarily by dynamic pressures, rather than by buoyant forces. The "planing area" or "planing bottom" is that part of the hull surface which is shaped so as to permit such a motion with the minimum of drag, and which has sufficient structural strength to withstand the forces involved. The conventional form of the hull with such a planing bottom is shown on Fig. 1. On this figure the letters designate the following elements:

- D - Bow
- E - Stern
- K - Keel
- C - Chine
- S_m - Main Step
- S_s - Second Step
- T - Tail Cone
- L_f - Forebody Length
- L_a - Afterbody Length
- h - Main Step Height
- α - Afterbody Keel Angle

σ = Sternpost Angle
V_1 = Straight Vee Bottom
V_2 = Vee Bottom with the Chine Flare
V_3 = Concave Vee Bottom
V_4 = Scalloped Vee Bottom
β = Angle of Deadrise
W = Warp, i.e. the change of the deadrise β with length

Figure 1 shows the hull with transverse steps. Figure 2 shows the Vee main step, and the pointed second step. Figure 3 shows the pointed main step. The variety of the pointed main step hull in which the height of the step is large, and the afterbody is long, so that the stern E serves as the second step S_s is called the "planing-tail hull".

While the hull is designed to be as perfect a streamline body as possible, certain deviations and sacrifices are necessary to insure satisfactory water planing action. The water in motion clings to, and exerts the suction on any curvex surface which comes in contact with it. This is the most important fact which the seaplane designer must constantly and vividly keep in mind. It is impossible to avoid the use of convex surfaces at the bow, but these are in water only at low speeds, and are raised above it even at moderate speeds. The lines of the bottom formed by the intersection of it with the vertical planes parallel to the hull centerline plane are called the "buttock lines". Aft of approximately the midpoint of the forebody length these lines must be straight in order to avoid the harmful suction, and to permit the dynamic pressure to be generated efficiently. These lines must terminate at their aft ends in discontinuities called "steps", as any upward change of direction of the continuous line would cause the suction to be generated.

The drawing giving all details of the external shape of a hull or a float is called the line drawing. Such a drawing in a somewhat simplified form is shown on Figure 3a for a seaplane float. The part of the line drawing showing the front or rear elevations with the contours of all stations is known as the "body plan". The notes "1.71 buttock" and "3.43 buttock" designate the lines formed by intersection of the planing bottom with the vertical planes spaced at a distance of 1.71 and 3.43 inches from the centerline plane of the float. In this case they are used to supply the additional information about the bottom shape only.

Quite frequently they are used in the same way for the upper part of the float as well. The "table of offsets", such as Table I also forms an integral part of a line drawing. The line drawing contains only a few fundamental dimensions on the drawing itself, while all dimensions defining the contours of all stations are collected in the table of offsets.

2. Buoyancy and Static Stability

2.1 Submerged Displacement, Normal Flotation and the Center of Buoyancy

Seaplane floats are built as ~~the~~ entirely watertight structures, with exception of the small air vent holes, usually incorporated in the handhole covers. The float will retain therefore its buoyancy even when completely submerged, and this buoyancy is called the "Submerged Displacement". The excess of the submerged displacement over the normal flotation, expressed in per cent of the latter, is called the "Reserve Buoyancy", and represents the most common measure of the adequacy of the float for the airplane it has to support. For instance if the float completely submerged has the buoyancy of 3800 pounds, and in normal flotation has to support the load of 2000 pounds, the reserve buoyancy is

$$100\frac{3800 - 2000}{2000} = 90\%$$

As a common and good practice in float design the reserve buoyancy of 100% is recommended, i.e. the submerged displacement is made equal to twice the normal displacement. 90% is the minimum permitted by the Civil Aeronautics Administration, as low as 65% and as high as 130% was used by Military Services on special occasions.

In order to determine the submerged displacement, the cross sectional areas of the float are measured at each station of the line drawing, and are plotted against the float length as shown by the curve "submerged displacement" on Figure 4. On this plot the abscissae are the distances of a given station from the bow of the float. The station numbers are also marked for the convenience of reference. It is a common practice, however, to use the distance from some reference line as a station number, thus avoiding the confusion of two numbering

systems. The ordinates are the sectional areas of the float stations in square inches. The area under the curve thus plotted on Figure 4 is again planimetered, giving the total displacement. Let A be the scale of ordinates, such for instance as 1" = 400 sq. in., and L the scale of abscissae, such as 1" = 30" of float length. The scale of the area of the diagram is then 1 sq.in. = A x L, in this case 400 x 30 = 12,000 cu.in. The total area under the curve of Figure 4, as measured in square inches, is multiplied by this scale, divided by 1,728 to convert into cubic feet, and multiplied by 62.5 or 64 to convert into the pounds of displacement of fresh or salt water respectively. Thus in the example cited in connection with Figure 4 , the submerged displacement in salt water is:

$$S.D. = 35 \times 12{,}000 \times 64/1728 = 15{,}500 \text{ pounds.}$$

If the stations of the line drawing are spaced so that the length of the float is divided into an even number of equal spaces, the volume can be obtained by Simpson's rule:

$$\text{Volume} = \frac{1}{3}\frac{L}{n}\left(a_1 + a_2/4 + a_3/2 + a_4/4 + \ldots\ldots + a_{n-2}/2 + a_{n-1}/4 + a_n\right) \qquad (1)$$

where L is the length of the float, n = the number of spaces, and a_1, a_2 . . . a_n are the sectional areas of the float sections.

The preliminary estimates of the float size can be made on the basis of the "block coefficient", i.e. the ratio of the float volume to the volume of the rectangular block, the length, width and height of which are equal to these of the float. The average value of .45 can be assumed for this coefficient.

Example:

A seaplane float has a length of 21 feet, a beam of 3 feet and a depth of 2 feet. The probable submerged displacement is:

$$.45 \times 2 \times 3 \times 21 = 56.7 \text{ cu. ft.}$$

or, in sea water at 64 lb./cu.ft.:

$$64 \times 56.7 = 3630 \text{ lb.}$$

In order to determine the "normal flotation", the estimated position of the water line is drawn on the side elevation of the float

or hull, the intersection of this water line with each of the hull stations is measured, and the water line of each station is drawn on the front elevation of the line drawing, known as the "body plan". The sectional area below this line is measured for each station, and the same procedure is followed as described previously for the submerged displacement. The first estimate of the position of the waterline and of the normal flotation is facilitated by computing the draft on the basis of the block coefficient, based in this case on the length of the waterline, the maximum beam, and the draft. In this case .38 can be taken as the average value of the coefficient. If the normal displacement is found to be larger or smaller than the weight of the aircraft, the waterline is lowered or raised, and the procedure repeated until the displacement is exactly equal to the weight.

Next, it is necessary to check the position of the center of buoyancy, i.e. of the center of gravity of the displaced water. For this purpose the sectional areas below the water line are multiplied by the distance from the main step, and the resultant area moments are plotted, as shown by the curves "forebody moment" and "afterbody moment" on Figure 4 . The distance x from the step to the center of buoyancy is determined as:

$$x = \frac{\left(\begin{array}{l}\text{Area under the forebody}\\ \text{moment curve}\end{array}\right) - \left(\begin{array}{l}\text{Area under the afterbody}\\ \text{moment curve}\end{array}\right)}{\left(\text{Area under the curve of the normal flotation}\right)} \qquad (2)$$

x is taken, of course, to the scale of abscissae of Figure 4 .

In the example used above:

Scale of the displacement area . . . 1" = 12,000 cu.in.
Scale of the moment area . . . L" = 20,000x30 = 600,000 $in.^4$

$$x = \frac{600{,}000\ (15 - 5)}{12{,}000 \times 17.5} = 28.6 \text{ inches.}$$

The vertical position of the center of buoyancy is seldom computed, and can be taken with sufficient accuracy to be located between 35 and 40 per cent of the draft below waterline. The line passing through the center of buoyancy and drawn normal to the waterline must pass through

the center of gravity of the seaplane. If it passes forward of it, it means that there is too much buoyancy in the forward part of the hull, and too little in the aft part. The assumed waterline is then tilted, so as to reduce the draft of the bow sections, and to increase the draft of the stern sections. Several trials and adjustments are usually needed. The change of the trim will affect the buoyancy, and the changes of draft, made to correct the buoyancy will affect the trim. Therefore both sets of computations must be carried out concurrently, and the results tabulated to permit the interpolation between trials.

2.2 Static Stability - Metacentric Height - Application to Twin-Float Seaplanes.

We will consider now the principles of static stability for a body floating on water. Assume Figure 5 to represent a cross section of a boat's hull, or more precisely a slice of a hull between two transverse planes spaced by the distance dx. Assume the hull to be inclined by a small angle θ, so that the triangular area g_1 is emerged, and the area g_2 is immersed, shifting the center of buoyancy from B to B_1. The vertical force of buoyancy now passing through B_1 will intersect the centerline plane at the point M, called "Metacenter". If G is the center of gravity, we evidently have the stabilizing moment formed by the couple of the weight and buoyancy forces equal to:

$$W \times MG \times \theta$$

The location of the metacenter M generally depends on the angle of heel θ, but it is reasonably constant for small values of θ, say up to 15°. When the metacenter is referred to, it usually means the initial metacenter for the infinitely small angle θ.

The moment due to the transfer of the buoyancy of the emerged triangle having its center of gravity at g_1 to the immersed one g_2 is

$$2 \times \frac{2}{3} y \times \frac{y^2 \theta}{2} = \frac{2}{3} y^3 \theta \, dx \qquad (3)$$

or integrating for the length L of the hull:

$$\frac{2}{3} \int_0^L y^3 \, dx \qquad (4)$$

This moment is evidently equal to the moment produced by the entire submerged volume of the hull V times the displacement of the center of buoyancy BB_1, or

$$BB_1 \times V = \frac{2}{3}\theta \int_0^L y^3 dx \qquad (5)$$

Substituting $BB_1 = BM\theta$, cancelling θ and transposing:

$$BM = \frac{\frac{2}{3}\int_0^L y^3 dx}{V} \qquad (6)$$

the numerator of this expression is recognized as the moment of inertia of the waterplane, and the expression is rewritten therefore as

$$BM = \frac{I}{V} \qquad (7)$$

Flying-boat hulls, and the floats of single float seaplanes are usually long enough to give the satisfactory longitudinal stability, so that special calculations are not needed. The floats of twin-float seaplanes must be checked for the longitudinal as well as lateral stability by the method described above. If I is the moment of inertia of the waterplanes, and D is the displacement in cubic feet of both floats:

$$I = 2(I_o + Ab^2) \qquad (8)$$

where I_o is the moment of inertia of the waterplane of each float about its own centerline, and A is the area of the waterplane, i.e. of the intersection of the water surface with the float. b is the distance of the float centerline from the plane of symmetry, i.e. the half spacing of two floats. I_o is quite small compared to Ab^2, and usually can be

neglected, assuming $I = 2Ab^2$.

Since the distance BG is known from the design data, we get:

$$MG = MB - BG$$

The minimum spacing of the floats is determined by the requirement of the Civil Aeronautics Administration for the minimum metacentric height MG:

$$MG = 4\sqrt[3]{\Delta} \qquad (9)$$

The same expression $MB = I/\Delta$ is used for checking the longitudinal stability, but in this case I is the longitudinal moment of inertia of the waterplane of two floats:

$$I = \frac{2}{3}\int_0^L yx^2\,dx \qquad (10)$$

where y is the breadth of the waterplane, and x is the distance of the particular station from the centroid of the area. The outline of the waterplane is drawn by measuring the half breadth at each waterline on the body plan, and by plotting it against the length of the float. The waterplane area is either measured by the planimeter, or is computed by Simpson's Rule. The products yx^2 are tabulated, and are plotted on the length basis. The longitudinal moment of inertia of one float is obtained as the area under the curve. This is found either by the planimeter or by the Simpson's Rule. As before, MG = MB - BG, but in this case CAA regulations require that:

$$\text{Longitudinal MG} = 6\sqrt[3]{\Delta} \qquad (11)$$

2.3 Lateral Stability of Flying Boats and of Single Float Seaplanes

The narrowness of flying-boat hulls and of single floats, and the resulting small moment of inertia of the waterplane area results in the transverse metacenter M being located below the center of gravity, i.e. the metacentric height MG is negative. This indicates the lateral instability, which must be corrected by auxiliary means. Figure 6-a shows the "stubs" or "sponsons" introduced by Dornier, and used in this

country by Boeing. By providing larger breadth, and therefore larger lateral moment of inertia of the waterplane, the stubs provide positive MG, and permit to attain the practical amount of stability. Figure 6-b shows the use of two auxilliary floats located near the main hull, and so disposed as to have sufficient waterplane area and moment of inertia to provide the necessary amount of stability. This arrangement was introduced by Rohrbach, and was used in this country by Sikorsky. Both of these arrangements are now abandoned, because of the weight involved, and of the added water resistance during take-off, in favor of auxiliary floats of small size located near wing tips, as shown on Figure 7. The floats, known as "auxiliary floats" or "wing tip floats" are so located vertically that they about touch the water surface, some times immersed an inch or two, some times a few inches above water level. The flying boat is permitted to list a certain amount before sufficient buoyancy is developed in the auxiliary float for equilibrium. In this case it is not practical to compute the metacentric heights, and the size of auxiliary floats is determined by empirical rules. We will quote E. G. Stout (Reference 1): USE Navy Spec SR-59

"The minimum submerged displacement for each auxiliary float is given (in SR-59) by the expression:

$$\Delta = \frac{W}{l}\left[h_e \sin\theta + \frac{0.10\,b}{(W/S)} + 0.06\sqrt[3]{W}\right] \qquad (12)$$

where Δ is submerged displacement of each side float, lb.; W, normal gross weight of seaplane, lb.; l, distance between C.B. of side float and center line of seaplane, ft.; h_e, effective height of C.G. above C.B. of main float or hull, ft.; θ, angle of heel required to submerge side float, deg.; b, wing span, ft.; and S, total wing area, sq. ft. . . . . First term within brackets is the result of the inherent upsetting moment caused by the effective destabilizing height of C.G.; second term is result of the effect of wind on wings; and third term represents a reasonable excess restoring moment based on accumulated experience".

It is noted that in the second term the upsetting moment due to the side wind is taken to be proportional to the span and to the area of wings, since W in the denominator is cancelled by W in front of brackets.

It is evident from the above that required size of the auxiliary float increases as the float is moved inboard, and increases with the angle of list θ needed to submerge the float. For this reason the floats are placed as low as possible, and as far outboard, as the strength of the wing permits. If the floats are located too low, they cause additional drag during take-off, and are more exposed to the danger of the damage during landing, so that making the keel of the float just touch the surface, or to be submerged only an inch or two appears to be the best compromise.

While only the buoyancy was treated in the above discussions, it is equally important for the float to have a satisfactory planing bottom to furnish dynamic lift at high speed. The general shape of the float must be such as to continue to generate the lift force when moving through water in fully submerged condition. Some streamline shapes suffer the rapid reduction of the lift force, or even change to the downward suction, if submerged while moving forward at sufficient speed. Figure 8 gives the outline of the float which was used on naval float seaplanes.

3. Planing, Resistance and Take-Off

3.1 General Considerations

Figure 9 shows a flat surface of the beam B planing at the angle of trim τ and wetted length ℓ. At the trailing edge the water breaks away forming a wave in the wake of the surface. It also breaks away cleanly on two sides leaving the upper part of the planing body dry. The exact speed at which this condition occurs is indetermined, and in this course we will generally consider speeds corresponding to C_V (to be defined in the following paragraph) $\geqslant 2.5$. In front of the planing surface the water surface rises first gently, then makes a quick turn up and forward, forming a thin sheet of water flowing forward. The streamline, separating the part of the water eventually directed forward from that flowing aft, meets the

surface at the point called "stagnation point". At this point the maximum water pressure on the surface is developed. Forward of this point the pressure drops sharply, aft of it the pressure drops more rapidly at first, then more gradually towards the trailing edge. The drop of the pressure aft of the stagnation point occurs more rapidly at small angles of trim τ, and less rapidly at large angles. The region of rapidly curving water surface and in the vicinity of the stagnation point is given the name "spray root" by H. Wagner, who formulated the theory of its formation (Ref. 3a). It was first observed experimentally by W. Sottorf (Ref. 3).

Figure 10 shows a vee planing surface. At the point B, where the keel meets the water surface, there is no discernible rise of the surface, and this point can be assumed to lie on the undisturbed water surface. Aft of this point the water surface rises forming the spray root, so that wetted area at chines is at the point C, above and forward of the intersection with undisturbed water at D. H. Wagner established the relation $b_1/b_2 = \pi/2$, from which it follows that $L_1/L_2 = 2/\pi$. If we denote by λ the ratio of the wetted length ℓ to the beam B, we obtain the expressions:

Wetted length of keel = $B\ (\lambda + \tan \beta/2\pi \tan\tau)$

Wetted length of chine = $B\ (\lambda - \tan \beta/2\pi \tan\tau)$

These deductions are demonstrated to agree well with experimental data (pages 12, 13 and 14 of Ref. 5).

3.2 General Expression of Hydrodynamic Force

It is shown by dimensional analysis that a hydrodynamic force acting on a submerged body, located far away from any boundaries, has the form

$$\text{Force} = k \times \frac{1}{2}\rho V^2 L^2 f\left(\frac{VL}{\nu}\right) \qquad (13)$$

where:

ρ is the density of water in mass units

V = velocity in feet per second

L = any characteristic linear dimension of body

k = a non-dimensional constant

ν - kinematic viscosity, defined as μ/ρ, where μ is the viscosity

the ratio VL/ν is known as Reynolds number, and is frequently denoted by R_e.

$f(VL/\nu) = f(R_e)$ is an unknown function of the Reynolds number.

In the case of a body moving on water surface, the force acting on the body is further affected by the gravity (resulting from the wave making), and by the surface tension of water, which resists the distortion of the initially flat surface. The expression for the force then takes the form:

$$Force = k \times \frac{1}{2}\rho V^2 L^2 f\left(\frac{VL}{\nu}\right) F\left(\frac{V}{\sqrt{gL}}\right) \varphi\left(\frac{V^2 L}{\sigma/\rho}\right) \quad (14)$$

where: g is the acceleration of gravity

σ is the surface tension of water

F and φ denote unknown forms of the functions.

The ratio $V/\sqrt{gL}$ is known as Froude number. If this number is squared, the ratio takes the form V^2/gL. Since for a given mass V^2 is proportional to dynamic pressure, while gL is proportional to the force of gravity, the Froude number indicates the ratio of dynamic forces to the force of gravity. The ratio $V^2L/(\sigma/\rho)$, known as the Weber number, likewise indicates the ratio of dynamic forces to the forces of surface tension. The detail treatment of the dimensional theory by which Eq. (14) is derived, as well as of the boundary layer theory and laws of skin friction, to be discussed later, is beyond the scope of these notes. References to the simple treatment of these subjects in readily available books are given on page .

It is not always necessary to consider all three of the functions f, F and φ. Thus, the influence of the Weber number is felt only at low speed and in case of very small models, and in our study of planing we can consider is as constant equal to unity, i.e. we can disregard it. The Reynolds and Froude numbers will be considered separately in the problems involving the lift force and the drag force.

3.3 The Lift Force

The vertical component of the forces acting on a body is called the lift force, and will be designated by L. It is known from experience that Reynolds number has very little influence on the lift, and that only the Froude number need be considered. In the study of the planing process it became customary to take the beam B as the characteristic length, and in such case give the Froude number the special term "speed coefficient", and to designate it by C_V. Thus

$$C_V = V/\sqrt{gB} \qquad (15)$$

Disregarding Reynolds and Weber numbers, and including the $F(C_V)$ into the non-dimensional lift coefficient C_L, we can rewrite Eq. (14) as

$$\left.\begin{aligned} \text{Lift} &= C_L \times \tfrac{1}{2}\rho V^2 B^2 \\ \text{where} \quad C_L &= f(\tau, \lambda, C_V, \beta) \end{aligned}\right\} \qquad (16)$$

It has not been possible to evaluate the coefficient C_L analytically, and the value of it is established by the empirical analysis of the test data. It is found convenient to separate the effect of the deadrise β from the effect of τ, λ and C_V, and to define first the lift coefficient C_{L_o} of a flat planing surface.

L. I. Sedov (Ref. 4) gave the following expression for the value of $C_{L_o} = f(\tau, \lambda, C_V)$:

$$C_{L_o} = \tau\left[\frac{0.7\lambda}{1+1.4\lambda} + \lambda(0.92\lambda - .38)/C_V^2\right] \qquad (17)$$

At the Experimental Towing Tank (Ref. 5), this expression was simplified, and was written

$$C_{L_o} = \tau^{1.1}\left[0.0120\,\lambda^{1/2} + 0.0095\,(\lambda/C_V)^2\right] \qquad (18)$$

The first of these two expressions is particularly interesting in indicating the proportionality of C_L with τ, which is only slightly modified by the second expression. The second expression is slightly more accurate for the range of C_V used in seaplane design, and brings out more clearly the significance of λ and of C_V.

The lift coefficient C_{L_β} of a prismatic Vee planing surface is given in terms of a flat surface (Ref. 5) as:

$$C_{L_\beta} = C_{L_0} - 0.0065\beta C_{L_0}^{0.6} \qquad (19)$$

For convenience of use the expressions (18) and (19) are given in the form of charts on Figure 11, taken from Ref. 5.

Example: 1. Find the lift Δ of a flat surface 1 foot wide planing at the angle of trim τ of 5 degrees at the speed of 20 feet per second on fresh water with the mean wetted length of 2 feet.

$$\tau^{1.1} = 5.87 \qquad \lambda = l/B = 2.0$$

$$C_V = V/\sqrt{gB} = 20/\sqrt{32.2\times 1} = 3.5$$

$$C_L = 5.87\left[.0120\times 2^{1/2} + .0095\,(2/3.5)^2\right] =$$

$$5.87(.0170 + .0031) = .118$$

$$\Delta = .118\,(62.5/2\times 32.2)\times 20^2\times 1^2 = 46 \text{ lbs.}$$

2. Find the lift of the above surface assuming that it has a Vee shape with the angle of deadrise β of 20 degrees:

$$C_{L_\beta} = .118 - .0065\times 20\times .118^{.6} = .082$$

$$\Delta = .082\times(62.5/2\times 32.2)\times 20^2\times 1^2 = 31.8 \text{ lbs.}$$

All of the expressions in this article were given in the form $\Delta = f(\lambda)$, since it is not practical to give Eqs. (17 and (18) in the inverse form $\lambda = \Phi(\Delta)$. In the actual work it is the latter relation

that is usually required, and can be easily obtained from the chart on Fig. 11. In the usual statement of a problem B, β, Δ and V are given. The trim τ is taken as a parameter, and the λ and ℓ are determined. In case of the aerodynamic analysis of an airplane, the wing area is fixed, and the computations are arranged so as to determine the lift coefficient and the angle of attack. In the case of a planing surface the wetted area (i.e. the λ) is variable, so the angle of trim τ is taken as a parameter, and the computations are arranged so as to determine λ. Conversely, if the resultant force is to pass through the center of gravity of a seaplane, the wetted length ℓ must be held constant, and the angle of trim τ is the variable to be determined.

The knowledge of the wetted length for every speed and trim angle during the take-off run of a seaplane will prevent many errors in the design. For instance were too small a beam B assumed, the calculations would immediately show excessive wetted length, with wetting of the curved areas of the bottom near the bow, and with resultant increase of the resistance and spray. For all planing conditions the wetted area must be confined to the region in which the buttock lines are straight, and the forward area of the bottom where the buttock lines are curved must remain above water. In the same way the computations of the wetted length $\ell = \lambda B$ will indicate the maximum load Δ which can be used for a given B and τ, or the minimum value of the angle of trim τ which can be used for a given load Δ. It should be particularly emphasized that the important first term of Eq. 18 shows that wetted length varies as the square of the loading, and inversely as the square of the beam.

3.4 Resistance of Prismatic Planing Surfaces

The resistance of a planing surface is found to depend both on the Froude number and the Reynolds number and for this case Eq. (14) is rewritten as:

$$\text{Resistance} = k \times \tfrac{1}{2}\rho V^2 B^2 \, F\left(\frac{V}{\sqrt{gB}}\right) f\left(\frac{VL}{D}\right) \qquad (20)$$

It was assumed, and subsequently verified experimentally that effects of the Froude number and of the Reynolds number can be separated and Eq. (20) can be rewritten as:

$$C_D = \frac{\text{Resistance}}{\frac{1}{2}\rho V^2 B^2} = k_1 F(C_V) + k_2 f(R_e) \qquad (20a)$$

Thus, total resistance R can be considered as the sum of two distinct parts: the resistance which is due to the normal pressures on the surface, which would exist even in frictionless fluid, and one due to tangential, or frictional force.

Normal pressures acting on a surface produce the lift as well as the drag, and for a prismatic surface two are connected by simple relation, resulting from Figure 12:

$$R = \Delta \tan \tau$$

and, dividing by $1/2\rho V^2 B^2$, and denoting the dynamic drag coefficient by C_{dd}:

$$C_{dd} = C_L \tan \tau$$

The effect of C_V is here already included in C_L obtained from Eqs. 17 and 18.

Friction drag coefficient, resulting from $f(R_e)$ and referred to the square foot of area can be estimated on the basis of Schoenherr's Formula:

$$\frac{0.242}{\sqrt{C_f}} = \log_{10}(R_e \cdot C_f) \qquad (20b)$$

For convenience of use the values given by this formula were tabulated in Reference 9. The plot of C_f obtained by Schoenherr's Formula vs. R_e is given by the curve (144) on Figure 12a. The value of Schoenherr's Formula lies in its applicability to a wide range of values of Reynold's number. If Reference 9 or the plot similar to Figure 12 are not available, and if the Reynold's number does not exceed 2×10^7, the simpler Prandtl-Karman formula can be used:

$$C_f = .074 (VL/\nu)^{-0.2} \qquad (20c)$$

While for $10^6 < Re < 10^9$ Schoenherr's formula agrees closely with Schlichting's formula

$$C_f = \frac{0.455}{(\log_{10} Re)^{2.58}} \qquad (20d)$$

In Eqs. 20b, 20c and 20d the coefficient C_f is referred to the actual wetted area, i.e. is determined as

$$C_f = \frac{\text{Frictional Resistance}}{\frac{1}{2}\rho V^2 (\text{Wetted Area})} \qquad (20e)$$

For use in Eq. 20a it must be converted to beam squared basis, i.e. it must be multiplied by λ and by Sec. β, so that we have finally

$$C_D = C_L \tan\tau + C_f \lambda \sec\beta \qquad (20f)$$

The above equations refer to the turbulent boundary layer, which can be assumed to exist on the full-scale floats and hulls. In the testing of the small models the turbulent layer can be assumed to exist only if special measures are taken to induce it, as for instance, towing of a vertical wire in front of the model. Without such a precaution, the boundary layer will be often turbulent with laminar approach (Reference 7 - Figure 2), and the value of the frictional drag will be lower and the data will be less consistent.

3.5 Ratio of Resistance to Lift

The ratio of the resistance to lift R/Δ is often designated by ϵ and called the "Planing Coefficient". In the previous discussion the lift and drag coefficients were referred to the square of the beam as the characteristic dimension, and were designated as C_L and C_D. For the following discussion it will be more convenient to refer them to the bottom area BL, i.e. to λB^2, and in this form we will designate them

as C_ℓ and C_d. In this form Eq. (20a) becomes:

$$C_d = C_\ell \tan\tau + C_f \sec\beta \qquad (20g)$$

and

$$\epsilon = \frac{C_d}{C_\ell} = \frac{C_\ell \tan\tau + C_f \sec\beta}{C_\ell} \qquad (20h)$$

On the basis of Equation 17, the lift coefficient C_ℓ can be assumed to be approximately proportional to $\tan\tau$, i.e. $C_\ell = K \tan\tau$, and Equation 20h takes the form:

$$\epsilon = \frac{\tan^2\tau + \text{Const.}}{\tan\tau} \qquad (20i)$$

The form of this function is shown by Figure 13, which represents the plot of the experimental data of Sottorf (Reference 7), obtained from tests on the planing surfaces 30 cm wide at the speed of 6 m/sec., or C_v of about 3.5. ~~The dotted line represents the extrapolation of the test data on the basis of the above formula.~~ This diagram is very useful in understanding the influence of the angle of trim τ. It is noted that minimum resistance for Vee surfaces occurs at the angle of trim of approximately 6 degrees, and the seaplanes are usually maintained at this attitude at high speed, when the pilot has the control power to do so. At smaller angles of trim the drag rises rapidly, due to the predominence of the second (friction) term, with $\tan\tau$ in the denominator being small. At the larger angles the first term predominates, and the curves approach asymptotically the line $\epsilon = \tan\tau$, indicating relatively unimportant effect of the friction. It should be emphasized that these curves apply to the prismatic Vee planing surface of sufficient length. In the actual seaplanes the prismatic section cannot be made to support the load at, or slightly above the hump speed at the angle of the minimum drag, and the drag increases rapidly as the curved, upswept part of the bottom is wetted. In this case the angle of the minimum drag becomes much larger, usually between 9 and 12 degrees,

and the drag is correspondingly large. In analyzing the hull performance it is always necessary to keep in mind these two factors: the angle of trim, and the corresponding wetted length.

3.6 The Attitude and Balance of the Planing Seaplane Hull in Two-Step Planing

Figure 13a shows the seaplane hull in the planing condition approximately at the hump speed. The hull is supported by water pressures on the forebody, the resultant of which is $\Delta - \delta$, and by the pressures on the afterbody near the second step, the resultant of which is δ. At a given angle of trim and a given speed, a certain wetted length L is required to support the load, and this can be determined from the formulae of Art. 3.3. In supporting the load the forebody deflects the water surface, forming the wave. The second step usually rides on the forward slope of the wave, somewhat below the level of undisturbed water. For the afterbodies of the length commonly used it can be assumed that τ at hump speed is equal to $1.2\,\sigma$, with $1.1\,\sigma$ for very long afterbodies, and $1.3\,\sigma$ for very short ones. A more accurate check on the estimated value of σ can be made by use of the data on the wave contours in the wake of planing surfaces given in Reference 8. Since this angle of inclination is not large we can assume the cosine of it to be equal to one, and can consider the resultant to be equal to $\Delta - \delta$ Then we have the positive pitching moment due to the forebody of $a(\Delta - \delta)$, from which the stern load is found to be:

$$\delta = \Delta a/(a+b)$$

It appears to be most advantageous to locate the center of gravity so that δ is 5% to 10% of Δ at the hump speed. With this load the hull is stably supported by the forebody and the afterbody forces. If the stern load is much lighter it will disappear with very small increase of speed, leaving the hull supported in complete balance by the forebody alone, with the probability of the low limit porpoising. If the stern load is much heavier, the variation of it will produce significant changes in the forebody load, and in the resultant wave form. This may lead to the high limit porpoising.

3.7 Towing Tank Data - Specific Test

The primary purpose of previous articles is to expose the basic principles involved in the process of planing, and to give the reader the understanding and the means of judging test data. The art of predicting the performance of a hull on the basis of its design characteristics is in its infancy, and in practice the design is laid out on the basis of the designer's experience, and usually is subjected to tests in the towing tank. There are three systems of planning the test, and of presenting the test data:

a. Specific test

b. N.A.C.A. General test

c. Experimental Towing Tank of the Stevens Institute of Technology collapsed data test.

3.71 The "specific test" is made to verify, and to present by graphs the characteristics of a specific design, at a specific initial load, and the specific take-off speed. It is the simplest test, and it gives the data usable directly with the minimum amount of calculations. Since the form of the function of the speed coefficient $F(C_V) = F(V/\sqrt{gb})$ or $F(V/\sqrt{gL})$ in Eq. 14 is unknown, the model and the full-scale prototype can be compared only at identical values of the speed coefficient C_V. Therefore the speed of the test is related to the size of the model by the Froude law of similarity:

$$V_m / V_{fs} = \sqrt{L_m / L_{fs}} = \lambda^{\frac{1}{2}}$$

where the subscript m denotes the model, the subscript fs denotes the full scale, and λ is the scale, i.e. the ratio of any linear dimension of the model to that of the full scale. The size of the model is chosen, after consultation with the test tank staff, to be as large as the capacity of the towing equipment permits in regards both to the weight and the speed, with the latter being usually the critical limit. The model is

supported by the pivoted connection placed at the point corresponding to the location of the center of gravity of the complete seaplane. The center of gravity of the model is brought to this point by a system of counter-weights. The weight of the model is also brought to the correct weight W:

$$W_m = \Delta_m = \lambda^3 W_{fs}$$

If the model is too light, the weights are added to it. If it is too heavy, it is counterbalanced, or "unloaded" by the means provided in the design of the towing carriage. Various features of the test are best explained by the reference to Figure 14, showing the form in which the results are usually reported. The "Load" curve gives the weight supported by the hull at any speed. The initial loading is equal to the weight of the seaplane to the proper scale, or otherwise to the displacement at rest Δ_o The wings are assumed to remain at a constant angle of attack, so that at any speed V the load on water is:

$$\Delta = \Delta_o (1 - V^2/V_o^2)$$

where V_o is the take off, or getaway speed at which the load on water $\Delta = 0$. This relation is referred to as the "parabolic unloading curve". Such an unloading is achieved in the test by either suitable adjustment of the model loading, or by a hydrofoil immersed in water, and adjusted so as to balance fully the weight of the model at the getaway speed.

With the model "free to trim", i.e. to assume any attitude solely under the action of the water forces, the following quantities are measured:

a. Vertical displacement of the model with respect to its position at rest, referred to as the "change of draft", "heave" or "rise".

b. The angle of trim the model assumes.

c. The resistance.

All of these quantities are plotted against the speed as shown on Figure 14. These tests are made for the series of speeds from the start to the highest speed at which the test can be safely performed. At too high a speed the model may develop the tendency to dive, endangering both the model and the apparatus. Usually the test can be carried to the speed at which the angle of trim, diminishing with it, drops to about 5 degrees. If the model tends to oscillate, this is eliminated by connecting it with a dashpot giving sufficient damping.

The hull design may be such that the model left to itself assumes the angle of trim different from the one desired for the best performance. To check this, certain test runs are repeated with the model restrained from pitching, i.e. are run at a "fixed trim", and the following quantities are measured:

a. The change of draft.

b. Pitching moment exerted by the model.

c. Resistance.

The range of these tests usually covers the most probable attitudes of the seaplane, i.e. the large trim angles at the hump, and the low trim angles at higher speed, so as to furnish additional data not obtained in the free-to-trim test. On Figure 14 the corresponding curves are distinguished by the indication of the angle of trim.

Now certain features of the test curves can be pointed. It is noted that both the "change of draft" and the "angle of trim" curves show a slight dip at (A) at very low speed, shortly after the start of the take-off run. This is primarily due to the suction generated by the water flow around curved bow sections of the hull.

In the satisfactory hulls this feature is of no importance. In certain hulls, however, the excessive curvature of the lines at the bow, combined with excessive draft at the bow, makes this small dip to develop into the complete diving.

The next point of importance is the maximum in the resistance curve at (B) usually referred to as the "hump". This is the critical point which often will determine the ability of the seaplane to take off, as this is described in greater detail in Section 3.9.

The hump in the resistance curve is usually associated with the maximum in the angle of trim curve, although often it may occur at a somewhat lower or higher speed. As can be seen from Figure 13a the higher the trim of the hull at the hump. the higher will be its resistance. To reduce the resistance it is necessary to reduce the angle of trim, and this can be achieved by either reduction of the sternpost angle, or by increasing the afterbody length. The reduction of the trim angle will decrease the resistance only if the region in which the buttock lines are straight is long enough to accommodate the increased wetted length, resulting from the decrease of the angle of trim. Because of these considerations it is highly desirable that during the test the wetted length be observed with respect to the suitable markings on the model.

After passing the hump speed, the slight break in the trim curve at (C) corresponds to the rise of the stern from water, and to the beginning of the planing on the forebody alone. At the hump the speed is low, the wetted area is large, and the stern load δ is therefore also large. The orientation of the force vector δ is such, however, that is does not contribute to the total drag, which therefore corresponds to the load $\Delta - \delta$ rather than Δ. The increase of the planing speed above the hump causes the decrease of the wetted length, although the rate of this decrease is tempered by the simultaneous

decrease of the angle of trim. Eventually the wetted length is shortened to such an extent that the resultant force acting on the forebody passes through the center of gravity, δ_A becomes zero, and the second step leaves the water surface. The angle of trim between the hump and the point (C) of Figure 14 is determined by the sternpost angle and the wake configuration, giving a broad low peak of the resistance curve. Were the sternpost angle increased so that the trim τ would become much larger, the wetted length would become shorter, the sternpost load δ at hump would would become light, and a very small increase of the speed would reduce it to zero. The points B and C would almost coincide. If no external moments were applied, the resultant of the forebody pressure would have to remain thereafter in one position determined by the position of the C.G. This means that the wetted length would have to remain essentially constant, and the increase of the speed would have to be compensated by the decrease of the angle of trim τ. The trim too high at the hump would tend to become too low at the high speed. The resistance curve would display a high and sharp peak at the hump, with the tendency to rise again at high speed.

3.72 General Tank Test

The drawback of the specific test is found in the lack of means of using the data for the speeds and loads other than those used in the test. The N.A.C.A. "General Tank Test" was devised to give the data which can be used for the wide range of loads, speeds, and hull sizes. For this purpose all test data are put into the form of non-dimensional coefficients:

$$\text{Load Coefficient } C_{\Delta} = \Delta/wb^3$$

$$\text{Resistance Coefficient } C_R = R/wb^3$$

Speed Coefficient $C_V = V/\sqrt{gb}$

Trimming Moment Coefficient $C_M = M/wb^4$

Draft Coefficient $C_d = d/b$

where:

Δ displacement in units of weight.
w weight of water per unit volume.
b beam.
d draft.
V speed.
M pitching moment about c.g. of the seaplane.
g acceleration of gravity.

any consistent system of units can be used such as pound-foot-second, or metric ton-meter-second.

C_R and C_M are determined by test, and are plotted against C_V, with C_Δ as parameter. A separate plot is made for each value of the trim angle τ. Figure 15 taken from Reference (20) gives the data for $\tau = 7^\circ$. This particular report covered the values of τ of 3,5,7,9, and 11 degrees.

The drawback of the plot shown on Figure 15 is that it is impossible to judge where the best value of R/Δ is. For this purpose the alternate way of presenting the general test data is shown on Figure 16, also taken from Reference (20). The resistance coefficient C_R is plotted against the angle of trim, with C_Δ and C_m as parameters. Thus for a given trim angle and loading, the resistance, and the pitching moment are readily read from the chart. A separate chart is prepared for each value of C_V, and two such charts for C_V of 3.5 and 4.0 are included on Figure 16.

Attention is called to the wide range of values of C_Δ used, so that every conceivable condition occurring

during the take-off run of a seaplane is represented. This is very important advantage for N.A.C.A. reports, which are used by many designers for many problems. The disadvantage is in that the plots do not convey directly the picture of the take-off performance and the data have to be read from the general test charts, and put into the form of the specific test for the analysis of the specific problem. While very large and expensive test schedule is needed to cover the broad field, for which the data are intended, the number of points which can be obtained for a specific problem is rather small, and there may be some difficulty in the precise definition of the specific curve.

Example: Assume a flying boat to which the data given by Figure 15 apply, with the beam of 10 feet, the gross weight of 64,000 pounds, and the getaway speed of 100 ft. per sec. operating in sea water. Find the resistance and the pitching moment occurring at 60 ft. per sec.

$$C_{\Delta_o} = 64{,}000/64 \times 10^3 = 1.00$$

$$C_{\Delta} = 1.00 \left[1 - (60/100)^2\right] = .64$$

$$C_V = 60/\sqrt{32.2 \times 10'} = 3.34$$

from Figure 15: $C_R = .117$ $C_M = +.06$

Resistance = $.117 \times 64 \times 10^3 = 7480$ pounds.

Moment = $.06 \times 64 \times 10^4 = 40{,}300$ ft.lbs.

The computations of this type can be readily arranged in a tabular form to cover a number of values of V throughout the speed range, thus furnishing the data for the plot of the resistance and moment curves. Making the computations for the several values of the angle of trim will indicate the most favorable attitude of the boat for any speed. The use of plots of the type shown

on Figure 16 will save some labor, since the best values of trim are directly indicated.

3.73 Stevens Collapsed Data Test

The method of plotting the data, originated at the Stevens Institute of Technology, and described in Reference 11 aims at giving the data of the General Test type with lesser number of test points, and in a more compact form. It also demonstrates more clearly how satisfactory test data can be obtained from a model which is too large for the available tank capacity to permit the straightforward specific test shown on Figure 14. It is the direct outcome of trying to get greater usefulness of test tanks which are much smaller than the tanks of N.A.C.A. The seaplane hull performance is considered in two separate parts — below and above the hump speed. Below the hump speed the attitude of the hull is determined by the hull interaction with the wave it creates, and very large moments would be needed to modify this natural angle of trim. The effect of aerodynamic controls is therefore weak, and to the first approximation can be neglected. The hull therefore is tested free to trim, and the angle of trim and the resistance are recorded. Below the hump, i.e. in the displacement range, the resistance coefficient is a function of the Froude Number:

$$R/\tfrac{1}{2}\rho V^2 L^2 = f(V^2/gL)$$

where L is any characteristic dimension. Defining L as $(\Delta/w)^{1/3}$, and substituting the N.A.C.A. coefficients puts the above expression into the form:

$$\frac{C_R}{C_\Delta^{2/3} C_V^{\,2}} = f\left(\frac{C_V^{\,2}}{C_\Delta^{1/3}}\right)$$

The typical free-to-trim test curve expressing the above relation is shown in the middle section of Figure 17.

Considerable range of the hull loadings C_Δ of a given hull is found to give the same curve, and conversely one curve can be taken to represent considerable range of loadings, so that it is not necessary to test actually for many loadings. The overloading may give, however, a somewhat higher resistance and a higher trim angle, and therefore tests should be made for this condition. With the general shape of the curve well established, relatively few check points are needed for this.

Above the hump speed and particularly at the important range near take-off or getaway speed the aerodynamic controls are effective, and a pilot is usually able to keep the hull at any attitude he chooses. Therefore the tests for the planing range above hump are made at a series of fixed trims. In this range the resistance can be assumed to be approximately independent of the Froude Number, and for a given angle of trim, dependent on the loading only. This statement is essentially equivalent to neglecting the second term in square brackets in Eq. (18), and in Eq. 20f neglecting the variation of C_f with Reynolds Number. The neglect of the effect of these variables permits to write in the coefficient form:

$$\frac{\text{Resistance}}{\frac{1}{2}\rho V^2 L^2} = f\left(\frac{\Delta}{\frac{1}{2}\rho V^2 L^2}\right)$$

or substituting the N.A.C.A. coefficients:

$$\frac{\sqrt{C_R}}{C_V} = f\left(\frac{\sqrt{C_\Delta}}{C_V}\right)$$

Test results are computed, and the above relation is plotted as on Figure 18, giving a curve for each angle

of trim. By cross plotting the curves of the trim vs. C_R/C_V with the C_Δ/C_V as parameter are finally obtained. These are shown separately on Figure 19, and as a part of the lower diagram on Figure 38-14.

Example: Assume the hull shown on Figure 17 to be used with the beam of 8 feet, gross weight of 27,000 pounds, and getaway speed of 90 ft. per sec., assuming the parabolic unloading curve. Find the resistance:

$$C_V = 70/\sqrt{32.2 \times 8} = 4.37$$

$$C_{\Delta_0} = 27{,}000/64 \times 8^3 = .82$$

$$C_\Delta = .82\left[1 - (70/90)^2\right] = .32$$

$$\sqrt{C_\Delta/C_V} = .13$$

From the lower chart of Figure 17:

$\sqrt{C_R/C_V} = .0625$ at the angle of trim of 9 degrees at which the pitching moment coefficient C_M is zero.

The Ratio

$$[\sqrt{C_R}/C_V] \div [\sqrt{C_\Delta}/C_V] = \sqrt{C_R/C_\Delta} = .0625/.13 = .48$$

$$C_R/C_\Delta = .23 \qquad C_R = .23 \times .32 = .0737$$

Resistance

$$.0737 \times 64 \times 8^3 = 2420 \text{ Lbs.}$$

The resistance can be reduced by applying a nose-down moment by means of elevators so that the angle of trim be reduced from 9 degrees to $6\frac{1}{2}$ degrees, at which $\sqrt{C_R/C_V}$ of .0575 is obtained, or $R/\Delta = .195$.

Insert page 29a

3.9 Take-off Calculations

In the problem of making the take-off calculations, the initial load and the getaway speed are determined by the design of the seaplane. Since the minimum drag of the hull at high speed occurs at the angle of trim of about 6 degrees, this angle of the keel is assumed, and the

Continue on p. 30

3.8 Turbulence Control and Correction of Frictional Drag for Changes in Reynolds Number

A small model tested in a towing tank at low speed may have a partly laminar flow, so that friction drag coefficient may be anywhere between the laminar and the turbulent (Schoenherr's) drag coefficient curves. In order to avoid the uncertainty in C_f value, the turbulence may be introduced by means of towing an approximately vertical piece of round rod or wire in front of the model and close to it. The turbulent wake of the rod induces the turbulence in the boundary layer, and raises the C_f value to the Schoenherr's curve, the use of which permits the recalculation of it from the Reynold's Number of the test model to that of the full-scale prototype. The measurements of wetted areas needed for direct application of friction drag formulae are very seldom made. However, a simple method of correction can be devised by using the ratio of Reynolds numbers Re_m/Re_s, where subscripts m and s designate the model and the full-size prototype. Using the exponential form of expression for C_f, such for instance as Prandtl-Von Karman formula, we can write:

$$\frac{C_{fs}}{C_{fm}} = \left(\frac{Rem}{Res}\right)^{.2} = \left(\frac{Vm\ Lm}{Vs\ Ls}\right)^{.2} = \left(\lambda^{\frac{1}{2}} \cdot \lambda\right)^{.2} = \lambda^{.3}$$

for the range of values of $R_e > 2 \times 10^6$, where the Prandtl-Von Karman formula does not apply directly, it can be made to approximate Schoenherr's line at Re_m and Re_s by replacing the exponent 0.2 by another suitable value. Since the specific test is made on the basis of identical Froude Number for the model and the full-scale prototype, the wave formation of the model is identical with that of the prototype, and the distribution of wetted area is identical. The friction resistance is therefore proportional to C_f. The procedure of making the correction, therefore, is as follows:

Total measured resistance at the angle of trim τ — — — =	say A
Resistance due to load $\Delta = \Delta \tan\tau$ — — — =	say B
Frictional Resistance — — — =	A-B

Corrected Frictional Resistance $(A-B)\lambda^{\circ 3}$ ——— = C

Total Corrected Resistance —— ——— ——— — = B + C

Care should be taken to define τ as the true mean inclination of the planing area and not as a nominal figure referred to an arbitrary reference line.

corresponding angle of incidence of wings is taken in computation of the take-off speed. The flaps are found usually beneficial when lowered for the take off to the angle of approximately half of that used for landing. The lift coefficient obtained on this basis is further increased by the ground effect, by the slipstream of the propeller, and by the vertical component of the propeller thrust. As a rough rule it is suggested that lift coefficient be increased by 25% to account for these factors.

The parabolic unloading curve can be usually assumed. For a given speed, the loading is read from this curve, the C_v and C_Δ are computed, and from these $C_v^2/C_\Delta^{1/3}$ and $\sqrt{C_\Delta}/C_v$. The corresponding values of C_R and of the trim τ are then determined from a suitable data report, such for instance as Reference (21). These are used to construct the curves, similar to the ones which are given directly by the specific test. Computations based on the general test data can be carried out directly in terms of the full-size seaplane, as this has been done in two examples above. The data of a specific test usually refer to the model of a certain scale λ, and have to be scaled up to the full size by the relations:

$$V_{fs} = V_m/\lambda^{1/2}$$

$$R_{fs} = R_m/\lambda^3$$

The angles of trim of the model and of the full-size seaplane correspond directly.

On Figure 20 the curve "hull drag" represents the sample plot of such a scaled-up drag. The aerodynamic drag is also plotted, and the two are added to form the total drag. The aerodynamic drag is computed for the attitude of the seaplane corresponding to the getaway angle of incidence, or approximately that of the steep climb. The increase of the drag due to the propeller slipstream is taken into account. The propeller thrust is computed by the methods given in various courses and data books on aerodynamics, and the curve of thrust vs. scale is plotted. The difference between the propeller thrust and the total drag represents the force available for the acceleration. Since this force varies with speed, the acceleration has to be integrated over the entire speed range.

This is accomplished most conveniently by the following graphical construction: compute the velocity reached in the first second $a = g \times \text{thrust/weight}$, where g is the acceleration of gravity = 32.2 ft./sec.^{2}, convert it into m.p.h., plot on the speed axis of Figure 20, and draw the lines b-c and b-d which make the angle $\pm$ with the vertical axis. The increment of speed a' gained in any of the following seconds is defined as $a' = a \times (\text{thrust less drag})/(\text{initial thrust})$, i.e. the increments of speed are proportional to the accelerating force. All that is needed, therefore, is to draw two series of the parallel strokes filling the space between the thrust curve and the total drag curve, each stroke inclined at the same angle $\pm \alpha$ to the vertical, where α is the angle of inclination of the initial stroke b-c. The number of strokes gives the number of seconds consumed in the process of take off. The zig-zag pattern of inclined strokes of Figure 38-17 permits to read off, and to plot the speed V versus time counted from the start. The take-off distance $S = \int_0^t V\,dt$ is determined as the area under such a curve.

The take-off time can be calculated also by an alternate method of integration. Writing formally:

$$t = \int_0^{V_0} dt \qquad (20j)$$

substitute

$$dt = \frac{1}{a'}\,dV \qquad (20k)$$

where: a' is the acceleration at a given instand defined as $\frac{(T-R)g}{W}$

$(T-R)$ is the effective or net thrust, i.e. the difference between the propeller thrust and the total resistance (in pounds) as given on Figure 17.

g = 32.2 ft./sec.^{2} the acceleration of gravity.

V is the speed at any given instant.

V_0 the getaway speed. W - the gross weight.

Substituting Equation (20k) into Equation (20j):

$$t = \int_0^{V_0} \frac{W}{(T-R)g}\,dV \qquad (20l)$$

The values of $\frac{W}{(T-R)g}$ are computed for a series of values of V from 0 to V_o, preferably using uniform and even number of steps or increments ΔV. The integral (23) can be evaluated then by Simpson's Rule.

For more detailed discussion of the take-off computations consult References 12, 14, 15 and 16.

It will be noted that there are two minima of acceleration: at the hump and near getaway speed. The relative importance of these varies with the value of C_v at getaway. Large flying boats usually have low $C_v = V/\sqrt{gb}$, even if V is large, because of the large value of b. The hump speed is usually critical in such a case, while at the getaway speed ample excess thrust is available for the acceleration. Relatively small sternpost angles, producing relatively low trim angles are, therefore, in order. On the other hand, a small twin-float seaplane may have low V, but b is so small that resultant C_v is large. In such a case the total drag near getaway speed may approach the available thrust, leaving only a small margin for acceleration. The high speed range now has to be favored, the sternpost angle has to be large to avoid afterbody interference, even at the expense of the increased trim and the drag at hump speed. By varying the beam or the sternpost angle, the best compromise between the hump and the high speed range is achieved.

4. Dynamic Stability - Porpoising and Skipping

4.1 Definition, Physical Nature and the Theory

The "porpoising" is defined as the combined oscillation of a seaplane in pitch and in heave of the sustained or increasing amplitude, occurring while planing on smooth water during take off or landing. In the violent case it may take the form of a series of jumps, during which the seaplane is thrown clear out of water; ordinarily the oscillation of the total amplitude of 2 degrees is recognized as the porpoising.

Figure 21 shows the seaplane planing on the forebody alone, with all forces in complete balance, i.e. with the vertical components of the wing lift and of the water pressure on the hull, designated to-

gether as $\sum Z$, equal to the weight W. Figure 21(a) shows the conditions modified by the decrease of the draft, i.e. by the rise of the seaplane, so that initial height of the center of gravity h is increased by Δh, without any change in the angle of trim. The wing lift (shown by the open arrow) is not changed, but the hydrodynamic lift (solid arrow) is decreased, due to shortening of the wetted area from L to L_1. The excess of the weight W over the lift forces $\sum Z$ imparts a downward acceleration to the seaplane. Figure 21(c) shows the reverse conditions, occurring when the height of the C.G. over water is decreased by Δh, causing increase of the wetted length from L to L_2. Now $\sum Z$ is larger than W, and the seaplane receives an upward acceleration. The oscillatory motion produced by these alternating unbalances of forces and moments is damped by the forces on wings and the hull resulting from the velocity of the motion. The final motion is defined by the equation:

$$\frac{d^2z}{dt^2} + Z_w \frac{dz}{dt} + Z_z z = 0 \qquad (21)$$

where: z is the vertical coordinate of the center of gravity.

t - time

Z - the resultant of all vertical forces, referred to the unit of mass.

$Z_w = \partial Z/\partial w$ - the rate of change of the force Z with the vertical velocity w, i.e. the damping in heave.

$Z_z = \partial Z/\partial z$ - rate of change of the force Z with the vertical displacement, due to the change of the wetted length and the displacement.

Similarly, Figure 22 shows the changes in the balance of moments. The middle sketch (b) shows the seaplane in the balanced condition in steady planing with $\sum M = 0$, the upper sketch (a) shows it with the angle of trim decreased, and the lower sketch (c) with the angle of trim increased. In the first case the wetted length is increased from L to L_1, and the vector of the water pressure is moved forward from the distance p forward of the step to p_1. As the seaplane is usually stable aerodynamically, the resultant air force is also moved forward. Both are producing now the positive pitching moment restoring the original trim. In the second case, with the angle of trim increased, the wetted length

is decreased from L to L_2, and both the hydrodynamic and aerodynamic force vectors are displaced aft, producing the diving moment. The resultant oscillatory motion is defined by the equation:

$$d^2\theta/dt^2 + M_q\, d\theta/dt + M_\theta\theta = 0 \qquad (22)$$

where: θ is the angular coordinate, such as the angle of trim, or the angle of attack of the wings.

$M_q = \partial M/\partial q$ - is the damping moment produced by the angular velocity in pitch q, mostly due to the aerodynamic action of tail surfaces.

$M_\theta = \partial M/\partial \theta$ - rate of change of the pitching moment with the attitude. This consists of two parts: aerodynamic $dM_a/d\alpha$ and hydrodynamic $dM_h/d\tau$, where M_a is the moment due to the air forces, M_h is the moment of all water forces, α is the angle of attack of wings, and τ is the angle of trim of the hull.

M - total pitching moment due to aerodynamic structure and the hull, referred to the unit moment of inertia.

The coefficients Z_w and M_q are always negative and represent the damping forces, while the coefficients Z_z and M_θ, also negative, represent the restoring forces. The damped system possessing the static stability is evidently stable in the sense that the effect of any accidental disturbance decays with time. Therefore, taken by themselves, the motions described by Equations (21) and (22) are stable, and towing tank tests demonstrated that porpoising does not occur if the model is free to move in heave or in pitch alone. However, it is clear from Figure 21 that a motion in heave produces also pitching moment due to the displacement of the hydrodynamic force vector with the change of the wetted length. Thus the upward displacement $+\Delta h$ is accompanied by the aft movement of the resultant water force, and therefore by the negative pitching moment. Likewise from Figure 22 it is clear that pitching motion produces changes in the vertical forces -- for instance, the reduction of τ means also the reduction in α, and therefore the reduction of the wing lift. Therefore, the motions in pitch and in heave are not independent, and the complete motion is not described by the independent equations (.21) and (.22), but by the equations which include also the "cross coupling

terms":

$$d^2z/dt^2 + Z_w\, dz/dt + Z_z z + Z_q\, d\theta/dt + Z_\theta \theta = 0$$

$$d^2\theta/dt^2 + M_q\, d\theta/dt + M_\theta \theta + M_w\, dz/dt + M_z z = 0 \qquad (23)$$

where the cross coupling terms are:

$Z_q = \partial Z/\partial q$ is the rate of change of the vertical force with angular velocity.

$Z_\theta = \partial Z/\partial \theta$ rate of change of the vertical force with the angle of pitch.

$M_w = \partial M/\partial w$ rate of change of the pitching moment with vertical translational velocity w.

$M_z = \partial M/\partial z$ rate of change of the pitching moment with the heave.

Since the porpoising motion is described by the solution of simultaneous equations (23), the heaving and pitching motions occur simultaneously and with the same period, although not in the same phase. The complete solution of the pair of simultaneous differential equations (23) takes the form

$$z = Ae^{i\sigma_1 t} + Be^{i\sigma_2 t} + Ce^{i\sigma_3 t} + De^{i\sigma_4 t}$$

(with similar equation for θ)

expressing the vertical coordinate z as a function of time, of a certain set of magnitudes σ_1, σ_2, σ_3 and σ_4 which depend on the hydrodynamic and aerodynamic properties of the seaplane and indicate the rate at which oscillations increase or decay, and of coefficients A, B, C and D dependent on the initial conditions. The solution in this form is very cumbersome, and is of little interest in the study of porpoising, since the interest lies in avoiding the oscillations, rather than in the study of their properties. What is desired is to find the conditions at which the accidentally introduced disturbances with decay, i.e. the conditions at which all σ's become negative. This condition is indicated by a simpler form of solution known as "Routh's Criterion", which merely indicates whether the motion is a stable one or unstable, i.e. whether oscillations caused by an accidental disturbance decay or in-

crease with time.

It has been shown (Ref. 22) that accelerations and forces in the direction of planing can be neglected, and they are not represented therefore in the system of equations 23. There are nevertheless 8 stability derivatives to determine the combined pitching and heaving motion, and most of these are composed of aerodynamic and hydrodynamic effects, the relative contribution of which varies with speed during the take-off run. The difficulty in visualizing the aggregate effect of so many parameters, the uncertainty in evaluating the derivatives, and the labor involved in applying the above theoretical method prevented the use of this theory in the practical design work, and limited it to improving the understanding of the porpoising phenomenon, although stopping far short of making it clear. This being the case, the subject will not be pursued further, and merely the references will be cited: (22) and (23) for the basic theory, (24) and (25) for certain applications and experimental verifications, and (26) for the excellent experimental study of the effect of each of the derivatives, and of the certain hull proportions, varied one at a time. Reference (26) and a similar to it unpublished work of Sottorf indicate that characteristics of the hull itself strongly predominate over aerodynamic characteristics of a seaplane, and that aerodynamic changes within the limits permissible in practice have little effect. Of these the changes of the damping characteristics of tail surfaces are most important. Changes of the wing lift, however, produce changes of the hull loading Δ, which is an important parameter in the hull action.

Reference to Figure 22 and to Equations (17 and 18) shows that as the angle of trim is decreased for a given load and speed, the wetted length $L = \lambda B$ gets larger, the movement of the force vector increases, thereby increasing pitching moments, and the derivatives M_θ and M_z increase. The damping moment derivative M_q on the other hand depends mostly on the tail surfaces of the seaplane and on the conditions at the spray root of the planing bottom, and vary but little with the trim angle. As the trim is decreased, therefore, sooner or later the point is reached when the planing ceases to be steady, and spontaneous oscillations develop. The trim at which these oscillations

acquire the total ($\pm$) amplitude of 2 degrees is known as "the lower limit" of stability. Since for any given seaplane it depends primarily on the wetted length, which in turn depends on the speed and loading, the most consistent graphical representation is obtained by plotting the trim at the lower limit against the parameter :

$$\sqrt{C_\Delta}/C_V = \sqrt{\frac{\Delta}{\rho V^2 B^2}} = f(\tau, \lambda) \qquad (24)$$

Reference to Eq. 18 shows that for any particular angle τ the parameter (.24) defines the λ, i.e. the ratio of the wetted length to beam. The plot of the lower limit is shown by two lowermost curves in the lower section of Figure 17, which is also used for plotting of the drag data in the planing range.

4.2 Porpoising in Two-Step Planing at High Speed

In the previous article the planing on the forebody alone was considered. Figures 23 and 24 show the effect of the heave and pitch respectively on the seaplane planing on two steps. In each case the middle diagram (b) shows the steady planing when $Z = 0$ and $M = 0$, and the moments of hydrodynamic forces acting on the forebody are balanced by those acting on the afterbody. Since the hydrodynamic lift is produced by the downward deflection of water, the depth of the wave depends on the forebody load. The decrease in the draft, i.e. the upward heave, as shown on Figure 23, reduces the hydrodynamic force on the forebody, the resultant wake depth η becomes smaller, and the wetted length and the force on the afterbody are increased. In extreme case, when the forebody keel at the step just leaves the water, the wake disappears, and the afterbody meets the full impact of the undeflected water. While the total force $\sum Z$ is decreased with elevation of the center of gravity, and the net force $W - \sum Z$ gives the downward acceleration, the powerful diving moment is simultaneously generated, i.e. the cross coupling derivative $M_z = \partial M/\partial z$ becomes extremely powerful. The oscillatory pitching motion here is only partly due to the shifting of the resultant force on the forebody, but is primarily

due to the variation in the magnitude of the afterbody force. In heave oscillations it is the see-saw effect of the force increment acting alternatively on the forebody and the afterbody, which produces the pitching moment, and the cross coupling derivative M_z. While pitching moments are large, the actual angular motion is often not large, because of the long distance between the forebody and the second step. Furthermore, changes of the wetted length and of the angle of incidence of water impinging on the afterbody are not only due to changes in trim, but to the larger extent are due to changes of the wave depth η in the wake.

The oscillatory motion in two-step planing occurs in the region of the hump speed, where the plot representing it blends gradually into the low-limit porpoising curve, as the stern leaves the water surface with increase of the speed. It is seldom important in this region. It occurs again at the speed somewhat above the hump speed and up to the getaway speed, when the angle of trim is increased sufficiently to produce the two-step planing. In this region it is known as the "upper limit porpoising, trim increasing". If the upper limit porpoising occurred as the result of the increasing trim, and the attempt is made to stop it by decrease of the trim, the oscillations often will stop only at a much lower trim than the one needed to start it. The resultant new limit is known as "upper limit, trim decreasing", or as the "secondary upper limit". The region between these two limits is one of the potential instability: a steady planing is possible, but sufficient disturbance will produce sustained oscillations. This is important because such a disturbance is actually produced on the landing at a higher angle of trim, followed by the nose-down pitching motion towards the lower trim of steady planing.

4.3 Experimental Technique

In the absence of a theory sufficiently developed for the practical use, the designer can get the estimate of porpoising characteristics of a new design only from model tests. While testing a hull model for the resistance, it can be made to run steadily by the use of sufficient damping in pitch, which may be anywhere from 5 to 80 times

that produced by the tail surfaces of an actual airplane. The presence or absence of oscillation in such a model, with or without the damping, has no relation whatsoever to the oscillation of the complete airplane, since aerodynamic effects and moments of inertia are not represented correctly to scale. For predicting porpoising characteristics, not only the model of the hull should be correctly scaled down in dimensions to the scale λ, and the weight to the scale λ^3, but the aerodynamic structure must be correctly represented in the slope of the lift curve $dC_L/d\alpha$, the maximum lift coefficient $C_{Lmax.}$, the slope of the pitching moment curve $dC_m/d\alpha$, and the damping in pitch dC_m/dq. The moment of inertia in pitch also must be correct to scale λ^5, since the mass is scaled as λ^3, and the radius of gyration squared as λ^2. Three types of testing of such "dynamically similar" models are now in use in the U.S.A.:

a. Complete radio-controlled model, powered with gasoline engines, as used by Convair under guidance of Ernest G. Stout (Ref. 27 and 27a).

b. Complete model, without power, or with the power derived from electric motors, used in a large towing tank, the carriage of which restricts the model in roll and in yaw, and sometimes controls its forward velocity, while leaving it free for all motions in pitch and heave. This method, originated by L. P. Coombes in England (Ref. 28), was developed and used in the U.S.A. by the N.A.C.A. under the guidance of Starr Truscott and John B. Parkinson (Ref. 29).

c. The model of the hull only is correctly represented in its geometry, with the weight and the moment of inertia corresponding to the complete seaplane. The effect of wings is represented by suitably arranged hydrovane or by a spring counterbalance, and the aerodynamic damping moment is represented by the properly calibrated dashpot. This method, permitting the use

of smaller and simpler models, has been developed by Dr. K. S. M. Davidson, F. W. S. Locke, Jr. and W. C. Hugli, Jr., and is used by the Experimental Towing Tank of the Stevens Institute of Technology (Ref. 26).

In all of the above methods the model is made to plane at a series of speeds covering the complete range from the hump to the getaway speed, and a series of trims covering the range between the upper and the lower limits of stability. In the methods (a) and (b) above, the trim is controlled by elevators, while in (c) by application of the equivalent pitching moment by means of a calibrated spring incorporated in the test apparatus. The test data are expressed by means of four curves shown on Figure 17:

a. Free-to-trim track, i.e. the plot of the angles of trim assumed by the model with zero applied moment, or the elevator in the neutral position. This is sometimes supplemented by a similar curve with applied stalling or diving moments, or with displaced elevators.

b. The lower-limit curve, i.e. the curve of the lowest trim at which the amplitude of oscillations does not exceed 2 degrees.

c. The upper limit, trim increasing.

d. The upper limit, trim decreasing (the secondary upper limit).

The free-to-trim angles may be found not to correspond to the angles of least resistance and good spray characteristics, or may come too close to the stability limits. Since the aerodynamic configuration is determined and controlled by flight conditions, it is not practical to change it to correct the free-to-trim track. This is done by shifting the position of the step with respect to the center of gravity, either bodily or by modifying the shape of it. Thus, introduction of the Vee step may move the centroid of the step forward, while leaving

the structure at the keel unchanged. Moving the step forward will raise, and moving it aft will lower the free-to-trim track. In this way, it can be readily adjusted to the desired position within the stable region between stability limits. The designer has very little control over the lower stability limit, which is determined primarily by the relation of the load and speed, and therefore is well represented by the plot of τ vs. $\sqrt{C_\Delta}/C_v$, as explained above. Any decrease of the load for a given speed will lower the lower limit, any increase of the load will raise it. Since the load on water is equal to the weight, less the lift of wings, the same float may exhibit porpoising within usable range of trim angles when installed on a heavy airplane with small wing area, and may be free of porpoising when used on a lighter airplane of lighter wing loading, in which case the lower limit may be lowered below the trim angles likely to be actually used in practice. The expression $\sqrt{C_\Delta}/C_v$ is a measure of the wetted length for any particular angle of trim. Anything decreasing the lift coefficient C_L will raise the lower trim track, usually raising the free-to-trim track at the same time. Thus, for example, the increase of the deadrise will raise simultaneously the lower limit, and the free-to-trim track.

The above remarks refer specifically to the part of the lower limit curve in which the hull planes on the forebody alone. Both the theory and experiments indicate that in this region the afterbody has no effect on the motion. In the region of the hump the lower limit curve is due to two-step planing. In this region the speed is low, there is practically no way to increase the hydrodynamic forces over the amount needed to support the seaplane, and therefore the propoising of significant amount does not develop. The critical point is the one of somewhat higher speed, when the second step leaves water, and the planing on the forebody alone begins.

The upper-limit porpoising occurs due to interaction of the forebody and afterbody at a higher speed, where the planing is possible either on two steps, or on the forebody alone. Figuratively speaking, it is the objection of the hull to being forced to plane on two steps, when the planing on the forebody alone is possible. The upper limit depends, therefore, on the design of the afterbody. Any measure, such

as the reduction of the sternpost angle, or the increase of the afterbody length, which tends to bring the afterbody into contact with the wave in the wake of the forebody at the lower angle of trim, also lowers the upper limit, and thereby reduces the stable range between the upper and lower stability limits. Conversely, the increase of the sternpost angle, and shortening of the afterbody increase the angle at which the second step touches water, and also raise the upper limit. This discussion is valid for the hulls of the normal design, and cannot be applied directly to the planing-tail hulls, on which no sufficient test data is available.

The bulk of the published test data refers to specific designs, and in the absence of the unifying theory the basic test data are not sufficient to form quantitative relations. The above discussion is given to help the designer to foresee the probable effect of changes in the loading, speed and geometry when laying out a new design starting from a known prototype. Care should be exercised to use the significant design parameters, rather than accidental drawing reference data. Thus the increase of the warp, i.e. of the rate of increase of the deadrise from the step to the bow, is approximately equivalent to the upward rotation of the original bottom with respect to the design reference line. The test data based on this reference line evidently will show the lowering of the lower limit, and simultaneous lowering of the free-to-trim track. On the other hand it will represent the effective increase of the sternpost angle, and therefore can be expected to raise the upper limit, at the same time raising the trim angle and the resistance at the hump speed. The warp of the afterbody, i.e. the increase of the afterbody deadrise with the distance aft of the step will primarily have the same effect as the increase of the sternpost angle, with only secondary effect due to the deadrise itself.

The high-limit porpoising is also affected by the depth and ventilation of the step. Deep step raises the upper limit, shallow step lowers it. The step ventilation added to the shallow step acts as the increase of the step depth, and raised the upper limit, i.e. widens the stable range between the upper and lower limits. To be effective the ventilating ducts must deliver the air near the keel at step, and must

have the sectional area of about .02(beam)^2. This is the measure used sometimes to improve the hull when major redesign of the structure is not practical.

4.4 Landing and Skipping

The term "skipping" is applied to describe the phenomenon of the seaplane leaving water upon landing, or bouncing even after a good landing. From one to several skips may occur in landing. The skipping may be manifested also in take-off as a jump take off, rather than smooth transition from the water borne planing to the air borne flight. To quote from Reference (30): "Skipping is associated with conditions whereby the forebody carries most of the water borne load and at the same time a large amount of water is washing over the afterbody bottom".

Prior to the contact with water, there exists the established air flow over the forebody, step and afterbody. At the instant of the contact this flow of air is interrupted at the step, while the inertia of the air moving along the afterbody, and the entrainment of this air by the water moving in close proximity to the afterbody generate the suction. The suction force distributed over the large area of the afterbody produces the downward force and the stalling moment. The downward force causes greater submergence, and brings into action greater wetted area than is required to support the small part of the seaplane weight which is not supported by wings. Subsequently, the water surface in the rapidly developing wake is deflected downwards, greater clearance is created under the afterbody, and the suction is broken. The excessive lift of the forebody, caused by the excessive submergence, as well as by the increase of the trim, accelerates the seaplane upwards, throwing it out of water. These events occur in such a rapid sequence that the period of time from the first contact with water to the emergence from it is a fraction of a second for a dynamic model, and is found to be about one second in a certain 8000 pound flying boat (Reference 31).

The primary remedy against skipping is the adequate ventilation of the step, which is achieved best by making it deep enough. For a given hull loading, and a given sternpost angle, the step height needed

for, and sufficient to prevent skipping must be such that the ratio (step height in % of beam)/(sternpost angle in degrees) plotted against the load coefficient C_{Δ_0} will fall between two oblique lines of Figure 25. The hull exhibiting unsatisfactory skipping characteristics due to the insufficient depth of step may be corrected by addition of the ventilating ducts extending from the keel to not over half beam in breadth, and having the sectional area of about $.02(\text{beam})^2$. The supply of air is needed instantaneously at the time of the contact with water, and therefore it is not necessary to extend ducts through the deck, but is sufficient to have them open to the interior of the hull. It is important however to guard against any constriction, or other impediment to the air flow, which is large for an instant of time.

The skipping is tested for in towing tanks by using dynamic models, and simulating the landing by means of gradual deceleration of the towing carriage. In simpler tests the number of skips is noted, in more complete research, the entire time history of the pitching and heaving motions is recorded by suitable instruments. The landings are made at a number of trims, the number of skips usually increasing with increase of the trim angle.

5. Directional Stability and Control

The directional characteristics of Seaplanes are considered under two headings:

a. Directional control in taxiing.

b. Directional stability during take off.

At the low speed of taxiing the hull is acting as a displacement vessel, with rather deep draft in forebody sections, and a small draft and small side area of the submerged portion at the stern. In case of a small yaw, say due to side wind, the resultant reaction of water acts forward of the center of gravity, increasing the initial yaw, i.e. making the hull unstable in yaw. Due to the presence of the vertical tail surface the side wind force acts aft of the center of gravity. Thus the couple formed by the side wind force and the water reaction tends to turn the seaplane into the wind, i.e. makes it "weathercock". At the low speed

and the small engine power used for taxiing the air velocity over the rudder is small, and the rudder often does not have sufficient power to overcome this weathercocking couple. In order to gain the necessary control under these conditions, the single engine seaplanes are usually equipped with water rudders placed at the stern of the float, or aft of the second step of the flying boat. The area of the rudder should be equal approximately to 4% of the side area of the submerged part of the hull or float, and the rudder should extend as far as possible into the undisturbed water, i.e., appreciable area of it should be placed below the afterbody keel. The rudders of small height located at water surface, and rudders located wholly in the wake of the stern are not efficient. The multi-engine flying boats usually depend on the unbalanced engine thrust, and are not equipped with rudders. The engine thrust may be controlled by manipulation of throttles, but greatly superior control is obtained by the use of reversible pitch propellers.

The stability of the hull during take-off run is easily tested in the towing tank by placing the model at the angle of yaw Ψ, and measuring the yawing moment acting on it by means of the calibrated spring. The moment coefficient C_{M_Ψ} is defined as M_Ψ/wb^4, where M_Ψ is the yawing moment in pound-foot units at the angle of yaw Ψ, w - weight of water per cubic foot and b - the beam in feet. The moment coefficient is plotted against the yaw angle, as shown on Figures 26, 27 and 28. Figure 26 shows the conditions of a certain flying boat at $C_v = 1.04$, at which the hull is in displacement condition, as shown by the small values of trim τ and the negative value of the heave coefficient h/b. As was described above, the hull is distinctly unstable in this condition, and this is shown by the positive slope of the moment coefficient curve. Figure 27 refers to the higher speed at $C_v = 2.17$. This is still far from the planing condition, but the dynamic forces are sufficient to cause certain increase of the heave coefficient h/b and the angle of trim τ. The fin area forward of the center of gravity is thereby reduced, and that at the stern is increased. The negative slope of the curve in the range $\Psi = \pm 2^\circ$ indicates the positive stability, and outside of this limited range the stability is essentially neutral. Figure 28 at a slightly higher speed with $C_v = 2.33$

illustrates the condition termed "hooking instability". There are two stable branches of the curve at the yaw larger than 3 degrees, with a highly unstable range between. It appears that this small increase of the speed changed the conditions of the wake at the second step, reducing the effective fin area at stern, and making the second step to plane in a middle of a wave hollow in the unstable condition. A small yaw brings the stern into contact with sides of the hollow, opposing further increase of the yaw, i.e. producing a stable branch of the curve on the plot. Three plots of test data discussed above illustrate the complex conditions governing the directional stability of the flying boat in the pre-hump region: they start at low speed with the natural instability of a displacement vessel, are modified by changes of trim as the speed increases, and then become dependent on the shape of the wake, which is rapidly changing with the speed and in the process of transition from the displacement to the planing condition. The conditions producing instability are further aggravated by details of the water flow at the stern of the boat, particularly by the suction generated at any convex curved surface. At a pre-hump speed large areas on the sides of the boat at stern are wetted. The curvature of these sides in the plan view of a pointed second step produces suction forces which often cause large unstable yawing moments to appear. Likewise, the water flow clinging to the rounded tail cone aft of the second step is the frequent cause of instability.

The seaplane float has a simpler shape than a typical flying-boat hull, has much smaller area of sides near stern, and has no structure to interfere with water aft of the second step. The difficulties with the directional stability in float seaplanes therefore occur but seldom.

In a flying boat the difficulties due to directional instability are confined to the "displacement" or the "pre-hump" region. At the planing speed the wetted area forward of C.G. is small, the aerodynamic stability is significant, and with the increase of speed, and the slip stream of the propeller, the rudder acquires ample power for the control.

The above discussion points to the nature of the problem of the directional stability, and to the towing tank tests by means of which the

stability can be measured, and quantitatively described. No criterion exists, however, to indicate whether the degree of the instability of the particular model is acceptable for the practical use or not. The behavior of the actual flying boat, the model of which gave the plots illustrated by Figures 26, 27 and 28, is described by the following quotation from Reference (32): ". . . . at speeds below the hump constant attention must be given to keep the flying boat headed very close to the course, and unbalanced power must be applied rapidly to check any deviation from the course. If corrective moment is not applied rapidly to check the first sign of yawing, the boat may become unmanageable. Cross-wind taxiing may be very nearly impossible, even with maximum unbalanced power."

6. Spray

Reference to Figure 14 shows that at a certain speed between the start of the take-off run and the hump speed, such as about 10 ft./sec. in this case, there is hardly any change in the draft, and only a small change in trim, yet the resistance is already about 2/3 of the maximum. The water surface meets the hull bottom not far aft of the bow at large angles of incidence, producing high local pressures. These pressures cause some of the water to flow in a thin sheet along the bottom of the hull in the outward and aft directions. This sheet of water breaks away at the chine, forming the spray blister . In a small model this blister has the form of a dome of thin water sheet, on a full-size hull the sheet breaks into a mass of water drops without changing the general form of the blister. Figure 29 shows the contour map of a typical spray blister. In a flying boat the spray interferes with propellers, and impinges on wing flaps, often causing structural damage. The spray therefore is one of the important factors determing the seaworthiness of the boat, and the experimental quantitative measurement of it represents an important phase of the towing tank testing. For this prupose the grid of the vertical and horizontal lines is painted on the side of the hull, and the side view of the spray is photographed against this grid. Simultaneously the photographs of the plan and front views are also taken. When the spray blister contours for several

speeds of the seaplane are superimposed, the conical surface can be drawn tangent to all blisters, i.e. enveloping all individual blister plots. The points of tangency of the blister to this envelope for each speed is defined by dimensions X, Y and Z, as shown on Fig. 29 . For the beam of the hull b, the coefficients are defined (Ref. 33 and 34):

Longitudinal Spray Coefficient	$C_x = X/b$
Lateral Spray Coefficient	$C_y = Y/b$
Vertical Spray Coefficient	$C_z = Z/b$

Since the spray can be considered as a form of the wave, these coefficients can be presumed to be functions of the Froude Number, and can be plotted against $V^2/g \times (\text{submerged Volume})^{1/3}$, or using N.A.C.A. coefficients $C_v^2/C_\Delta^{1/3}$. Furthermore the use of coefficients X/b, Y/b and Z/b would be sufficient for the hulls differing in size but of geometrically similar form. To make coefficients applicable to hulls of the different length/beam ratio, they are divided by functions of C_Δ, finally expressing the relationships to be plotted as:

$$C_x/C_\Delta^{1/3} = \Phi_1 (C_v^2/C_\Delta^{1/3})$$

$$C_y/C_\Delta^{1/3} = \Phi_2 (C_v^2/C_\Delta^{1/3})$$

$$C_z/C_\Delta^{1/3} = \Phi_3 (C_v^2/C_\Delta^{1/3})$$

The plot of the first of these relationships, defining C_x, is shown on Fig. 30 . It is observed that spray characteristics for a wide range of loadings for a flying-boat hull are well represented by a single curve. Equally good agreement is shown in Reference (34) for second and third relationships, defining C_y and C_z. Three curves describing the height and position of the spray blister are therefore included in the summary sheet of hull characteristics, as shown by the upper section of Fig. 17.

At speeds above the hump, the bow sections of the hull are clear of water, and the spray coming off the main planing bottom is located further aft, and is of low height, so that it does not strike any part of the seaplane, and therefore is of no interest to the designer.

The spray described above is usually referred to as the "main spray". In addition to this the bow spray has to be considered. At very low speed, say about 5 ft./sec. on Figure 14, both the heave and the pitch are below these of the static flotation. The hull settled in water, and trimmed by the bow. This causes water at the bow either to break into spray, or to envelope the bow in a thin sheet of water clinging to the surface, eventually breakijg into spray at the upper part of the hull bow. These conditions are very much aggravated during operation in waves, when the bow plunges into the oncoming wave. The bow spray is important in that it wets the windshield, thereby temporarily obscuring pilot's vision, and also leaves the deposit of salt, thus impairing the visibility for the entire duration of flight. In single engine, twin float seaplanes the bow spray of floats is primarily responsible for the wear of the propeller.

The bow spray in calm water and in waves is studied in towing tanks, and results are reported qualitatively by a series of photographs. Extensive study of the bow spray, as it is affected by the bow shape, is given in Reference (35). Quoting from this reference: ". . . . the height and the volume of spray at the windshield can be reduced by (1) increasing the hull length and especially the forebody length, (2) increasing the "sharpness" of the bow lines below the chine, (3) increasing the static trim when the bow form is such that relatively bad spray otherwise occurs, and (4) decreasing the waterborne load. These changes are listed approximately in the order of their importance from the point of view of reducing spray". As a corollary to the item (3) above, the piloting technique for reducing the bow spray calls for the use of the full-up elevator at the start as the throttle is opened until the bow comes up, or for the entire duration of the low-speed taxiing. Moreover the taxiing at the speed of the bad spray should be reduced to the minimum; it is usually possible to taxi at either lower or higher speed.

7. Impact

7.1 Introduction, Statement of the Problem

When a seaplane makes a perfect landing on smooth water, the series of events are similar to the ones occurring during take-off, but

taken in the reverse order: after flare-out of the glide, the velocity becomes practically tangential to the water surface, which is penetrated without any shock. With engines throttled the seaplane decelerates under action of the air and water drag, and, as the speed is decreased, the hull wetted area and the angle of trim increase, with constant increase of the drag. The hump speed, i.e. the speed of the maximum resistance is reached, after which the planing ceases, and the seaplane settles to the displacement phase, and finally to static flotation. Often, however, the flare-out of the glide is far from being perfect, and the flight path at the instant of the contact with the water surface is inclined at the angle γ_0, as this is shown on Figure 31. It is convenient to trace the subsequent motion of the seaplane by reference to the keel at step - point 0 on Figure 31. This motion is shown on Figure 32(a). The downward component of the velocity is gradually decreased by the reaction of water, then is reversed in sign accelerating the seaplane upward till it leaves the water at a certain point P. The water reaction is shown on Figure 32(b). At the point of entry 0 the velocity is high, but the wetted area is nil. Subsequently a point is reached where the remaining velocity and the wetted area of the bottom are such that maximum reaction is produced, and finally the reaction becomes zero again at the point of exit P. The maximum reaction usually occurs somewhat before the maximum draft is reached, and before the chine becomes wetted. Indeed, in the case of the flying boats the entire cycle of the impact-rebound often occurs without wetting of chines, so that in theoretical study it is possible to assume a Vee shape of infinite width. Furthermore the duration of time from the entry to exit is so short that angle of trim does not change appreciably, and in theoretical studies the constant angle of trim τ is assumed. Thus the conditions preceding the impact can be described by three parameters: velocity V_o, the glide path angle γ_0, and the angle of trim τ. Here the subscript zero indicates conditions at the first contact with water, both V and γ varying subsequently under the action of water forces, while τ remains sensibly constant.

Since the force of the impact determines the strength which the hull must possess, the theoretical and experimental study of it re-

ceived a good deal of attention, beginning with the work of G. H. Bottomley, Reference (36). This study has three basic objectives:

a. The determination of the total force of the water reaction, and of its variation with the time and submergence.

b. The intensity of the water pressure on the bottom plating and its distribution.

c. The effect of elasticity in the structure connecting the planing bottom with the masses of the seaplane.

Theoretical and experimental studies of the impact establish the form of relationship between the impact force, three approach parameters mentioned above, the mass of the seaplane and such parameters of its shape as the deadrise β or the curvature of the bottom. The actual magnitude of impact forces, however, is determined by magnitudes of the parameters occurring in practice. The frequency of the occurrence of different magnitudes of parameters is determined statistically from the analysis of the operational practice. Furthermore it is always possible to imagine conditions severe enough to break any seaplane hull. The most unfavorable combination of the parameters, indicating the maximum strength to be provided in the hull, is limited, therefore by the weight which can be tolerated in the aircraft. The final outcome of all these considerations takes the form of regulations established by the Bureau of Aeronautics for the seaplanes procured by the U. S. Navy, or by the Civil Aeronautics Board for the seaplanes to be licensed for civilian uses. The object of this chapter, therefore, is to give the reader the understanding of the phenomena of the impact, and to improve thereby his ability to interpret and to supplement the regulations, rather than to give any direct design data or instructions.

7.2 Theory and Tests Pertaining to the Impact in Smooth Water

Theory of the impact of the wedge dropped onto water vertically was originated by Th. von Karman - Ref. (37) - who established the concept that momentum of the wedge plus the momentum of the added mass of entrained water must be equal at all times to the initial momentum

of the wedge, i.e.:

$$MV_o = MV + mV \qquad (25)$$

where: M - mass of the wedge.

m - added mass of the entrained water.

V_o - velocity of the wedge at the instant of the contact.

V - vertical velocity of the wedge at any instant during immersion.

The movement of a body in the fluid causes various fluid particles to move in many paths with various velocities and various momenta. It is possible to imagine a certain mass of the fluid as moving with the same velocity as the body, and possessing the momentum equal to the sum of momenta of all fluid particles involved. Such a hypothetical mass of the fluid is known as the "additional mass". In case of the fluid flowing around a flat strip of a certain width 2C and of infinite length, the additional mass is shown by the hydrodynamic theory to be equal to the mass of the cylinder of the diameter 2C, i.e. $m = \rho\pi C^2$, where ρ is the mass density of the fluid, in this case of water. The case of the wedge penetrating the water surface - as on Figure 33(a) - was compared by Th. von Karman to the flat plate having water on one side of it, i.e. was associated with additional mass of water equal to one half of the cylinder, or $\rho\pi C^2/2$. In the process of immersion of the wedge the half breadth C is continuously increasing, and the additional mass m is also continuously increasing, so that both V and m in Equation 25 are considered as variables.

Using the concept of virtual mass described above, equations of motion will be developed defining the impact process for the case of a vertical drop of an infinitely long prismatic section at zero trim angle. For this condition of vertical drop the fluid flow over the bottom is of a two-dimensional nature and the flow can be considered as being in planes normal to the keel.

Two-Dimensional Case

The action of a unit slice of the wedge and a unit slice of the fluid is considered herein. The momentum of the fluid is equal to the product of the "additional mass" m and the instantaneous velocity

of the float $\dot{z}$. The impact force is equal to the time rate of change of the momentum. The displacements, velocities, and accelerations are considered positive downward, and the effects of buoyancy and viscosity are assumed negligible. Also, it is assumed that the wedge has a 1 g lift force acting on it which corresponds to the wing lift of an actual seaplane hull.

$$F = \frac{d}{dt}(m\dot{z}) = m\ddot{z} + \dot{m}\dot{z}$$

also: $F = -M\ddot{z}$

Therefore: $M\ddot{z} + m\ddot{z} + \dot{m}\dot{z} = 0$ (26)

Let $m = Kz^2$

$\dot{m} = 2Kz\dot{z} = \frac{2m\dot{z}}{z}$ (26a)

Substituting for $\dot{m}$ and dividing by M:

$$\ddot{z}\left(1 + \frac{m}{M}\right) + \frac{2\frac{m}{M}\dot{z}^2}{z} = 0$$

Let $\frac{m}{M} = R$

$$\ddot{z}(1+R) + \frac{2R\dot{z}^2}{z} = 0 \qquad (26b)$$

This equation defines $\ddot{z}$ in terms of the unknown instantaneous values of $\dot{z}$ and z. The analysis will now proceed with an evaluation of the relation between $\dot{z}$ and z.

From (26a):

$$\frac{dR}{dt} = \frac{2R\dot{z}}{z}$$

$$R = \frac{dR}{2dt}\frac{z}{\dot{z}}$$

Thus Eq (26b) becomes:

$$\frac{d\dot{z}}{dt}(1+R) + \frac{z}{z}\frac{dR}{dt}\frac{z}{\dot{z}}\frac{1}{z}\dot{z}^2 = 0$$

$$\frac{d\dot{z}}{\dot{z}} + \frac{dR}{(1+R)} = 0 \qquad (26c)$$

Now integrating:

$$\log \dot{z} + \log (1 + R) = \log c$$

To solve for the constant of integration, substitute the conditions just prior to impact:

$$t = 0;\ z = 0;\ R = 0;\ \dot{z} = \dot{z}_o = \text{initial contact velocity.}$$

Thus: $\log \dot{z}_o = \log c$

and $$\dot{z} = \frac{\dot{z}_o}{(1 + \frac{m}{M})} = \text{Vertical Velocity} \qquad (26d)$$

Solving the vertical velocity equation for acceleration gives,

$$\ddot{z} = \frac{-2 \frac{m}{M} \dot{z}_o^2}{z(1 + \frac{m}{M})^3} \qquad (27)$$

By differentiating the acceleration equation with respect to z and setting the quantity equal to zero, it can be shown that the maximum acceleration for the two-dimensional case occurs when the ratio $\frac{m}{M} = \frac{1}{5}$.

Although the two-dimensional analysis is of small practical value for design it serves to illustrate the fundamentals of the impact theory and is extremely useful in the development of the three-dimensional case of the more practical case of the oblique impact.

7.3 Three-Dimensional Case of Oblique Impact

In an actual seaplane landing, the hull usually penetrates the water surface with a definite trim angle and with a resultant velocity which is not normal to the keel of the hull. Also, the forebody of the hull has a definite length terminating at the step that results in certain end flow losses at the step which must be considered. The three-dimensional analysis will be made for an ideal prismatic float with no afterbody. The float is assumed to maintain a constant trim

angle and horizontal velocity throughout the impact period. In Figure 34 an ideal float is shown immersed in the water after having travelled alohg a path of motion indicated by the dotted line. Mayo (Ref. 47 & 48) and Benscoter (Ref. 50) applied the two-dimensional theory to the solution of the case of the oblique impact of a Vee shaped surface. The fluid beneath the float is imagined as subdivided into slices of length ds by planes drawn normal to the keel of the float. As the float moves through these slices, the flow in each slice is assumed to be two-dimensional and identical with the flow in the case of the wedge dropped vertically into water as treated in the two-dimensional case. It is necessary to assume that the fluid in each slice is independent of the motions in adjacent slices and that the reaction on the float is due to combined action of all the slices which have a total width equal to the wetted keel length.

Before presenting the analytical solution for the three-dimensional case, two additional factors must be considered -- one concerns the definition of the virtual mass and the other the effect of end losses at the step. von Karman initially defined the added mass m on the basis of the half breadth c of the intersection of the wedge with the undisturbed water level. Herbert Wagner (Ref. 38, 39, 40 and 60) took into account the rise of the water surface near the surface of the wedge and defined the diameter of the semi-cylinder of virtual mass on the basis of deadrise and depth of immersion. Thus, referring to Fig. 33b, the effective diameter 2c is defined by Wagner as follows:

$$c = f(\beta)z$$

$$c = \left(\frac{\pi}{2\beta} - 1\right)z \qquad \beta \text{ in radians.}$$

A correction factor for approximating the three-dimensional condition on the basis of a two-dimensional calculation has been developed by Pabst (Ref. 41), who showed that the correction was a function of the length/beam ratio of the wetted area:

$$g(A) = 1 - \frac{\text{Tan } \tau}{2 \text{ Tan } \beta}$$

As in the two-dimensional case the analysis proceeds with the equation for change of momentum. The fluid in each slice exerts an elemental force f on the bottom:

$$f = \frac{d}{dt}(m\dot{z}) = m\ddot{z} + \dot{m}\dot{z}$$

$$m = \left[f(\beta)\right]^2 \frac{\rho\pi}{2} z^2$$

$$f = \left[f(\beta)\right]^2 g(A) \frac{\rho\pi}{2}\left[z^2\ddot{z} + 2z\dot{z}^2\right]$$

Integrating over the entire float length to obtain the total force F on the bottom:

$$F = \left[f(\beta)\right]^2 g(A) \frac{\rho\pi}{2}\int_0^{z_s/\mathrm{Tan}\tau} (z^2\ddot{z} + 2z\dot{z}^2)\, ds$$

substituting $z = s\tan\tau$

$$F = \left[f(\beta)\right]^2 g(A) \frac{\rho\pi}{2}\int_0^{z_s/\mathrm{Tan}\tau} (s^2\mathrm{Tan}^2\tau\,\ddot{z} + 2s\tan\tau\,\dot{z}^2)\, ds$$

Integrating and letting $F = -\frac{W}{g}\ddot{z}$

$$-\frac{W}{g}\ddot{z} = \left[f(\beta)\right]^2 g(A) \frac{\rho\pi}{2\mathrm{Tan}\tau}\left[\frac{z_s^3\ddot{z}}{3} + z_s^2\dot{z}^2\right] \qquad (27a)$$

which expresses the general relationship that exists among the variables at any time during the impact process.

For convenience in application of the results, the above equation is transformed to a coordinate system relative to the water surface using the following relations (with ref. to Fig. 34):

$$\dot{z} = \dot{x}\sin\tau + \dot{y}\cos\tau$$

$$V_p = \dot{x}\cos\tau - \dot{y}\sin\tau$$

$$\text{or } \dot{z} = \frac{\dot{y}}{\cos\tau} + k$$

$$\text{where } k = V_p \tan\tau$$

also:

$$z_s = \frac{y}{\cos\tau}$$

$$\ddot{z} = \frac{\ddot{y}}{\cos\tau}$$

Substitution of these relations into the general equation result in:

$$-\frac{W}{g}\ddot{y} = \frac{[f(\beta)]^2 g(A)\ \rho\pi}{6\sin\tau\cos^2\tau}\left[y^3\ddot{y} + 3y^2(\dot{y} + k\cos\tau)^2\right]$$

or

$$\left[1 + \left(\frac{\alpha g}{W}\right)y^3\right]\ddot{y} + 3\left(\frac{\alpha g}{W}\right)y^2(\dot{y} + k\cos\tau)^2 = 0$$

where

$$\alpha = \frac{[f(\beta)]^2 g(A)\ \rho\pi}{6\sin\tau\cos^2\tau}$$

(28)

The solution of the above equations for acceleration, velocity and draft has not been carried out analytically but a numerical solution is given in Reference 52. The results presented in Reference 52 are in coefficient form as follows:

$$\text{Draft coefficient} = C_d = yK$$

$$\text{Time coefficient} = C_t = \dot{y}_o tK$$

$$\text{Load factor coefficient} = C_\ell = \frac{n_w g}{y_o^2 K}$$

where

$$K = \left(\frac{g\alpha}{W}\right)^{1/3}$$

y = instantaneous value of draft at step

$\dot{y}_o$ = vertical component of the velocity at first contact with water

$\dot{y}$ = vertical component of the velocity at the instant under consideration, i.e. at the draft y and time t

t = time in seconds from the first contact with water to the instant under consideration

n_w = load factor; i.e., $\ddot{y}/g$

W = weight of seaplane.

The above coefficients are shown in Reference (52) to be functions of the approach parameter K, as defined on Figures 35 to 38. It is noted that approach parameter is a function of the trim angle τ and the glide path angle γ_o. For each value of the approach parameter K the values of coefficients are shown for the instant of maximum acceleration, the instant of the maximum immersion, and in some cases at rebound. All of the above data apply to the float of the uniform, straight Vee cross section throughout the wetted length. The method of using the data for the curved bottom sections is given in Reference (51).

Example: Consider the prismatic float of 22-1/2 degree angle of deadrise, loaded to 1100 pounds, landing with the flight path angle $\gamma_o = 8^\circ$, the angle of trim $\tau = 9^\circ$ and the velocity of 75 feet per second. Assume sea water with $\rho = 64/32.2 = 1.99$

$$\dot{y}_o = V_o \sin \gamma_o = 75 \times .1392 = 10.45 \text{ ft./sec.}$$

$$f(\beta) = \frac{3.14 \times 57.3}{2 \times 22.5} - 1 = 3.0$$

$$g(A) = 1 - \frac{.1584}{2 \times .4142} = .908$$ ← should be 0.808

$$K = \left(\frac{32.2 \times 3.0 \times .908 \times 1.99 \times 3.14}{1100 \times 6 \times .1564 \times .9877}\right)^{1/3} = 1.175$$

$$K = .1564 \times .956/.1392 = 1.08$$ ← should be squared?

At the instant of the maximum acceleration we have from Figures 37 and 38:

$$C_\ell = 1.6 \qquad C_t = .5$$

whence:

Load factor $n_w = 1.6 \times 1.175 \times 10.45^2/32.2 = 6.4$

Time from the moment of the first contact to the instant of the max. acceleration:

$$t = \frac{.5}{1.175 \times 10.45} = .04 \text{ sec.}$$

7.4 Impact Basin

Reference (53) describes the experimental tank constructed at N.A.C.A. laboratories specifically for the impact testing of large models - up to about 2400 pounds displacement. This float or model is attached to the carriage which is accelerated to the proper landing speed by means of a catapult. When the proper speed is reached the float with a certain part of the attaching structure is allowed to drop onto water, either smooth, or on waves as desired. The horizontal speed up to 110 feet per second and the height of drop up to 4 feet are available. The vertical travel of the float, and accelerations resulting from the impact are recorded. References (53) to (57) give results of such impact tests in smooth water on the prismatic float of 22-1/2 deadrise at several angles of trim from -3 to 12 degrees. Reference (52) indicates excellent agreement between these test results and the theoretical data represented by Figures 35 to 38.

7.5 Landing on Waves

In the previous paragraphs the impact of a Vee shape on smooth water was discussed. Figure 39 shows the seaplane landing on waves. All of the data of smooth water landing are applicable in this case, provided the angle of trim τ is measured with respect to that part of the wave surface at which the hull makes contact with water, and $\dot{y}_o$ used in the previous theory is replaced by v_n, which is the component of the velocity taken normal to the water surface, as shown on Figure 39. In a number of landings the contact will be made with a number of points on the wave profile; at certain points the combination of τ and v_n will produce the approach parameter K such that maximum acceleration at the impact will result. This will occur usually for the impacts at

the steepest slope of the wave flank, which varies with the ratio of the wave length to height (for further information on waves see Par. 7.8). By making a large number of tests in a towing tank, in waves of varying length, and with the model landing at random on any part of the wave profile, the curve can be drawn of the maximum impact acceleration vs. wave length. Such a curve is shown on Figure 40. As the wave length is decreased from about 750 feet to 250 feet, the maximum impact acceleration is increased, because the landings are made on progressively steeper slopes of shorter waves. As the wave length is decreased below 250 feet, the impacts become less severe, because the crest of the preceding wave begins to interfere, and the impacts can occur only on the higher points of the wave, where the slope is smaller.

Examination of the Figure 39 shows that in order to avoid a too small, or even a negative angle of trim τ the seaplane must be flown at a large angle of attack with respect to the flight path, and this in turn must be as flat as possible, i.e. γ_0 must be as small as possible. Furthermore the acceleration of the impact is proportional to the square of the speed, and the speed therefore must be as small as possible. All three of these objectives, large angle of attack, small γ_0 and the lowest possible speed, are obtained in a power landings. In these landings sufficient engine power is used to permit seaplane only a very slow rate of descent, while maintaining a very large angle of attack. The effect of the slipstream in this case gives added wing lift, and better elevator control, so that larger angle and lower speed can be obtained than would be possible in a power-off landing. Furthermore, should the seaplane bounce off severely, as it does all too often, sufficient increase of engine power can be quickly obtained to permit a gentle letdown for the next contact.

The bounce often results in the partial loss of control and speed, and the seaplane comes to the second and the subsequent contacts with waves at a steeper and steeper "glide path" angles, and smaller and smaller angle of trim. The conditions cease to correspond to the "step landing" discussed in theory, the resultant force moves towards the bow, and in addition to the vertical force a large nose-up pitching moment is developed. Figure 41 gives the envelopes of the maximum

translational acceleration and the maximum pitching acceleration for the various positions of the force along the hull length between the bow and the step. Excellent time history of the landing process obtained on two dynamic models in the towing tank will be found in Reference (59). Good data on the position of the resultant force will be found in Reference (42). These were obtained on the full-size tests of a Heinkel HE-9a twin-float seaplane.

7.6 Pressures Acting on the Hull Bottom

In the section 7.2 it was explained how Th. von Karman represented the water force acting on the wedge entering water by assuming the wedge to be equivalent to the flat plate of the same wetted width, and using the concept of the "added mass" associated with such a plate. Herbert Wagner (Ref. 38, 39, 40, 60 and 61) also used the concept of the expanding plate, but in addition to determination of the added mass he used the equations of the fluid flow about a plate. He has shown that immersion of the wedge is accompanied by the rise of water level in immediate proximity of the wedge, so that wetted width C becomes $\pi/2$ times the width defined by the intersection of the wedge with undisturbed water, as this is shown on Figure 33 b . The velocity of the fluid at any point of the wedge is obtained from flow equations, and is shown to vary from zero at the keel to the maximum at the chine. Since the velocity at any point is known, the pressures are readily obtained from this theory is shown by dotted lines on Figure 42. The conspicuous part of this diagram is the sharp peak of pressure at the edge of the wetted area, with lower pressures towards keel. When the chines are submerged, and the flow corresponds to the plate of a fixed width, the maximum pressure is at the keel, and corresponds to the stagnation pressure due to the vertical velocity V, i.e. to $\rho V^2/2$. The penetration of the Vee shape is shown to be analogous to the expanding plate, and even at the keel the pressure is shown to be several times higher than above, while the peak pressure now occurs at the edge of the wetted area.

The "expanding plate" theory gave excellent insight into the general pattern of the flow, and into the pressures connected with it. It is evident, however, that conditions at the edge of the wetted area,

point A on Figure 33b, require further study, since the presence of the high pressure peak at the edge of the free surface must cause some form of an intensive local disturbance. H. Wagner applied the term "spray root" to the vicinity of the point A, and developed the mathematical theory (Ref. 60 and 61) representing the fluid flow in this region. If the vertical velocity of the wedge be designated by V, the horizontal velocity v of the point A becomes:

$$v = dC/dt = \pi V/2\tan\beta \quad . \qquad (29)$$

Since the point A moves with velocity v with respect to the undisturbed water, the stagnation pressure at A is:

$$p_{max.} = \rho v^2/2 \quad . \qquad (30)$$

This pressure accelerates the fluid particles along the bottom (forming the spray sheet) to the velocity v with respect to the point A, or approximately 2v with respect to the undisturbed water. The existence of the spray, and of the high pressure peak are shown to be inseparably connected -- one cannot exist without the other. It is demonstrated in Ref. (60) that the same value of the peak pressure is obtained from either the "expanding plate" or the "spray root" theories.

It has been shown in Par. 7.3 and on Fig. 34 that planing of a Vee-shaped surface can be compared to the penetration of the wedge in each of the imaginary vertical slices of water. At the leading edge of the wetted area of the planing surface the "spray root" is formed, with its characteristic pressure peak, and with pressures dropping towards keel. These phenomena cease to exist as the chines become wetted, and all pressures drop to lower values. Figure 44 shows the pressure distribution as measured by Dr. W. Sottorf on a prismatic planing surface of 15 degrees deadrise, planing at the angle of trim of 6 degrees. Figure 45 shows the results of the pressure distribution measurements on a full-size flying boat. Here the regions of the peak pressure and of the reduced pressure aft are approximated by rectangular step diagrams. Figure 46 shows similar pressure distribution for a longer wetted length, with a certain length of the chine forward of step wetted. Reader's attention is called to the fact that these diagrams represent the instantaneous distribution of pressure. They should not be confused with

the diagrams often found in the literature on the subject, showing the maximum pressure occurring at any part of the bottom during a landing, which are the "envelopes" of the instantaneous pressure diagrams.

As the wetted length of the hull changes with the speed and load, the region of the peak pressure, always located at the leading edge of the wetted area, traverses the hull bottom area, so that almost any part of it is subjected to the high local pressure at some time. The bottom plating and stringers supporting a small bottom area must be designed therefore to withstand this high peak pressure. U.S. Navy, Bureau of Aeronautics calls for the yield strength of the plating and stringers of 25 pounds per square inch. The supporting structure, however, will be affected by the average pressure over a certain larger area, and can be designed for somewhat lower pressure.

Equations 29 and 30 show that velocity of the stagnation point A, and therefore the pressure, increase with decrease of the deadrise. Figure 43 shows how the magnitude of the maximum pressure is affected by the transverse shape of the planing bottom. In case of the straight Vee the pressures gradually drop towards the chine, because of the decrease of the vertical velocity with increasing penetration into water. With a slight concavity of the bottom, pressures increase gently towards the chine, because of the decrease of the local deadrise angle. With the deep curvature of the bottom the pressures peak sharply towards the chine.

7.7 Effect of the Elasticity of Supporting Structure

Figure 47 shows diagrammatically the main mass of the seaplane M attached to the mass of the planing bottom M'. Initially both masses have the same vertical velocity V_o, but during the impact the velocities become $\dot{y}$ and $\dot{z}$, using the notation shown on Figure 47. We have now two equations describing the motion: the conservation of momentum, expressed by Equation (25) for the rigid wedge, now becomes (according to Reference 46):

$$(M + M')\, V_o = M\dot{y} + (M' + m)\, \dot{z} \qquad (31)$$

and the force in the structure, or "spring", connecting masses M and M':

$$M\ddot{y} = -k(y - z)$$

where k is the spring constant.

Whilhelm Pabst (Ref. 41), neglecting the mass of the bottom structure M', writes:

$$\left.\begin{aligned} M\,(d^2y/dt^2) &= kf - nW \\ m\,(d^2z/dt^2) &= -kf \\ y - z &= -f \end{aligned}\right\} \quad (32)$$

In writing the above we modified the original notation of Pabst to correspond to the notation already used in Sec. 7.2 of this book. The additional symbols not used before are:

n - the fraction of the weight remaining after deducting the lift of the wings. It is often permissible to take n = 0, i.e. to assume the entire weight to be supported by wings, as indeed it must be just before the impact.

f - the deflection of the spring.

Differentiating twice the last one of Eqs. (32):

$$\frac{d^2y}{dt^2} - \frac{d^2z}{dt^2} = -\frac{d^2f}{dt^2}$$

and substituting from first two Eqs. (32):

$$\frac{d^2f}{dt^2} + kf\left(\frac{1}{M} + \frac{1}{m}\right) - ng = 0 \qquad (33)$$

the solution of this differential equation is:

$$\left.\begin{aligned} f &= A \sin \omega t + B \cos \omega t + ng/\omega^2 \end{aligned}\right\} \quad (34)$$

where

$$\omega^2 = k\,\frac{M + m}{Mm}\,; \quad A = \frac{V_o}{\omega}\,; \quad B = -\frac{ng}{\omega^2}$$

Eq. (34) can be written also in an alternate form:

$$f = X \sin (wt - \varepsilon) + ng/w^2$$

where

$$X = \frac{1}{w}\left[(ng/w)^2 + V_o^2\right]^{1/2} - ng/w^2$$

$$\beta = \text{arc tan}\frac{ng}{wV_o} = \tan^{-1}\frac{B}{A}$$

(35)

The important fact indicated by Eq. 35 is the oscillatory character of the deflection f of the structure supporting the mass, and the resulting oscillatory variation of stresses in the structure. This may be very important in many types of trussed structures, such for instance, as the struts connecting the floats of a float seaplane to the fuselage. Such a structure may contain slender tension members, which will be subjected to compression, and may fail in buckling in the reversal of stress after the impact. The theory outlined above does not take account of the damping, and indicates the reversal of the stress of full magnitude. Actually all structures possess a certain amount of damping, reducing the intensity of stress in consecutive oscillations. A good rule of thumb, based on the above reasoning, is to check the slender tension members for the compressive stress equal to about half of the design tensile strength.

7.8 Waves

A system of exact equations expressing a possible form of wave motion when the depth of the water is infinite was given as long ago as 1802 by Gerstner, and in 1862 independently by Rankine and by W. Froude (Refs. 63 and 64). If the axis of x be horizontal, and that of y be drawn vertically upwards, the formulae in question may be written

$$x = a + r\, e^{kb} \sin k(a + ct)$$

$$y = b - r\, e^{kb} \cos k(a + ct)$$

(36)

where a and b are two coordinates defining the original position of a particle, and x and y are the coordinates of this particle at time t.

The constant $k = 2\pi/L$, where L is the wave length, and c is the velocity of propagation (the celerity) of the wave. It is obvious from Eqs. (36) that the path of any particle (a, b) is a circle of radius re^{kb}. Since b is negative, the radius of the circle diminishes rapidly with the increase of the depth b of a particle. The surface particle moves through the height $\pm$ r, i.e. the height H of the wave from trough to crest is 2r. The velocities of the water particles resulting from the above circular motion are referred to as "orbital velocities".

The form of the wave resulting from the above motion of water particles is represented by the curve known as "curtate cycloid" or "trochoid", the construction of which is shown on Figure 48. The curve is traced by a certain point located at the radius r on a generating disk of radius R rolling along a straight track. The equations of the curve referred to the track are:

$$x = R\theta + r \sin \theta$$

$$y = R + r \cos \theta$$

where R, r, and the angle θ are as shown on Figure 48. The length of the wave is $L = 2\pi R$, and the height from the trough to the crest is $H = 2r$. The slope of the wave surface is:

$$\tan \Phi = \tan \beta = dy/dx = \frac{r \sin \theta}{R + r \cos \theta}$$

The celerity (the velocity of the wave propagation) is:

$$c = \sqrt{gL/2\pi}$$

and the period: $T = L/c = \sqrt{2\pi L/g}$.

The experimental verification of the wave theory is given in Reference (65), together with an excellent bibliography on the subject. A very close agreement between theoretical, and experimental wave shapes is indicated.

The waves are usually described by their height H, and the ratio of length to height L/H. Reference (66) gives the statistical data

on the wave height and the L/H ratio encountered at several stations in open sea. For the wave heights over 15 feet, the predominating frequency of occurrence of L/H is in the range of 20 to 30. L/H of 20 is adopted in the Naval Architecture as the basis for the strength calculations of ship hulls. In the wave heights of 4 to 10 feet, in which seaplanes often have to operate, the frequently encountered waves are in the L/H range of 20 to 60. In U.S.A. the height of waves is usually given in feet. In Europe the wave height is usually described by a number of the following scale:

Scale	Wave Height in Meters
0	0
1	0 - 1
2	1 - 2
3	2 - 3
4	3 - 4
5	4 - 5
6	6 - 7
7	8 - 9
8	10 - 15
9	over 15

The waves of three to six feet in height, for instance, are referred to as "sea 2". The size of the waves is connected with the wind velocity by the empirical formula due to Zimmermann (Ref. 63):

$$H = 0.65\ w$$

where wave height H is in feet, and the wind velocity w is in statute miles per hour. This formula appears to give good results for the waves over 15 feet in height, but for the smaller waves of less than 8 sec. period gives the wave velocities in excess of wind velocities, which does not seem reasonable for fully developed waves and constant wind velocity.

REFERENCES

1. Ernest G. Stout, "Static Stability Analysis for Flying Boats and Seaplanes", Aviation, February, 1947.

2. John R. Dawson and Edwin P. Hartman, "Hydrodynamic and Aerodynamic Tests of Four Models of Outboard Floats (N.A.C.A. Models 51-A, 51-B, 51-C and 51-D)", N.A.C.A. T.N. No. 678, December 1938.

3. W. Sottorf, "Analysis of Experimental Investigations of the Planing Process on the Surface of Water", N.A.C.A. T.M. No. 1061, March 1944 (originally Jahrbuch 1937 der Deutschen Luftfahrtforschung).

3a. H. Wagner, "Landing of Seaplanes", N.A.C. T.M. No. 622, 1931.

4. L. Sedov, "Scale Effect and Optimum Relations for Sea Surface Planing", N.A.C.A. T.M. No. 1097, February 1947 (originally Report No. 439 of the Central Aero-Hydrodynamic Institute, Moscow, 1939.

5. B. V. Korvin-Kroukovsky, Daniel Savitsky and William F. Lehman, "Wetted Area and Center of Pressure of Planing Surfaces", Experimental Towing Tank of Stevens Institute of Technology Report No. 360, August 1949, Sherman Fairchild Fund Publication No. 244, Institute of the Aeronautical Sciences.

6. W. Sottorf, "Scale Effect of Model in Seaplane-Float Investigations", N.A.C.A. T.M. No. 704, April 1933.

7. W. Sottorf, "Experiments with Planing Surfaces", N.A.C.A. T.M. No. 739, March 1934.

8. B. V. Korvin-Kroukovsky, Daniel Savitsky and William F. Lehman, "Wake Profile of a Vee Planing Surface, Including Test Data on a 30° Deadrise Surface", Experimental Towing Tank of Stevens Institute of Technology Report No. 339, April 1949, Sherman M. Fairchild Publication Fund Paper No. 229, Institute of the Aeronautical Sciences, New York.

9. "Uniform Procedure for the Calculation of Frictional Resistance and the Expansion of Model Test Data to Full Size", Bulletin No. 1-2 of the Society of Naval Architects and Marine Engineers 29 West 39th Street, New York 18, N. Y.

10.

11. F. W. S. Locke, Jr., "General Resistance Tests on Flying-Boat Hull Models", N.A.C.A. Wartime Report No. W-70 (originally ARR No. 4B19).

12. F. W. S. Locke, Jr., "A Graphical Method for Interpolation of Hydrodynamic Characteristics of Specific Flying Boats from Collapsed Results of General Tests of Flying-Boat-Hull Models", N.A.C.A. T. N. No. 1259, January 1948.

13. Ernest G. Stout, "Take-off Analysis for Flying Boats and Seaplanes", Aviation, August and September, 1944.

14. John D. Pierson and Joseph R. Burghardt, "A Specific Chart for Flying Boat Take-off Performance", Journal of the Aeronautical Sciences, April 1945.

15. Karl D. Wood, "Technical Aerodynamics", McGraw-Hill Book Company, New York, Second Edition, 1947, pp. 290-308.

16. Walter Stuart Diehl, "Engineering Aerodynamics", The Ronald Press Company, New York, Revised Edition, Fourth Printing, July 1940, pp. 498-505.

20. John R. Dawson, "A General Tank Test of a Model of the Hull of the P3M-1 Flying Boat Including a Special Working Chart for the Determination of Hull Performance", N.A.C.A. T. N. No. 681.

21. F. W. S. Locke, Jr., "A collection of the Collapsed Results of General Tank Tests of Miscellaneous Flying-Boat-Hull Models", N.A.C.A. T. N. No. 1182.

22. W. G. A. Perring and H. Glauert, "The Stability on the Water of a Seaplane in the Planing Condition", A.R.C. (British) R. & M. No. 1493.

23. Alexander Klemin, John D. Pierson and Edmund M. Storer, "An Introduction to Seaplane Porpoising", Journal of the Aeronautical Sciences, Vol. 6, No. 8, June 1939.

24. Kenneth S. M. Davidson, F. W. S. Locke, Jr. and Anthony Suarez, "Porpoising - A Comparison of Theory with Experiment", N.A.C.A. Wartime Report W-65 (originally ARR No. 3G07).

25. James M. Benson and Anton Freihofner, "Methods and Charts for Computing Stability Derivatives of a V-Bottom Planing Surface", N.A.C.A. Wartime Report L-349 (originally ARR No. 3L08).

26. Kenneth S. M. Davidson and F. W. S. Locke, Jr., "Some Systematic Model Experiments on the Porpoising Characteristics of Flying-Boat Hulls", N.A.C.A. Wartime Report W-67 (originally ARR No. 3F12).

27. Ernest G. Stout, "Experimental Determination of Hydrodynamic Stability", Journal of the Aeronautical Sciences, Vol. 8, No. 2, December 1940.

27a. Ernest G. Stout, "Development of Precision Radio-Controlled Dynamically-Similar Flying Models", Journal of the Aeronautical Sciences, Vol. 13, No. 7, July 1946.

28. L. P. Coombes, W. G. A. Perring and L. Johnston, "The Use of Dynamically Similar Models for Determining the Porpoising Characteristics of Seaplanes", A.R.C. (British) R. & M. No. 1718.

29. Method Used in N.A.C.A. Tank for the Investigation of the Longitudinal Stability Characteristics of Models of Flying Boats", N.A.C.A. Report No. 753.

30. F. W. S. Locke, Jr., "An Analysis of the Skipping Characteristics of Some Full-Size Flying Boats", N.A.C.A. Wartime Report W-104 (originally ARR No. 5J24).

31. John B. Parkinson, "Notes on the Skipping of Seaplanes", N.A.C.A. RB No. 3I27.

32. F. W. S. Locke, Jr., "Some Yawing Tests of a 1/30-Scale Model of the XPB2M-1 Flying Boat", N.A.C.A. Wartime Report W-66 (originally ARR No. 3G06).

33. F. W. S. Locke, Jr. and Helen L. Bott, "A Method for Making Quantitative Studies of the Main Spray Characteristics of Flying-Boat Hull Models", N.A.C.A. Wartime Report W-69 (originally ARR No. 3K11).

34. F. W. S. Locke, Jr., "General Main-Spray Tests of Flying-Boat Models in the Displacement Range", N.A.C.A. Wartime Report W-72 (originally ARR No. 5A02).

35. F. W. S. Locke, Jr., "Some Systematic Model Experiments of the Bow Spray Characteristics of Flying-Boat Hulls Operating at Low Speed in Waves", N.A.C.A. Wartime Report No. W-71 (originally ARR No. 3L04).

35a John D.Pierson, "Directional Stability of Flying Boat Hulls During Taxiing" Journal of the Aeronautical Sciences, Vol. No.

36. G. H.Bottomley, "The Impact of a Model Seaplane Float on Water", A.C.A. (British) R.&M. No. 583, 1919.

37. Th. von Karman, "The Impact on Seaplane Floats During Landing", N.A.C.A. T.N. No. 321, 1929.

38. H. Wagner, "Landing of Seaplanes", N.A.C.A. T.M. No. 622, 1931.

39. H. Wagner, "Uber Stoss- und Gleitvorgange an der Oberflache von Flussigkeiten", Z.f.a.M.M. Bd. 12, Heft 4, August 1932 pp. 193-215.

40.

41. Wilhelm Pabst, "Theory of Landing Impact of Seaplanes", N.A.C.A. T.M. No. 580, 1930.

42. Wilhelm Pabst, "Landing Impact of Seaplanes" N.A.C.A. T.M. No. 624, 1931.

43. R.L. Kreps, "Experimental Investigation of Impact in Landing on Water" N.A.C.A. T.M. No. 1046, 1943 (originally published as Report No. 438, Central Aero-Hydro Inst., Moscow 1939.

44. J. Sydow, "The Effect of Spring Support and Keeling on Landing Impact," Jarbuch der Deutschen Luftfahrtforschung, 1938, Vol. 1, (Available as British Air Ministry Translation No. 861).

45. E.T. Jones and R.W. Blundell, "Force and Pressure Measurements on V-Shapes on Impact with Water Compared with Theory and Seaplane Alighting Results," A.R.C. (British) R.&M. No. 1932, January, 1938. (Formerly Marine Aircraft Experimental Establishment Report No. F/Res/107).

46. S.V. Fagg, "A Theoretical Analysis of the Impact of an Elastic Body on Water," A.R.C. (British) R.&M. No. 1925, October 1941.

47. Wilbur L. Mayo, "Theoretical and Experimental Dynamic Loads for a Prismatic Float Having an Angle of Dead Rise of 22 1/2", N.A.C.A.RB No. L5F15, July, 1945.

48. Wilbur L. Mayo, "Analysis and Modification of Theory of Impact of Seaplanes on Water," N.A.C.A. T.N. No. 1008, 1945.

49. C.B. Lyman, "Water Load Criteria for the Design of Seaplanes," U.S. Navy Dep't., BuAer., a Paper for presentation at the Sixth International Congress for Applied Mechanics, Paris, 1946.

50. Stanley U. Benscoter, "Impact Theory for Seaplane Landing," N.A.C.A. T.N. No. 1437, October 1947.

51. Benjamin Milwitzky, "A Theoretical Investigation of Hydrodynamic Impact Loads on Scalloped-Bottom Seaplanes and Comparisons with Experiment," N.A.C.A. T.N. No. 1363, 1947.

52. Benjamin Molwitzky, "A Generalized Theoretical and Experimental Investigation of the Motions and Hydrodynamic Loads Experienced by V-Bottom Seaplanes During Step-Landing Impacts," N.A.C.A. T.N. No. 1516, February, 1948.

53. Sidney A. Batterson, "The N.A.C.A. Impact Basin and Water Landing Tests of a Float Model at Various Velocities and Weights," N.A.C.A. Report No. 795, 1944 (Originally ACR No. L4H15, 1944).

54. Sidney A. Batterson, "Variation of Hydrodynamic Impact Loads with Flight-Path Angle for a Prismatic Float at 3° Trim and with a $22\text{-}1/2^{\circ}$ Angle of Dead Rise," N.A.C.A. RB No. L5A24, 1945.

55. Sidney A. Batterson and Thelma Stewar, "Variation of Hydrodynamic Impact Loads with Flight Path Angle for a Prismatic Float at 6° and 9° Trim and a $22\text{-}1/2^{\circ}$ Angle of Dead Rise," N.A.C.A. RB No. L5K21, 1945.

56. Sidney A. Batterson, "Variation of Hydrodynamic Impact Loads with Flight-Path Angle for a Prismatic Float at 12° Trim and with $22\text{-}1/2^{\circ}$ Angle of Dead Rise," N.A.C.A. RB No. L5K21a, 1946.

57. Sidney A. Batterson, "Variation of Hydrodynamic Impact Loads with Flight Path Angle for a Prismatic Float at 0° and -3° Trim and with $22\text{-}1/2^{\circ}$ Angle of Dead Rise," N.A.C.A. T.N. No. 1166, April, 1947.

58. W. Sottorf, "Experiments with Planing Surfaces," N.A.C.A. T.M. No. 739, 1934 (originally Werft-Reederei-Hafen, Oct. 1, 1932, Feb. 15 and March 1, 1933).

59. Benson, J.M., Havens, R.F. and Woodward, D.R., "Landing Characteristics in Waves of Three Dynamic Models of Flying Boats," N.A.C.A. RM No. L6L13, May 7, 1947.

60. John D. Pierson, "On the Pressure Distribution for a Wedge Penetrating a Fluid Surface," Stevens Inst. of Tech., ETT Rep. No. 336.

61. John D. Pierson and Samuel Leshnover, "An Analysis of the Fluid Flow in the Spray Root and Wake Regions of Flat Planing Surfaces," Stevens Inst. of Tech., ETT Rep. No. 335.

62 F. L. Thompson, "Water Pressure Distribution on a Flying Boat Hull, N.A.C.A. Report No. 346.

63. "Principles of Naval Architecture" Vo. II, Chapter I, Section 1, The Society of Naval Architects and Marine Engineers, 29 West 39th Street, New York, New York.

64. Sir Horace Lamb, "Hydrodynamics," Sixth revised edition, Dover Publications, N. Y., p. 421.

65. "A Study of Progressive Oscillatory Waves in Water," Technical Report No. 1, Beach Erosion Board, Office of the Chief of Engineers, U.S. Government Printing Office.

66. "A Statistical Study of Wave Conditions," S.I.O. Wave Project, Report No. 53, Contract No. NObs2490 (Declassified).

67. "A New Approach to Determining the Hydrodynamic Characteristics of Flying Boats During Flight Tests," by F.W.S. Locke, Jr., Navy Dep't., Bu. Aero., Design Res. Div. Report No. 1063 (Preprint of Paper to be Presented at VII International Congress of Applied Mechanics Meeting in London on 6 September 1948.

The List of Captions

Fig. 1 The Elements of the Hull of Float Lines - Straight Steps.

Fig. 2 Vee Main Step and Pointed Second Step.

Fig. 3 Pointed Main Step.

Fig. 3a Like Drawing of NACA Model 4-A Single Float (Navy Mark V Float)

Fig. 4 Typical Set of Curves Used in Buoyancy Calculations.

Fig. 5) Definition of the Metacenter M, and of the Metacentric Height MG.
Fig. 5a)

Fig. 6 Sponsons and inboard Auxiliary Floats for Lateral Stability.

Fig. 7 Wing Tip Floats for Lateral Stability.

Fig. 8 Lines of NACA Model 51-B Wing Tip Float.

Fig. 9 Flat Planing Surface.

Fig. 10 Vee Planing Surface.

Fig. 11 Lift of Planing Surfaces (charts taken from Ref. 5).

Fig. 12 The Diagram Showing the Total Drag as the Sum of the Dynamic Drag and the Friction Drag.

Fig. 13 The Balance of the Forces and Moments in Two Step Planing.

Fig. 13a The Variation of the Planing Coefficient ϵ with the Angle of Trim τ for the constant Δ, and with the λ Variable (taken from Ref. 7).

Fig. 14 The Typical Set of the Resistance, Trim and Heave Curves from the Specific Test of a Model.

Fig. 15 The Plot of the General Tank Test Data for $\tau = 7^\circ$ from N.A.C.A. Tec. Note No. 681.

Fig. 16 The Alternate Way of Presenting the General Tank Test Data taken from N.A.C.A. Tech. Note No. 681.

Fig. 17 Typical Collarsed Summary Chart of the General Tank Test Data taken from N.A.C.A. Tech. Note No. 1182.

Fig. 18 The Plot of $\sqrt{C_R/C_V}$ vs. $\sqrt{C_\Delta/C_V}$ for the Fixed Trim Resistance Tests from N.A.C.A. Wartime Report No. W-70.

Fig. 19 The Angle of Trim vs. $\sqrt{C_\Delta/C_V}$ with $\sqrt{C_R/C_V}$ as Parameter Obtained by Cross Plotting the Data of Fig. 18 taken from N.A.C.A. Wartime Report No. W-70.

Fig. 20 The Typical Set of Curves for Calculation of the Take-off Time.

Fig. 21 The Unbalance of Forces due to Changes of the Heave with Constant Trim in a Seaplane Planing on the Forebody Alone.

Fig. 22 The Unbalance of Moments due to Changes of Trim with Constant Heave in a Seaplane Planing on the Forebody Alone.

Fig. 23 The Unbalance of Forces due to Changes in Heave h with the Constant Trim τ in a Seaplane Planing on Two Steps.

Fig. 24 The Unbalance of Moments due to Changes of the Trim τ with Constant Heave in a Seaplane Planing on Two Steps.

Fig. 25 The Plot of the Ratio (Step Height in % of Beam) (Sternpost Angle in Degrees) vs. Load Coefficient C_{Δ} taken from Ref. 30.

Fig. 25a Diagramatic Sketch of Apparatus for Yaw Tests (taken from Ref. 35a).

Fig. 26 The Curve of the Yawing Moment Coefficient vs. the Yaw Angle ψ for C_{Δ} = .89, C_V = 1.04, showing the Unstable Condition. Taken from Ref. (32).

Fig. 27 The Curve of the Yawing Moment Coefficient vs. the Yaw Angle ψ for C_{Δ} = .81, C_V = 2.17, showing the Stable Condition. Taken from Ref. (32).

Fig. 28 The Curve of the Yawing Moment Coefficient vs. the Yaw Angle ψ for C_{Δ} = .79, C_V = 2.33, Showing the "Hooking" Instability. Taken from Ref. (32).

Fig. 29 Schematic Diagram showing the Contours of the Main Spray blister, and the Location of its Point of Tangency to Spray Envelope. Taken from Ref. (34).

Fig. 30 The Plot Showing the Longitudinal Position of the Point of Tangency of the Main Spray Blister to Envelope Crests. Taken from Ref. (34).

Fig. 31 Seaplane at Instant of Entry into Water (taken from Ref. 50).

Fig. 32 Trajectory of the Step Point and Reaction During Impact Period (taken from Ref. 50).

Fig. 33 Half Cylinder of Water the Mass of which is Added to the Mass of the Wedge in Impact, a) as originally visualized by von Karman, and b) taking into account the rise of water as used by H. Wagner.

Fig. 34 Instantaneous Position of the Float During Impact (taken from Ref.50).

Fig. 35 Draft Coefficient vs. Approach Parameter (taken from Ref. 52).

Fig. 36 Ratio of the Instantaneous Vertical Velocity to Vertical Velocity at First Contact vs. Approach Parameter (taken from Ref. 52).

Fig. 37 Load Factor Coefficient vs. Approach Parameter (taken from Ref. 52).

Fig. 38 Time Coefficient vs. Approach Parameter (taken from Ref. 52).

Fig. 39 Landing on the Flank of the Wave (taken from Ref. 49).

Fig. 40 Acceleration plotted vs. Wave Length in case of a seaplane landing in oncoming 4.4 foot waves. (taken from Ref. 49).

Fig. 41 The Plot showing the magnitudes of the vertical, horizontal and pitching angular accelerations vs. position of the resultant force. (taken from Ref.49).

Fig. 42 Theoretical Pressure Distribution over Straight Sided Vee Compared with Experimental Results when Pressure Surface Reaches C = 1/6, 1/2 and 3/4 of the Distance between Keel and Chine (taken from Ref. 45).

Fig. 43 Peak Pressures across Several Typical Sections of Flying Boats (taken from Ref. 45).

Fig. 44 Pressure distribution in case of a 15° deadrise prismatic planing surface, planing at the angle of trim of 6° and speed of 6 m/sec. (taken from Ref. 58).

Fig. 45 Approximate distribution of the maximum vertical water reaction in landing--Total load 4.7 times weight of Seaplane (taken from Ref. 62).

Fig. 46 Approximate distribution of the maximum water pressures caused by impact with a wave in a take-off total load 3.0 times weight of seaplane (taken from Ref. 62).

Fig. 47 Sketch showing the effect of elastic connection between the mass of a seaplane and the planing bottom during impact (taken from Ref. 46).

Fig. 48 Diagram showing the generation of the trochoidal wave form (taken from Ref. 63).

TABLE I

Offsets for N.A.C.A. Model 41-A Single Float (Inches)

Station	Distance from F.P.	Distance from base line Half-breadths						Radius of flare	Radius of deck
		Keel	Chine	Deck	Tangent of flare	Chine	Tangent of flare		
						Tangent to F.P.			
F.P.	0.00	2.43	2.43	2.43					2.96
1	1.00	5.72	2.79	1.50	3.75	2.46	1.13	1.92	2.96
2	2.13	7.06	3.25	1.00	4.43	3.36	1.72	2.78	3.63
3	3.25	7.86	3.63	.74	4.86	3.93	2.06	2.98	4.12
4	5.50	8.79	4.29	.47	5.57	4.64	2.57	3.65	4.74
5	10.00	9.68	5.32	.22	6.54	5.32	3.15	4.71	5.31
6	14.46	10.00	6.14	.11	7.14	5.61	3.43	4.62	5.61
7	19.03	10.16	6.74	.03	7.61	5.78	3.61	5.16	5.78
7-1/2	23.52	10.25	7.15	.00	7.91	5.86	3.73	5.59	5.88
8	28.00	10.29	7.40	↑	8.13	5.93	3.80	6.02	5.93
8-1/2	32.50	↕	7.55	↕	8.27	5.98	3.84	7.29	5.98
9	37.00	↓	7.68	↕	8.36	5.99	3.86	7.34	5.99
10,F.	42.68	10.29	7.81	↓	8.43	6.00	3.86	6.97	6.00
10,A.	42.68	9.36	6.44						
11	46.00	↑	6.04	.00		5.90			5.90
12	53.68	↕	5.35	.02		5.25			5.25
13	61.36	↓	4.93	.15		4.05			4.05
14	69.04	5.90	4.73	.54		2.39			2.39
15,F.	71.75	5.73	4.91	.72		1.68			1.68
15,A.	71.75	4.88	4.06						
16	74.29	↕	3.05	.97		1.00			1.00
A.P.	76.21	3.93	3.93						

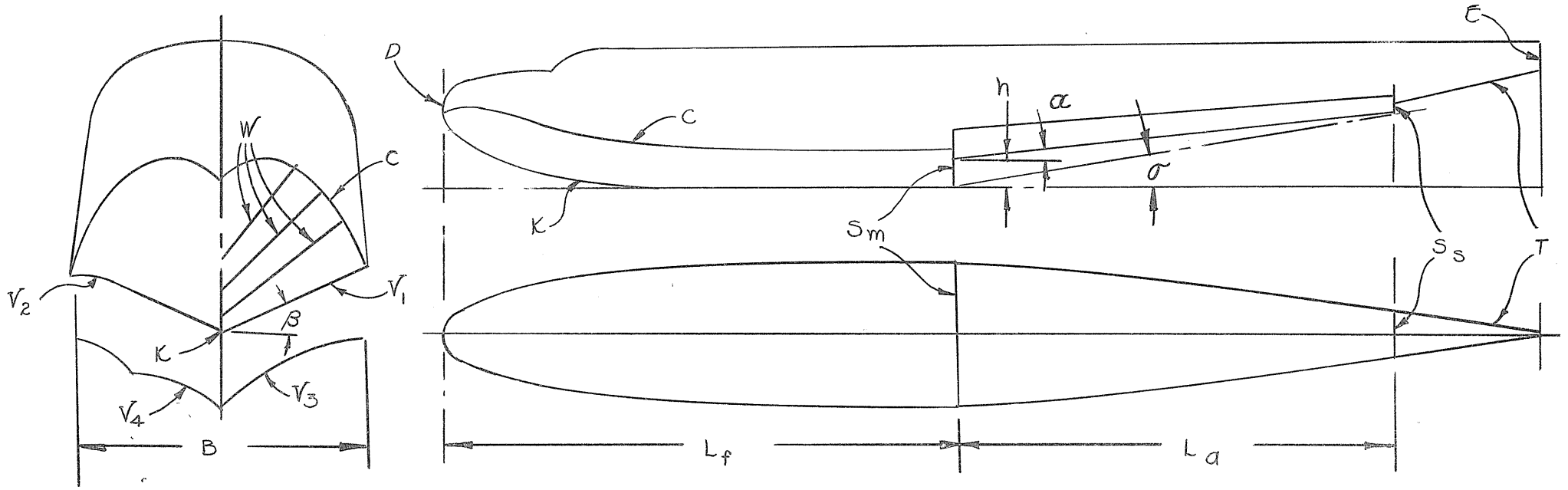

FIGURE 1

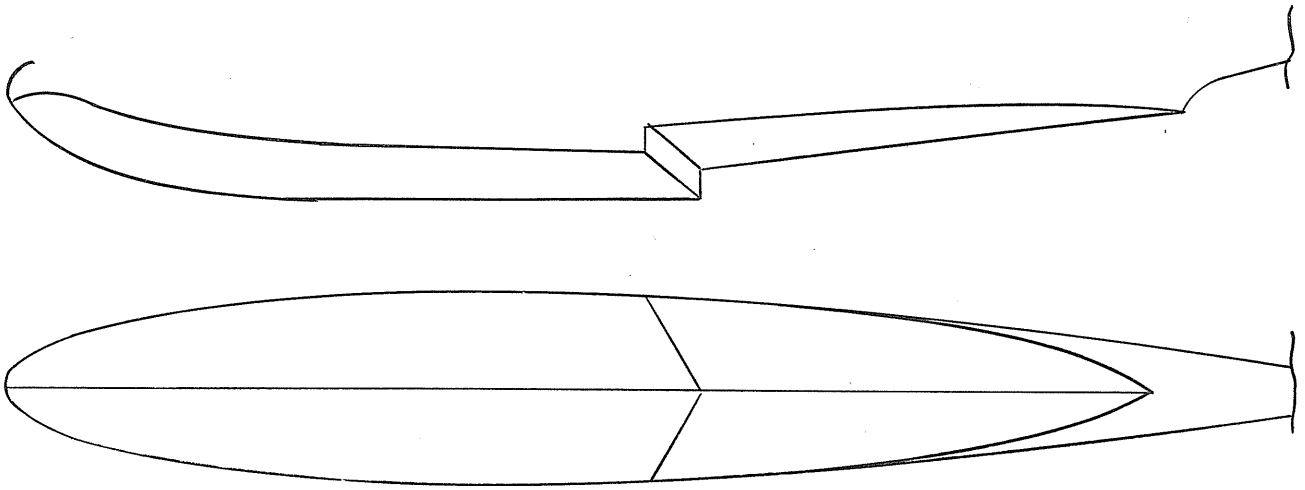

FIGURE 2

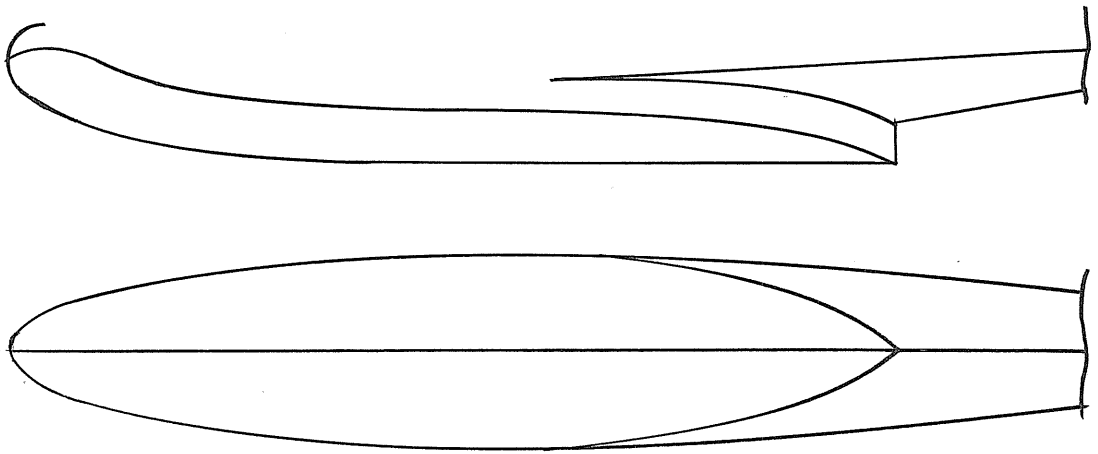

FIGURE 3

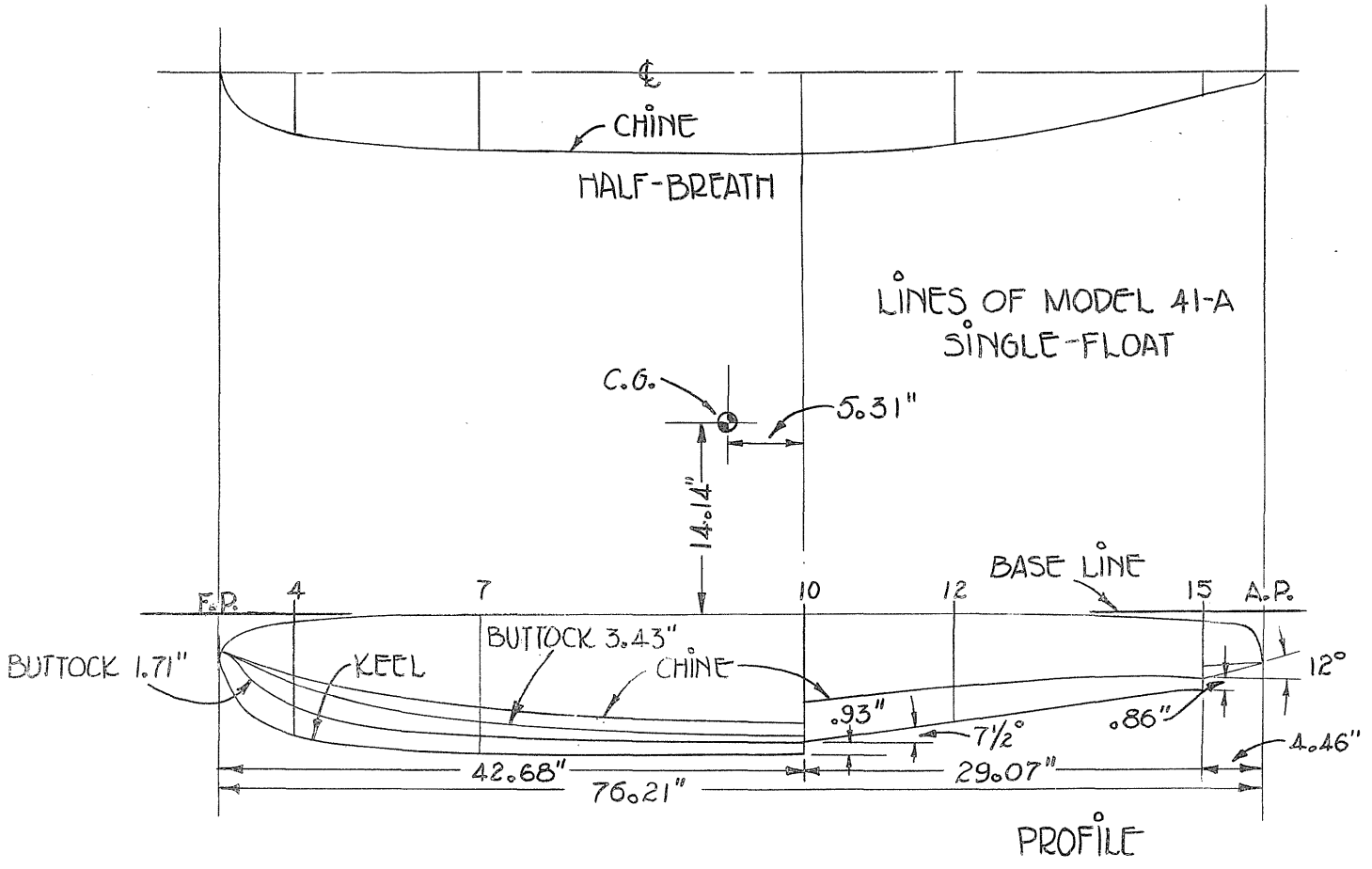

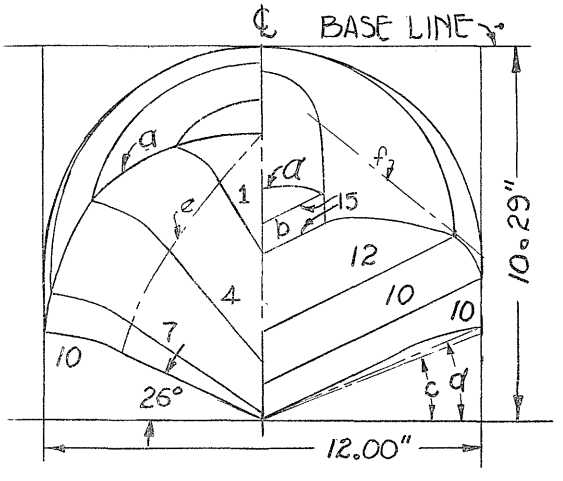

a. CHINE
b. STEP
c. 21½°
d. 22½°
e. TANGENCY OF FLARE
f. TANGENCY OF DECK RADIUS

BODY PLAN OF MODEL 41-A
SINGLE-FLOAT

FIGURE 3a

FIGURE 4

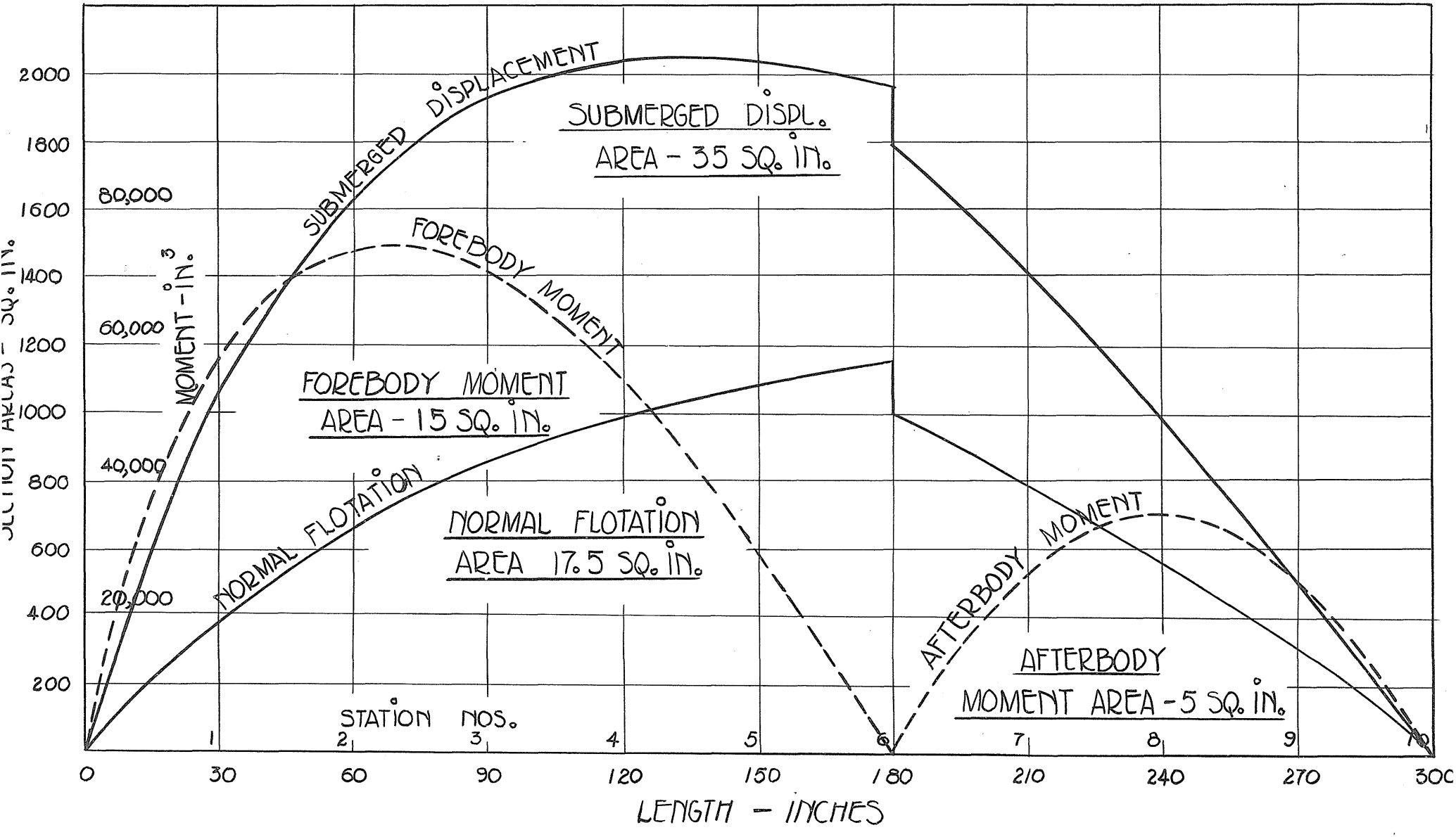
SUBMERGED DISPLACEMENT
SUBMERGED DISPL.
AREA - 35 SQ. IN.
FOREBODY MOMENT
FOREBODY MOMENT
AREA - 15 SQ. IN.
NORMAL FLOTATION
NORMAL FLOTATION
AREA 17.5 SQ. IN.
AFTERBODY MOMENT
AFTERBODY
MOMENT AREA - 5 SQ. IN.
SECTION AREAS - SQ. IN.
MOMENT - IN.³
80,000
60,000
40,000
20,000
2000
1800
1600
1400
1200
1000
800
600
400
200
STATION NOS.
1
2
3
4
5
6
7
8
9
10
0
30
60
90
120
150
180
210
240
270
300
LENGTH - INCHES

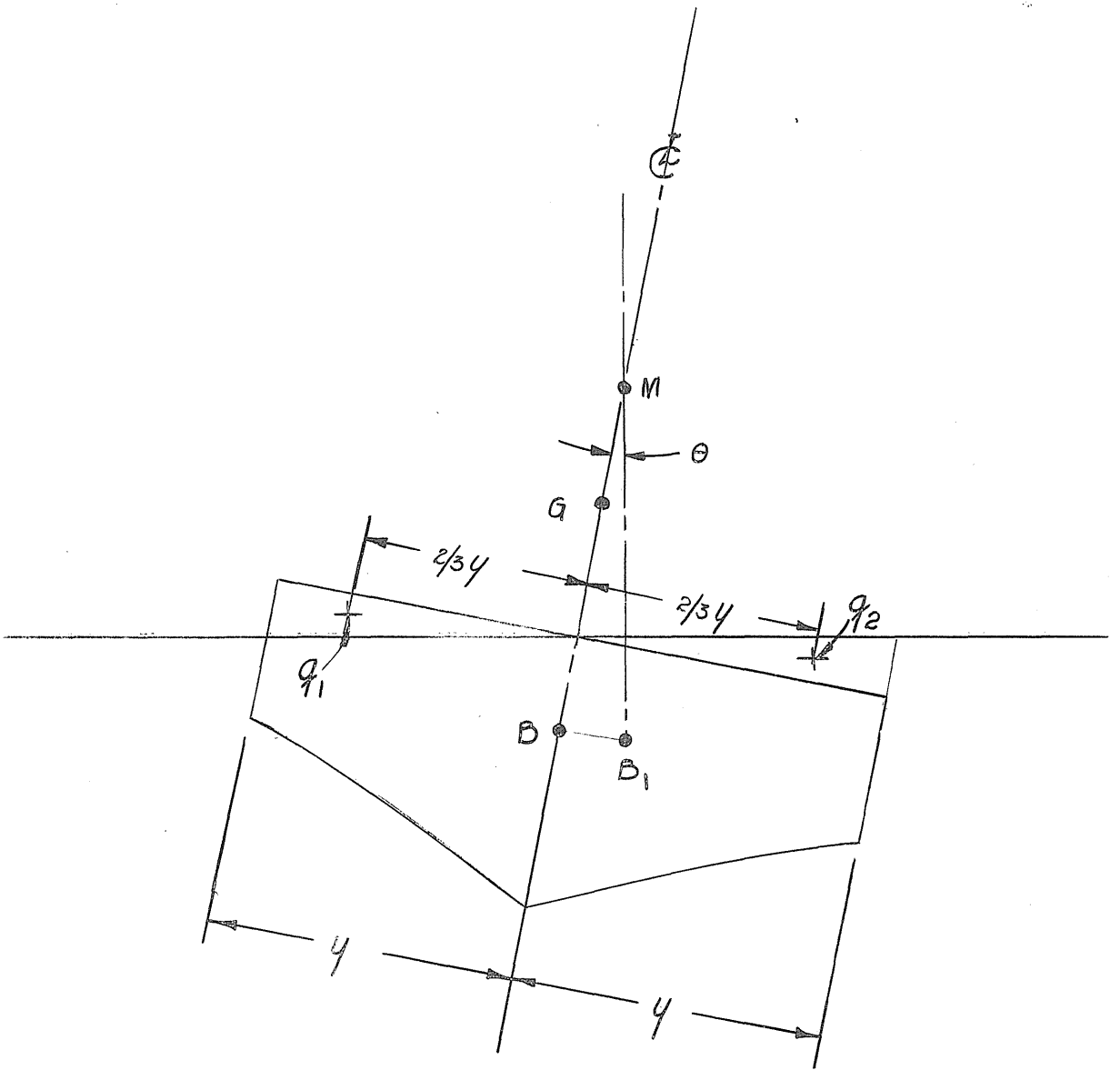

FIGURE 5

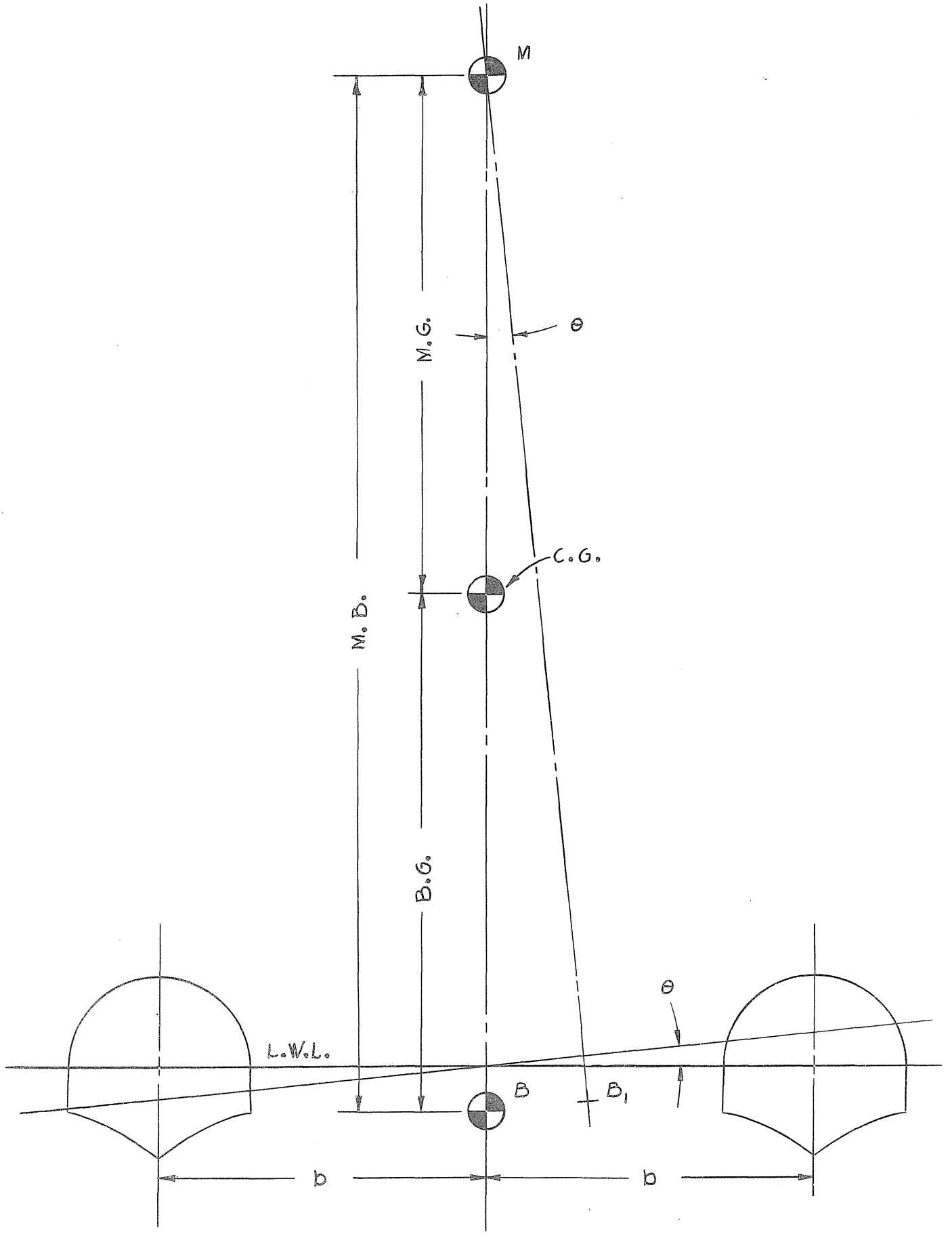

FIGURE 5a

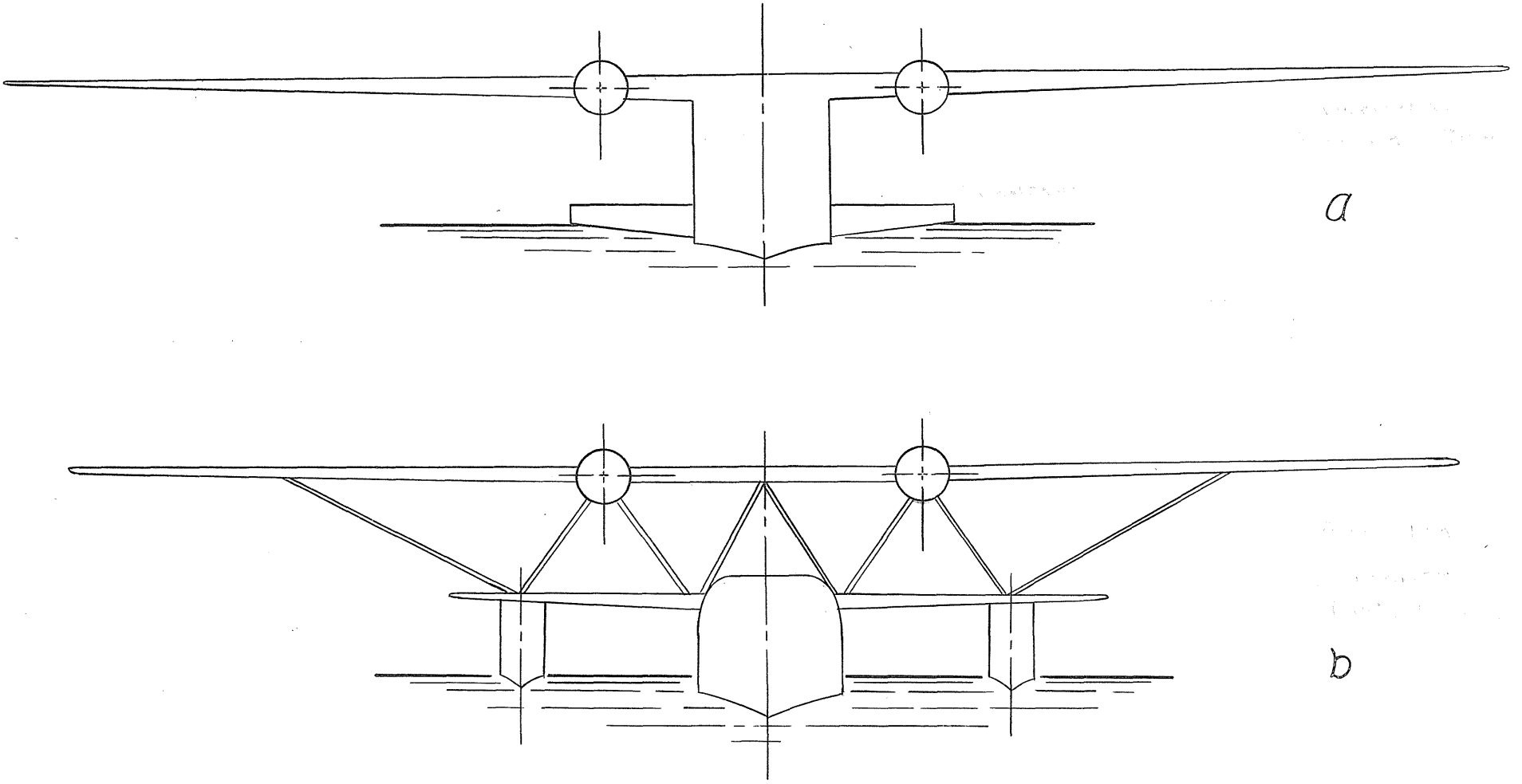

FIGURE 6

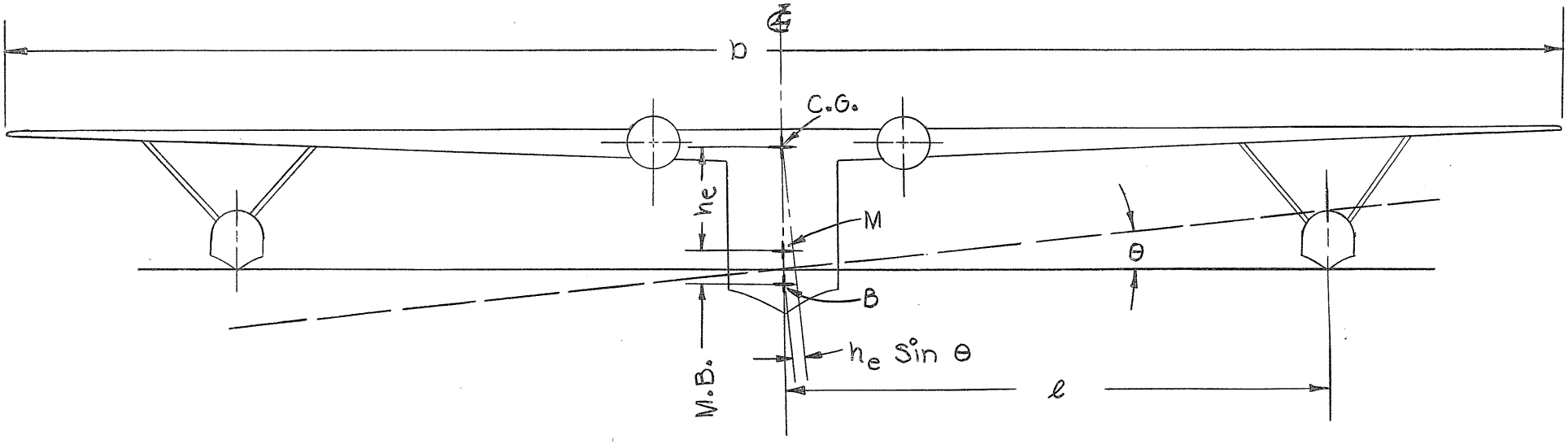

FIGURE 7

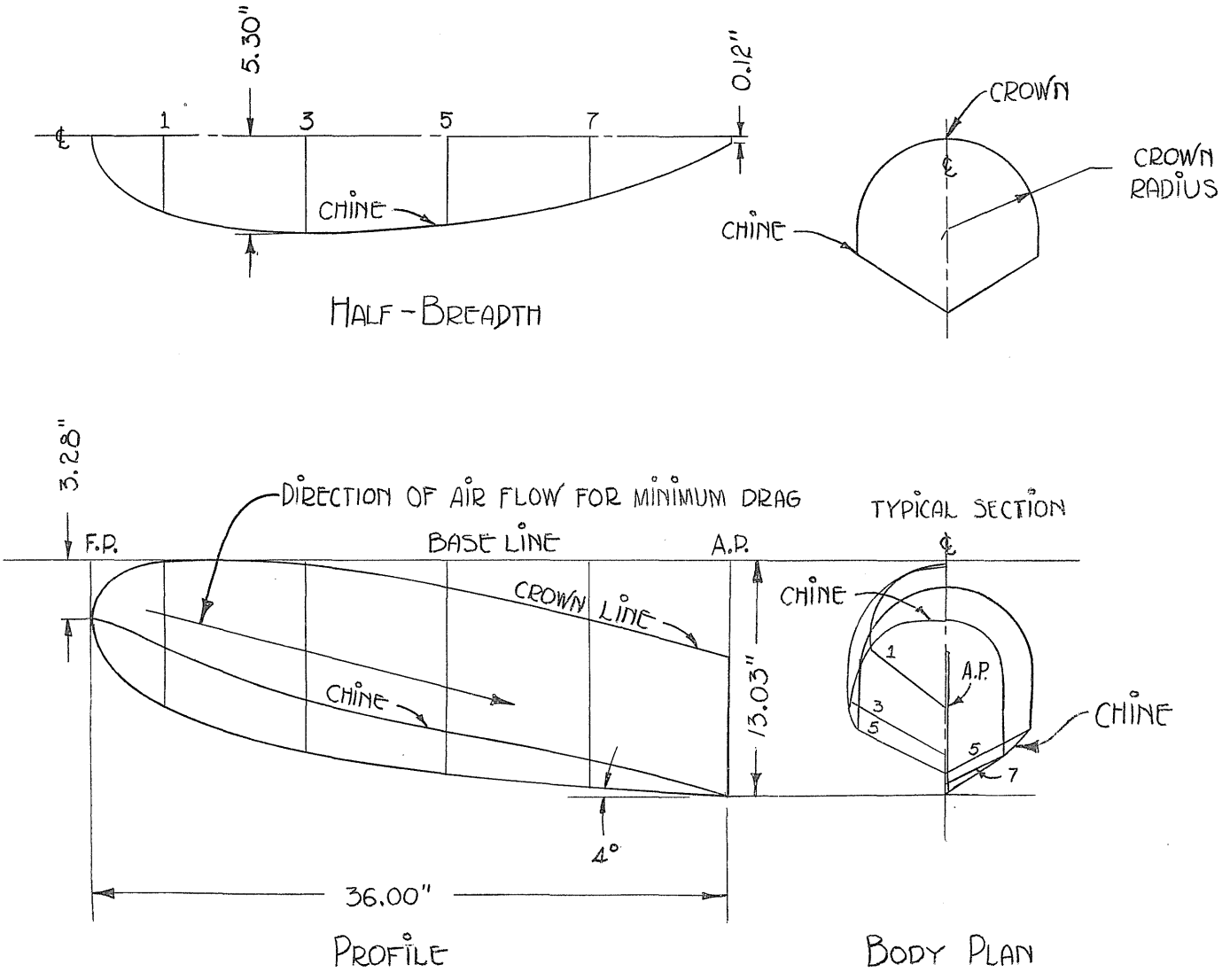

FIGURE 8

LINES OF N.A.C.A. MODEL 51-B. VOLUME = 1.200 CU. FT.

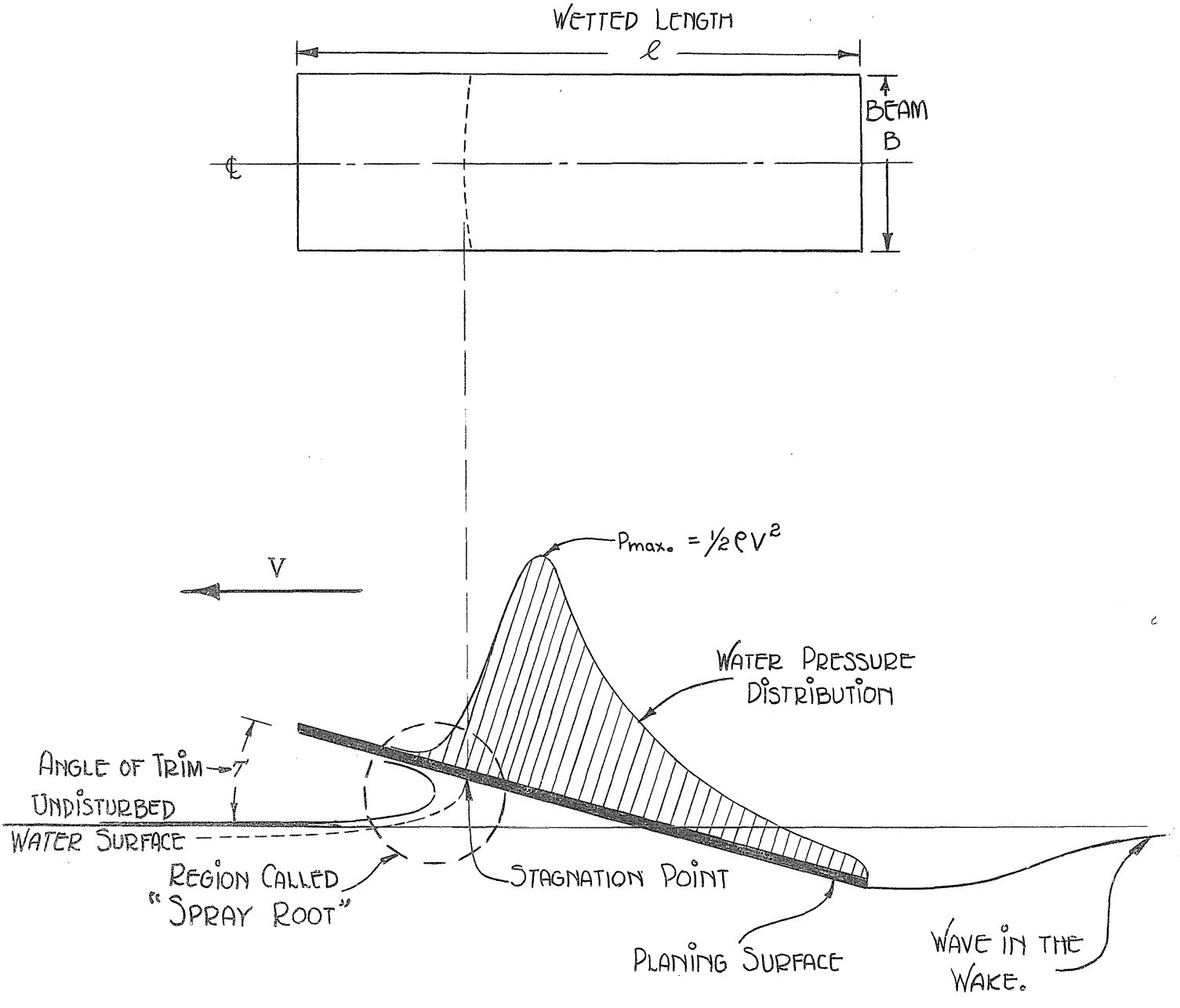

FIGURE 9

FLAT PLANING SURFACE

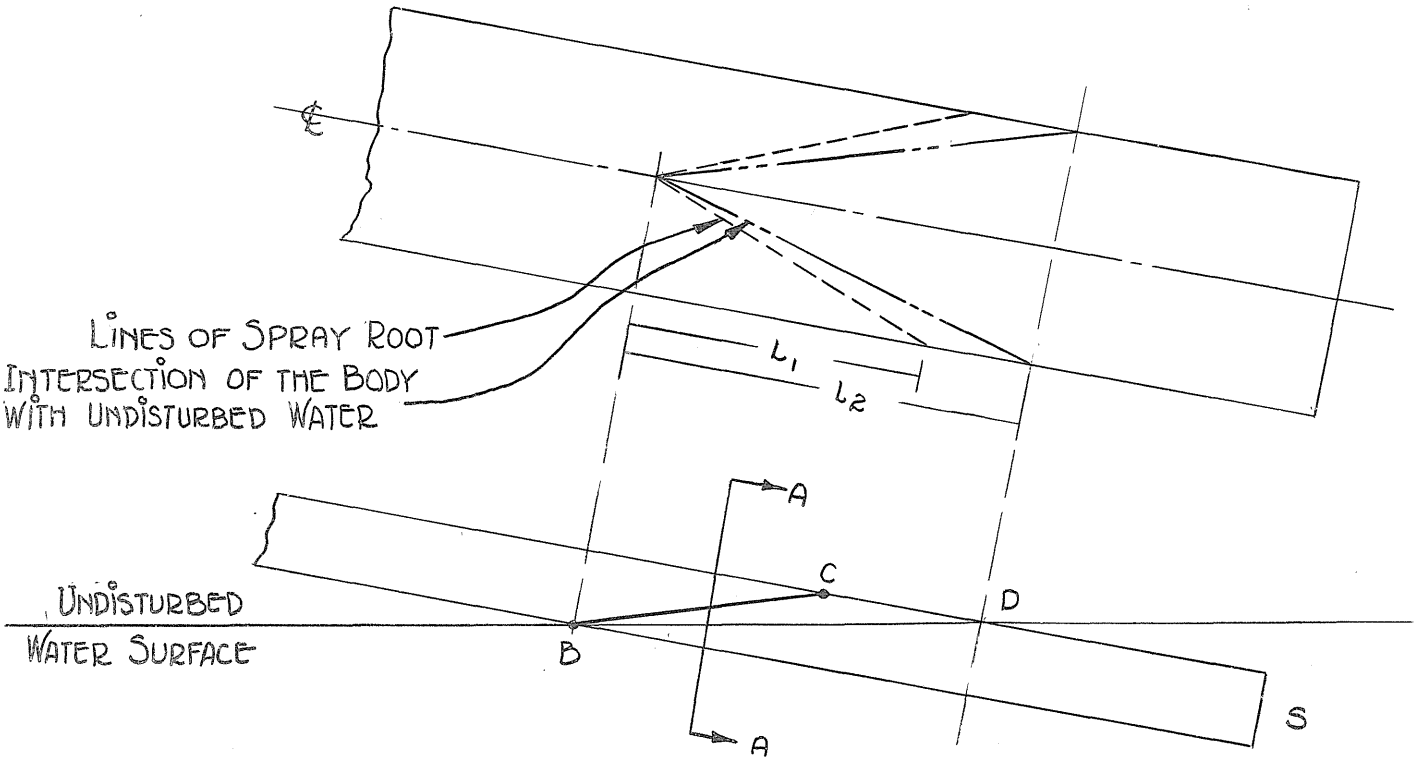

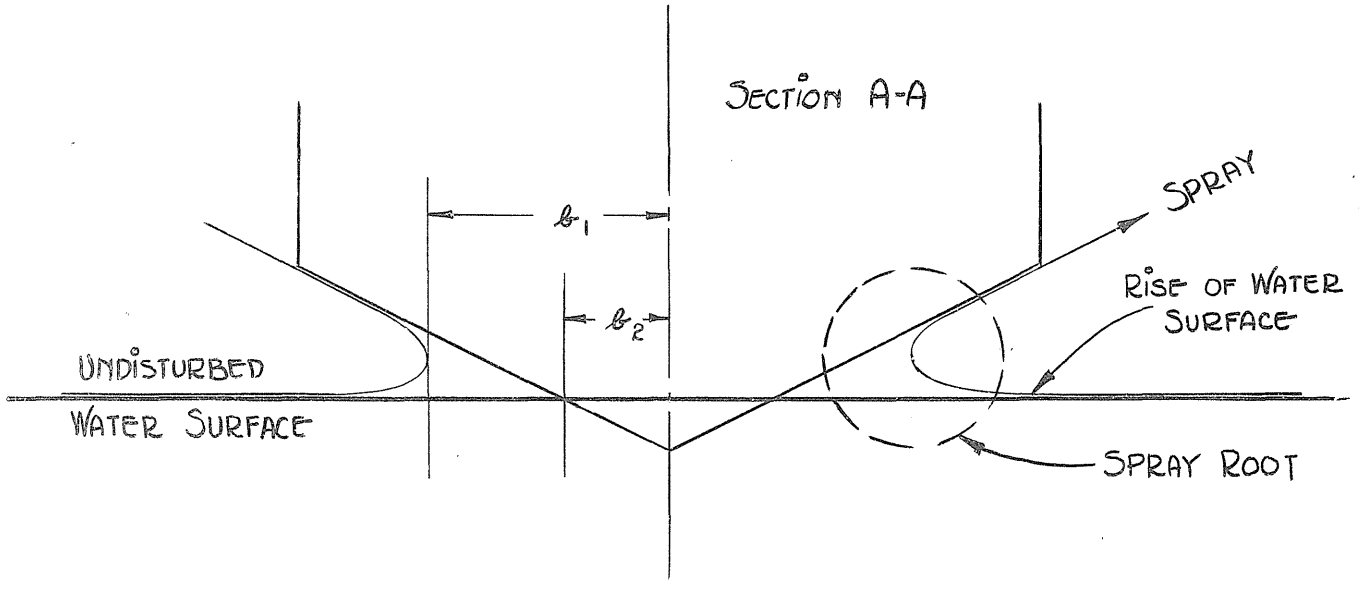

FIGURE 10
VEE PLANING SURFACE

LIFT OF PLANING SURFACES

LIFT COEFFICIENT IS DEFINED AS:

$$C_L = \Delta / \tfrac{1}{2}\rho V^2 b^2 = 2C_\Delta / C_V{}^2$$

FOR A FLAT PLATE - DEADRISE ZERO:

$$C_{L_0} = \tau^{1.1}(.0120\,\lambda^{1/2} + .0095\,\lambda^2 / C_V{}^2)$$

FOR A VEE SURFACE OF DEADRISE β:

$$C_{L_\beta} = C_{L_0} - .0065\beta\ C_{L_0}{}^{.6}$$

Δ - LOAD LB.
ρ - WATER DENSITY
b - BEAM IN FEET

V - VELOCITY IN FEET PER SEC.
τ - ANGLE OF TRIM IN DEGREES
β - DEADRISE IN DEGREES

λ - RATIO OF MEAN WETTED LENGTH TO BEAM
C_V - SPEED COEFF. = $V/\sqrt{gb}$

τ	$\tau^{1.1}$	τ	$\tau^{1.1}$
2	2.14	9	11.21
3	3.35	10	12.59
4	4.59	11	13.98
5	5.87	12	15.39
6	7.18	13	16.80
7	8.50	14	18.23
8	9.85	15	19.67

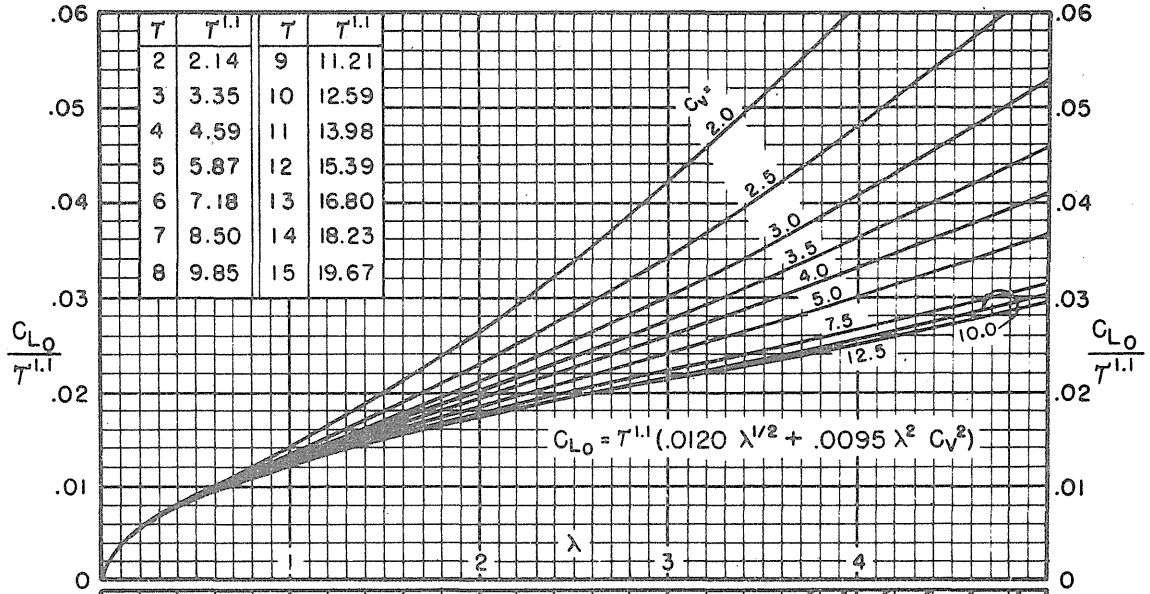

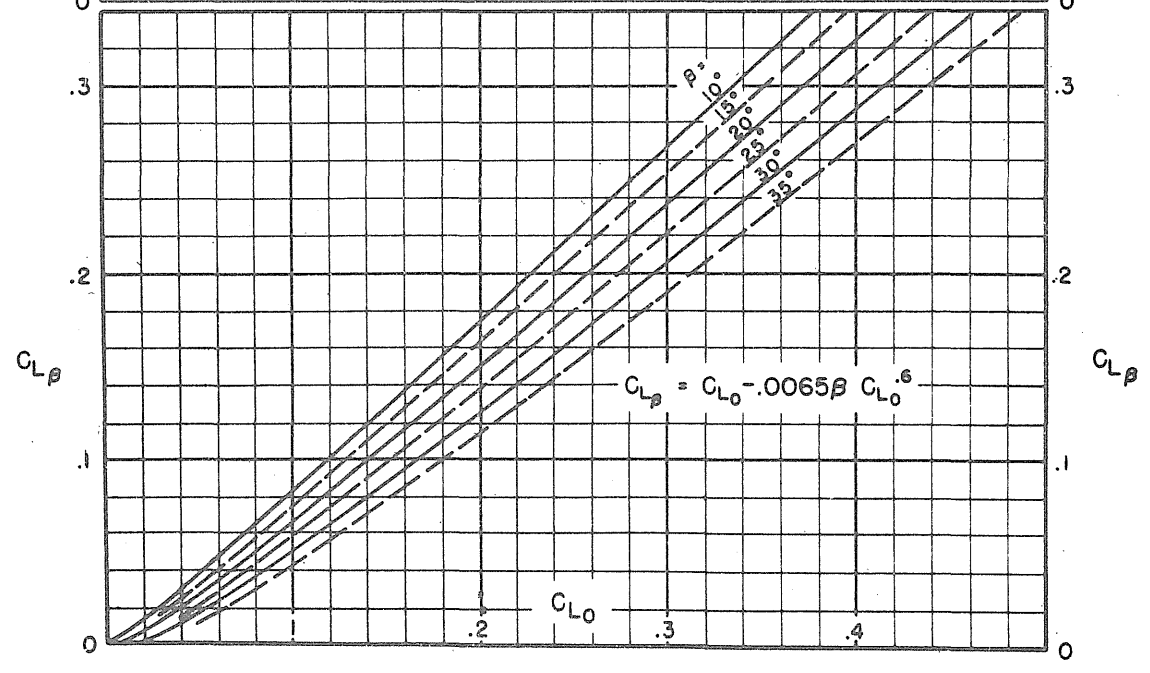

FIGURE 11

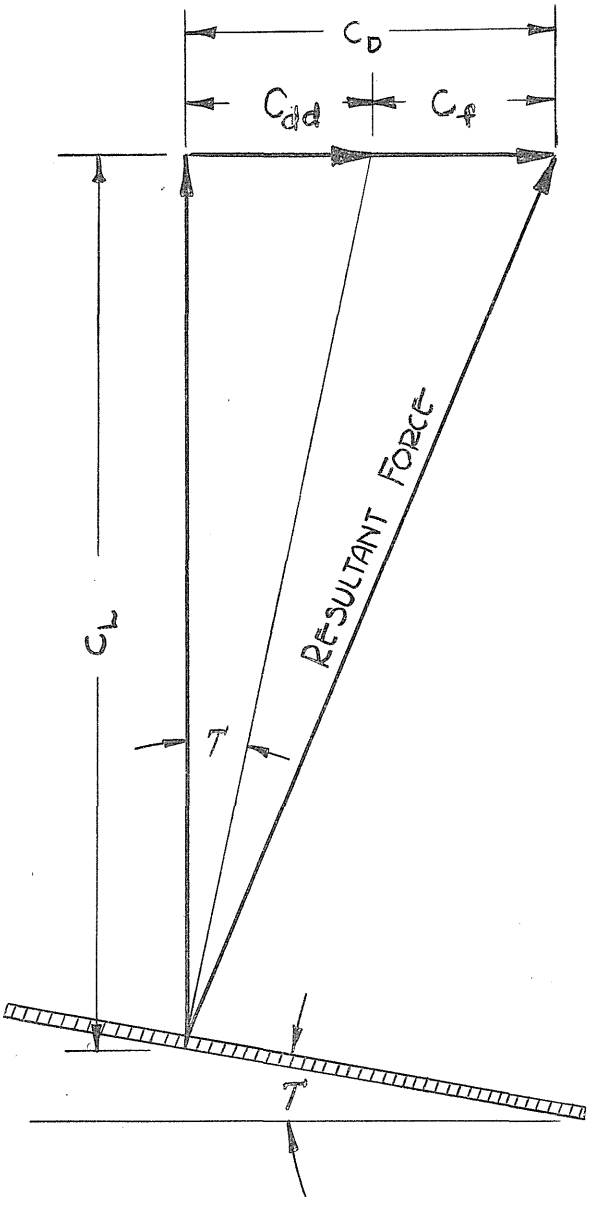

FIGURE 12

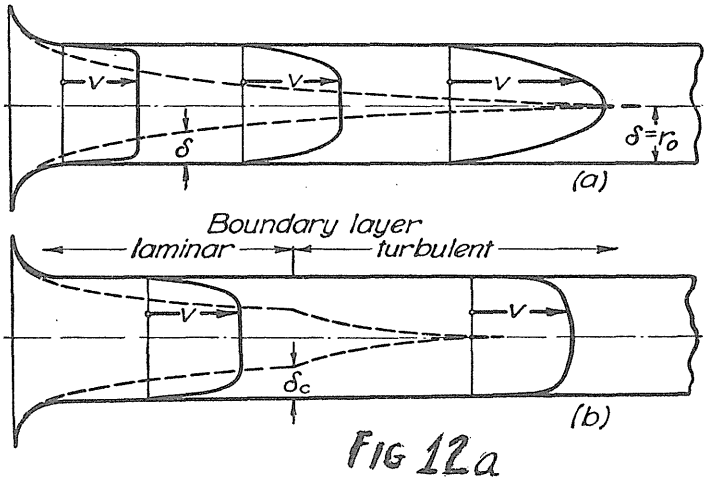

FIG 12a

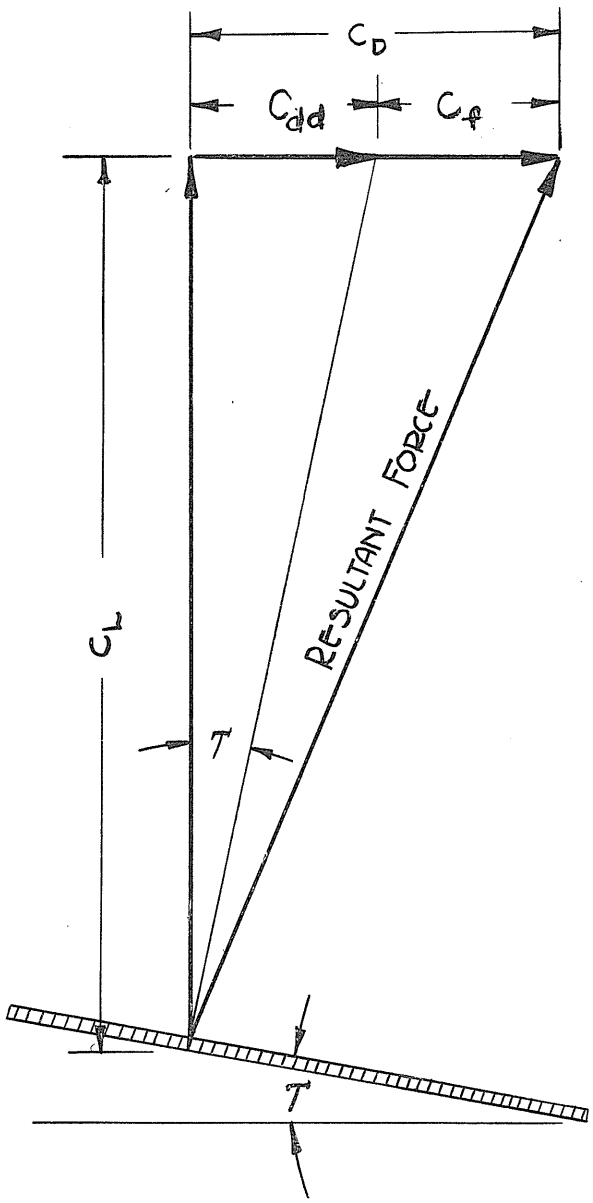

FIGURE 12

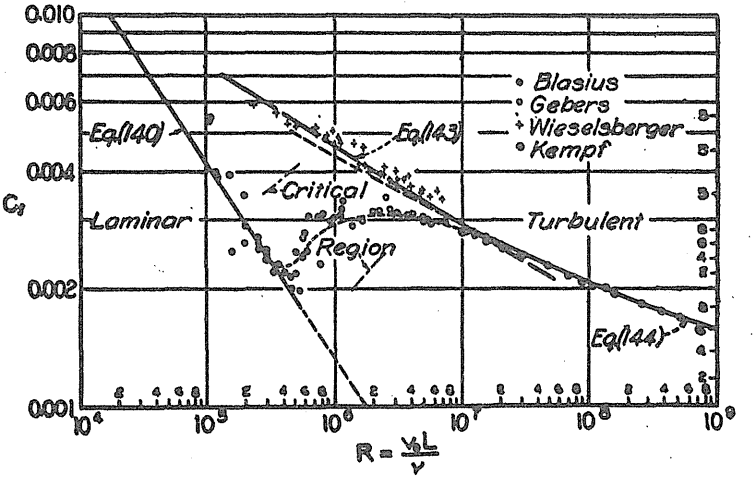
0.010
0.008
0.006
0.004
0.002
0.001
C_f
Eq.(140)
Eq.(143)
Eq.(144)
Laminar
Critical
Region
Turbulent
Blasius
Gebers
Wieselsberger
Kempf
10^4
10^5
10^6
10^7
10^8
10^9
$R = \frac{V_0 L}{\nu}$

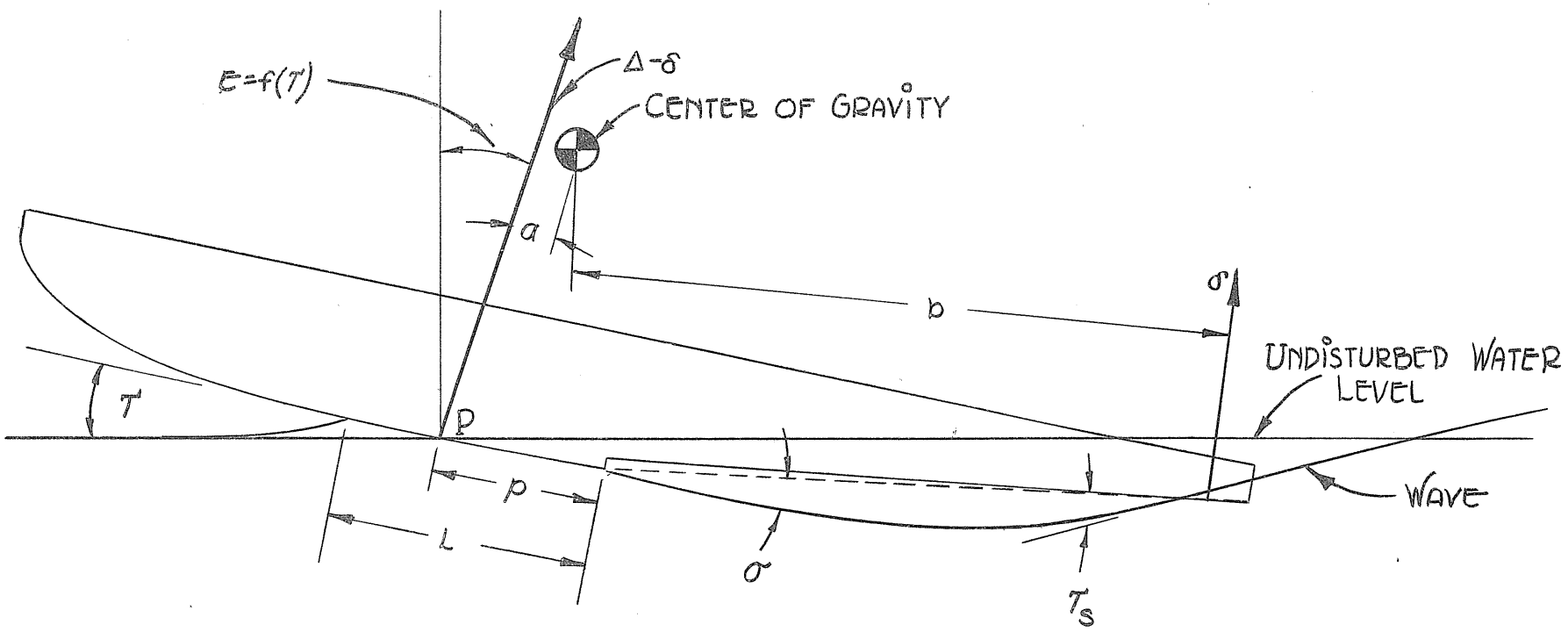
E=f(T)
Δ-δ
CENTER OF GRAVITY
a
b
σ'
UNDISTURBED WATER LEVEL
T
P
p
L
σ
WAVE
T_S

FIGURE 13

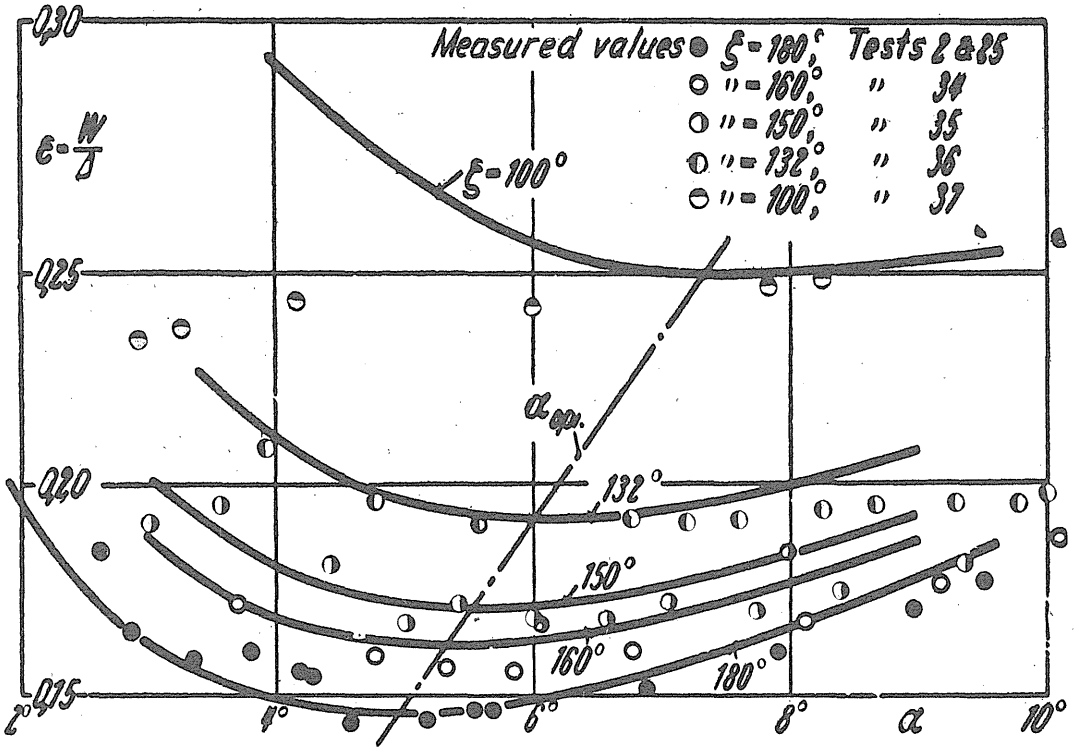
Measured values
ξ = 180°
" = 160°
" = 150°
" = 132°
" = 100°
Tests 2 & 25
" 34
" 35
" 36
" 37
ε = W/J
ξ = 100°
α ср.
132°
150°
160°
180°
0,30
0,25
0,20
0,15
1°
6°
8°
α
10°

Fig. 13a

FIGURE 14

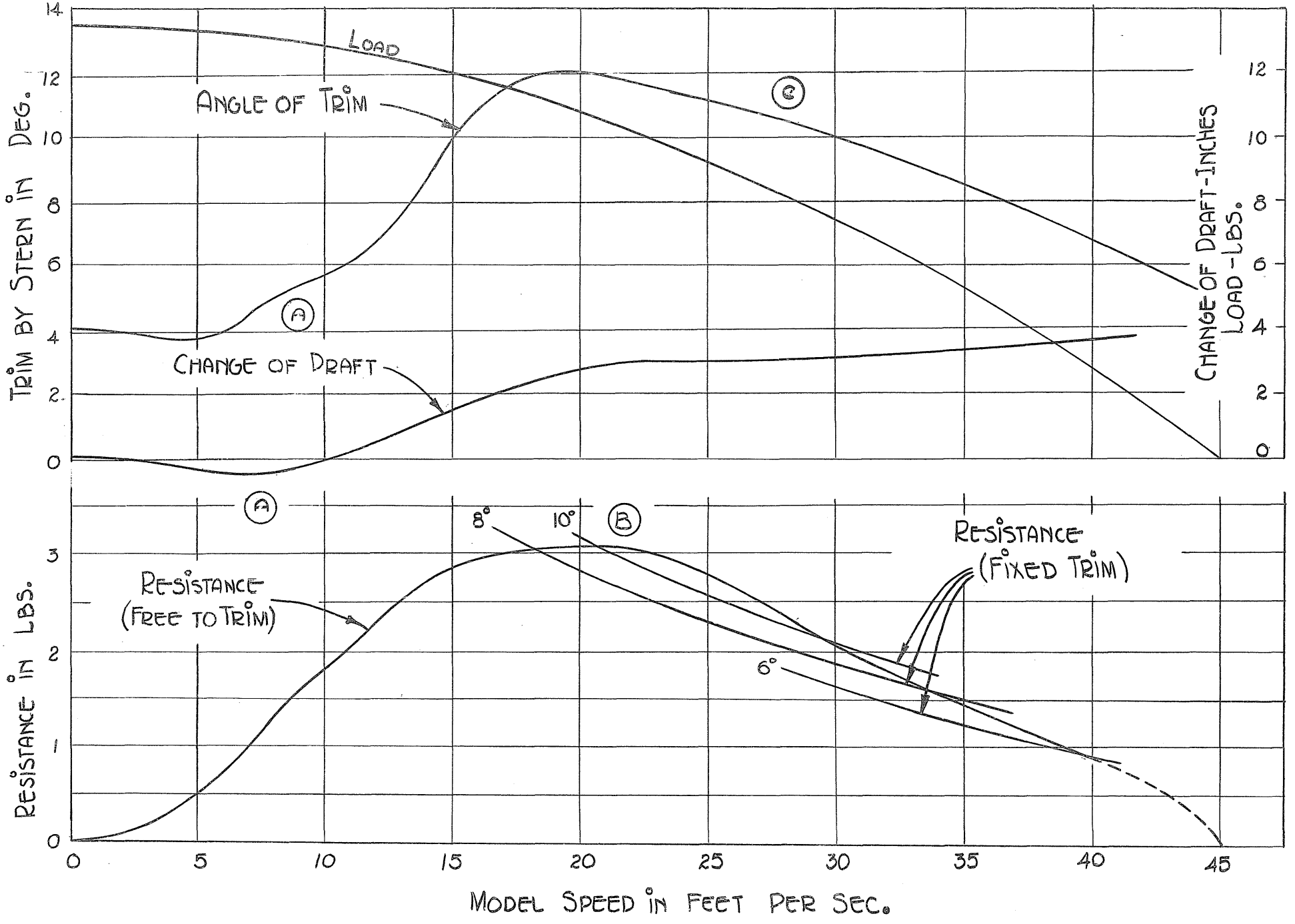
LOAD
ANGLE OF TRIM
CHANGE OF DRAFT
TRIM BY STERN IN DEG.
CHANGE OF DRAFT-INCHES
LOAD-LBS.
RESISTANCE IN LBS.
RESISTANCE (FREE TO TRIM)
RESISTANCE (FIXED TRIM)
8°
10°
6°
A
B
C
0
2
4
6
8
10
12
14
1
3
5
15
20
25
30
35
40
45
MODEL SPEED IN FEET PER SEC.

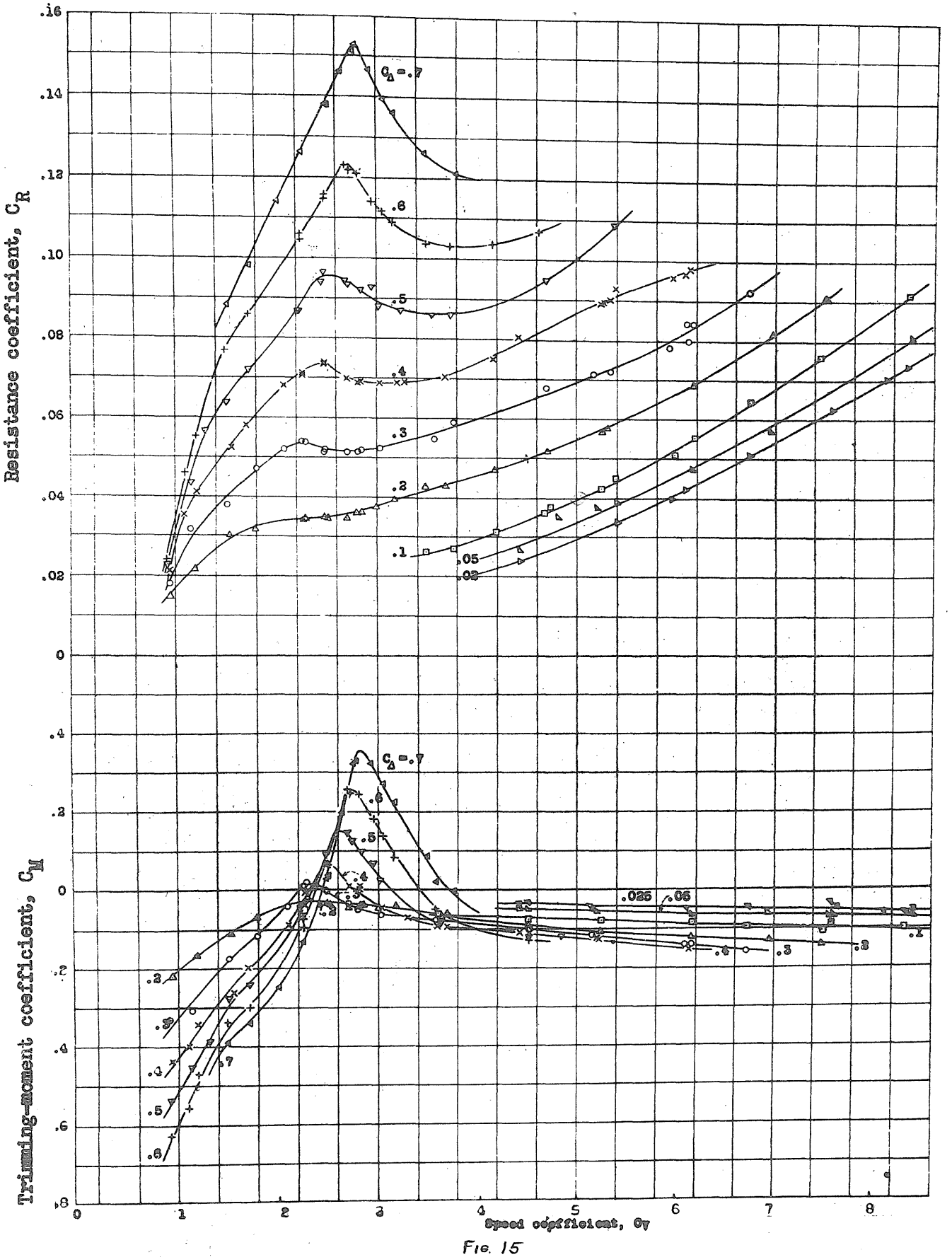
Resistance coefficient, C_R
Trimming-moment coefficient, C_M
Speed coefficient, C_V
$C_\Delta = .7$
.6
.5
.4
.3
.2
.1
.05
.025
.7

FIG. 15

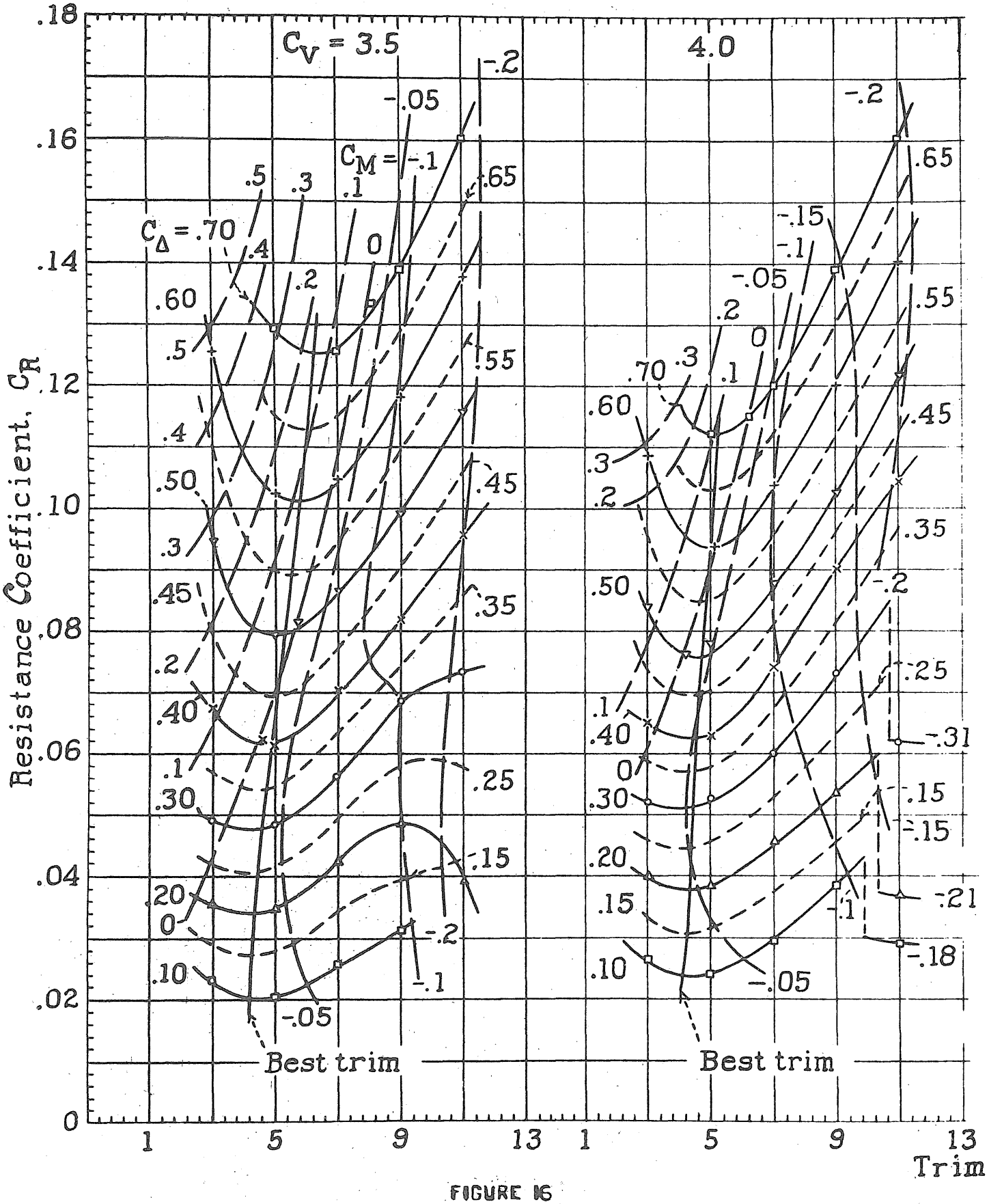
C_V = 3.5
4.0
C_M =
C_Δ = .70
Resistance Coefficient, C_R
Trim
Best trim
Best trim
.18
.16
.14
.12
.10
.08
.06
.04
.02
0
1
5
9
13

FIGURE 16

FIGURE 17

DESIGNATION: 3.25-1.04-20

MODEL NO. 1024-01
MODEL BEAM: 6.00"

C.G. = 0.25 b FWD. OF STEP
1.08 b ABOVE KEEL

C_{Δ_o} = 0.753 (NOMINAL)
k/L = 0.203

TESTED AT S.I.T. NO. 3 TANK
DATE: 6-8-49

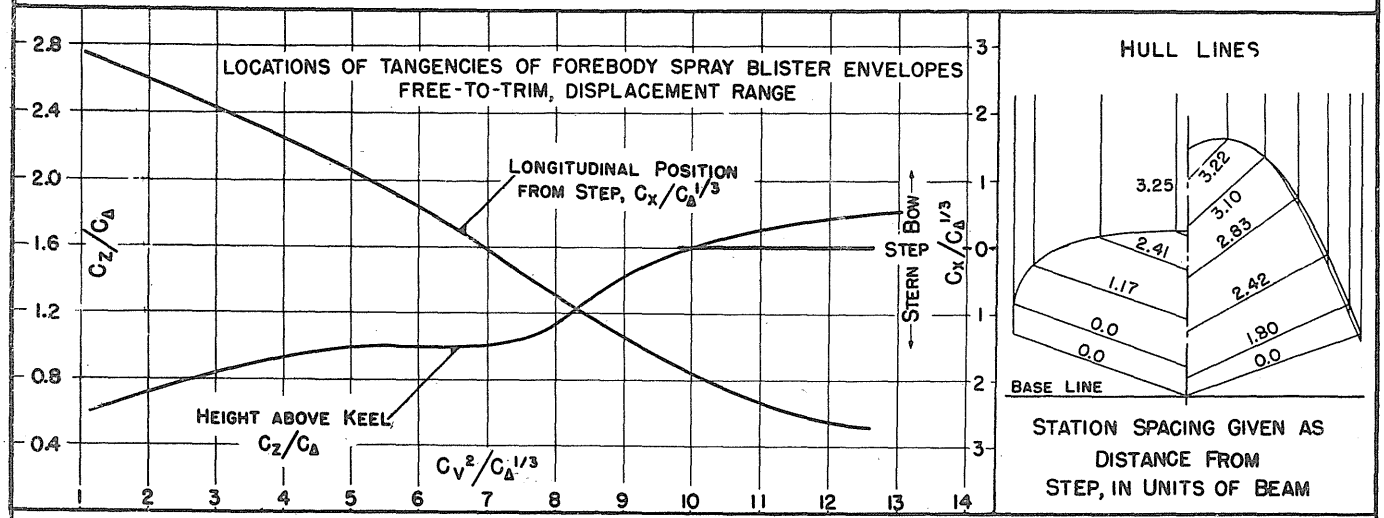

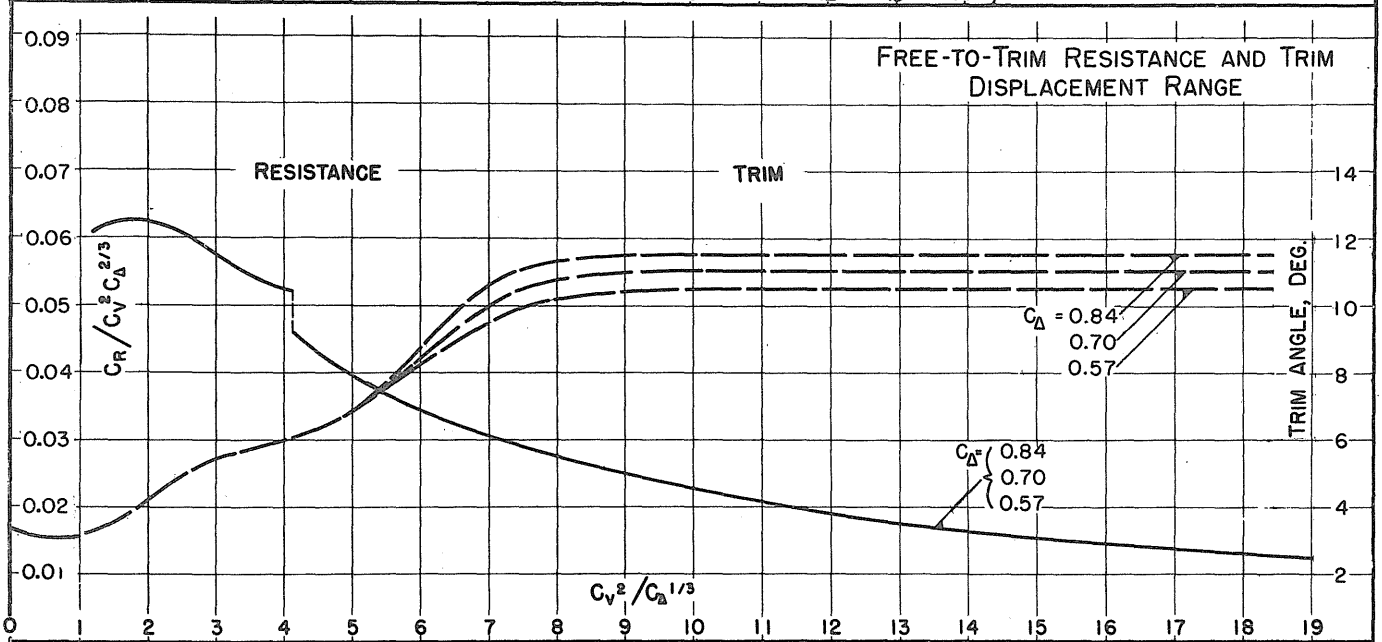

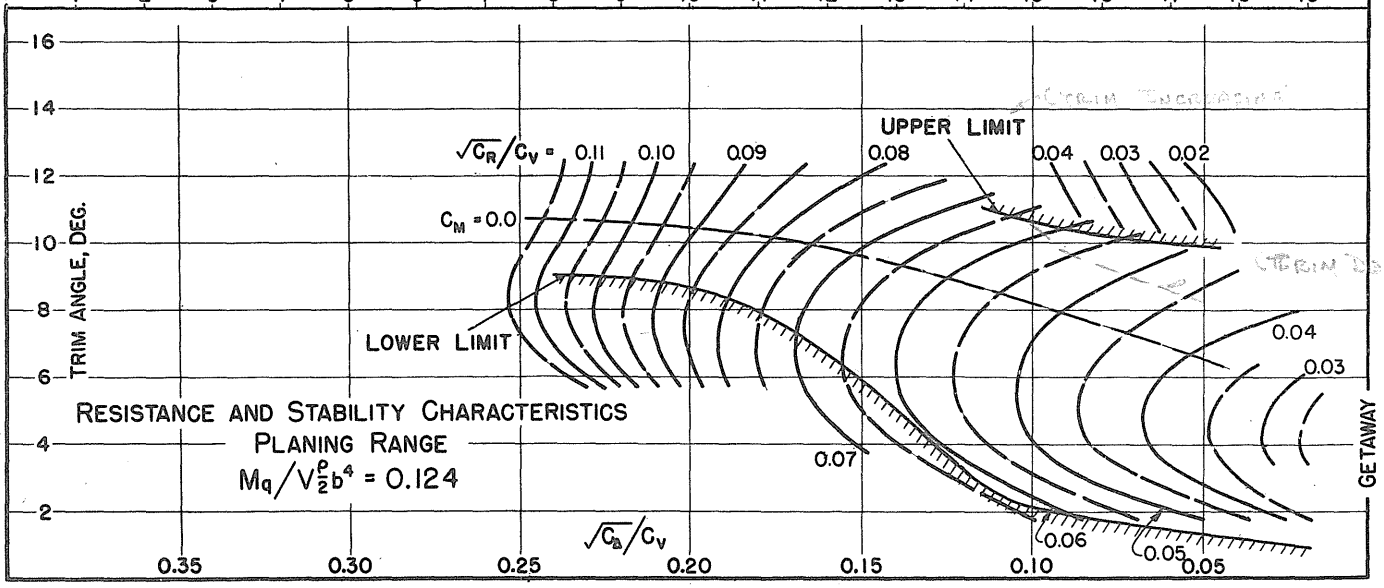

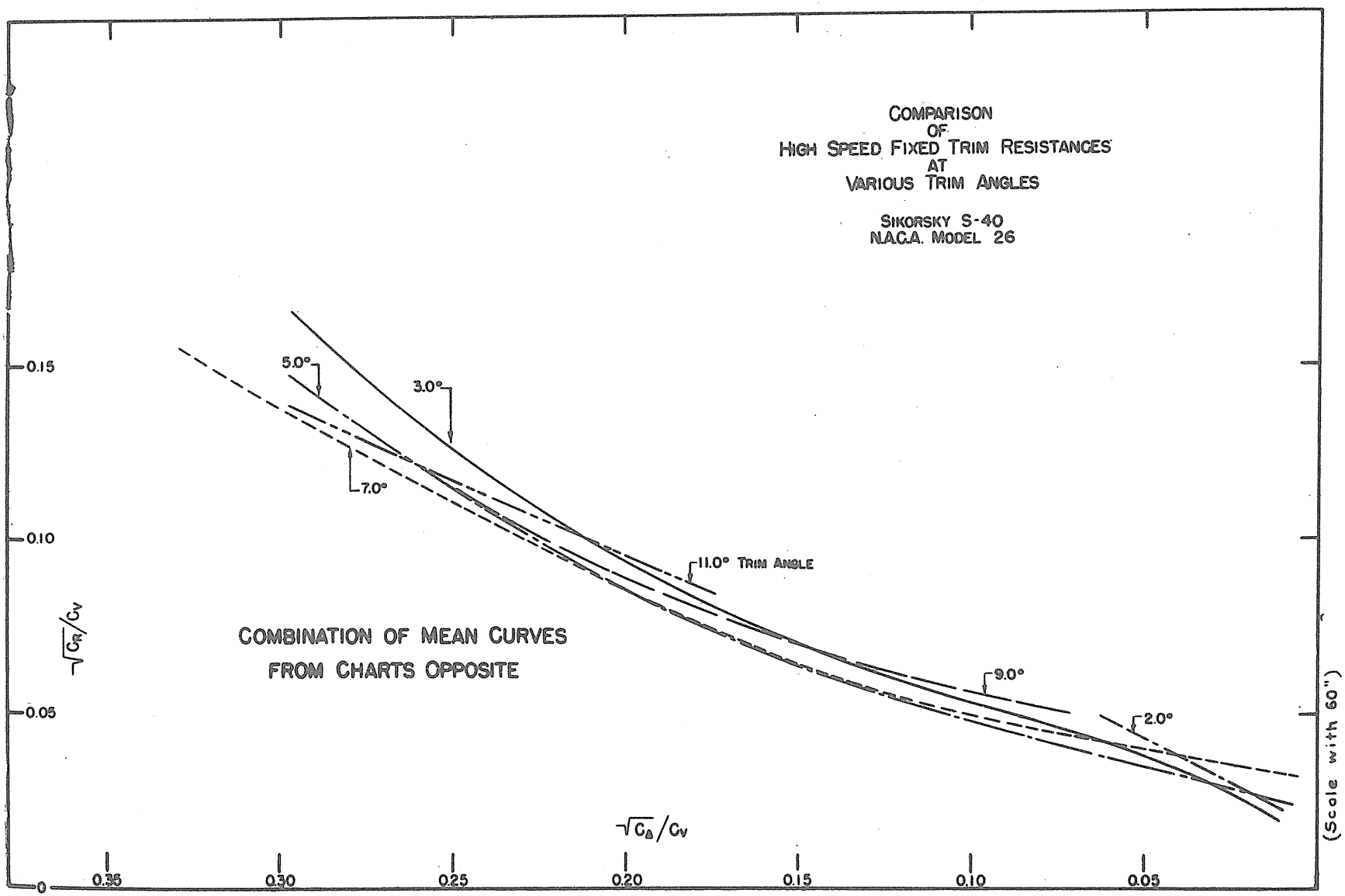
COMPARISON
OF
HIGH SPEED FIXED TRIM RESISTANCES
AT
VARIOUS TRIM ANGLES
SIKORSKY S-40
N.A.C.A. MODEL 26
5.0°
3.0°
7.0°
11.0° TRIM ANGLE
9.0°
2.0°
COMBINATION OF MEAN CURVES
FROM CHARTS OPPOSITE
$\sqrt{C_R}/C_V$
$\sqrt{C_\Delta}/C_V$
0.15
0.10
0.05
0
0.35
0.30
0.25
0.20
0.15
0.10
0.05
(Scale with 60")

FIGURE 18

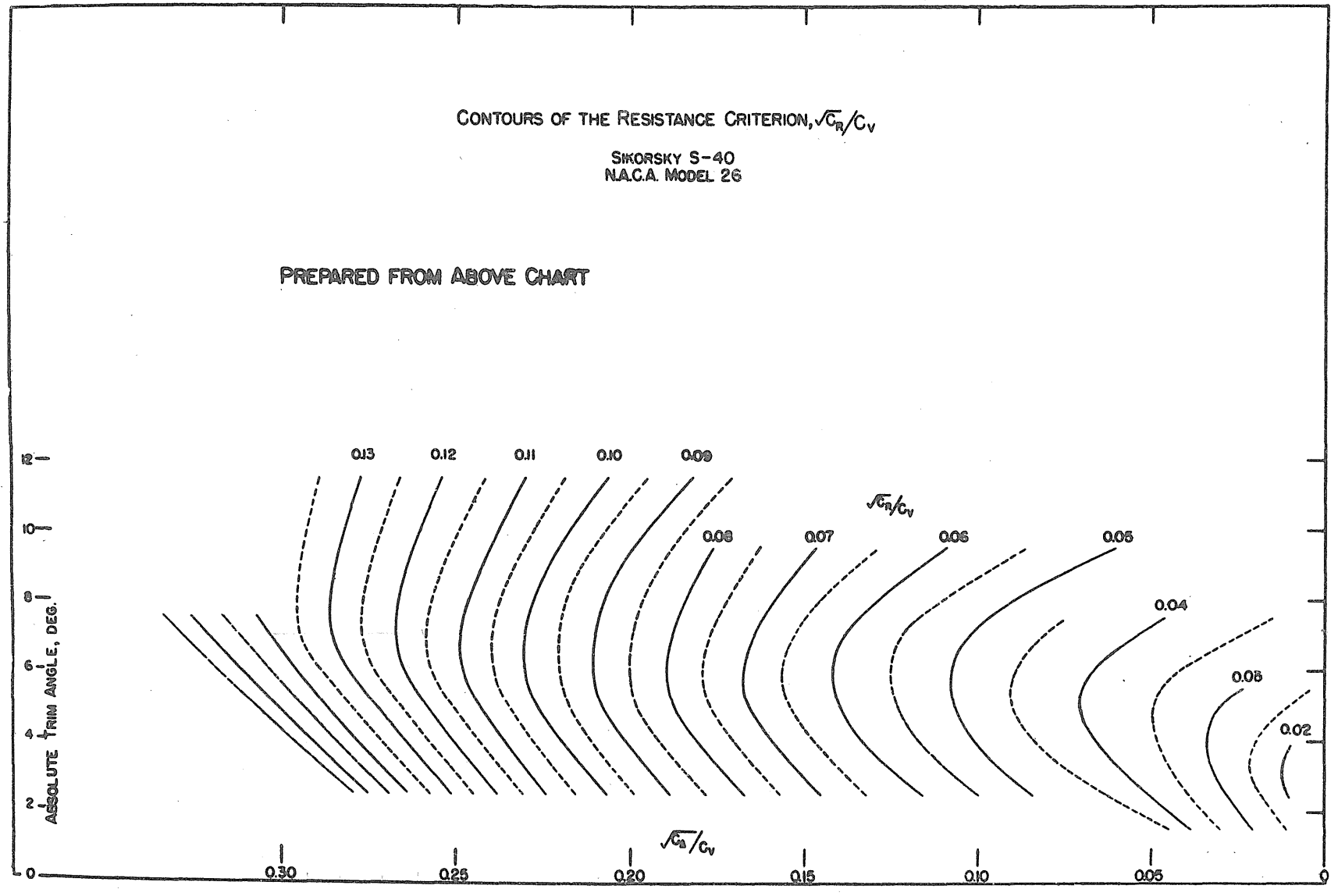
CONTOURS OF THE RESISTANCE CRITERION, $\sqrt{C_R}/C_V$
SIKORSKY S-40
N.A.C.A. MODEL 26
PREPARED FROM ABOVE CHART
ABSOLUTE TRIM ANGLE, DEG.
$\sqrt{C_R}/C_V$
0.13
0.12
0.11
0.10
0.09
0.08
0.07
0.06
0.05
0.04
0.03
0.02
0.30
0.25
0.20
0.15
0.10
0.05
0
2
4
6
8
10
12

FIGURE 19

FIGURE 20

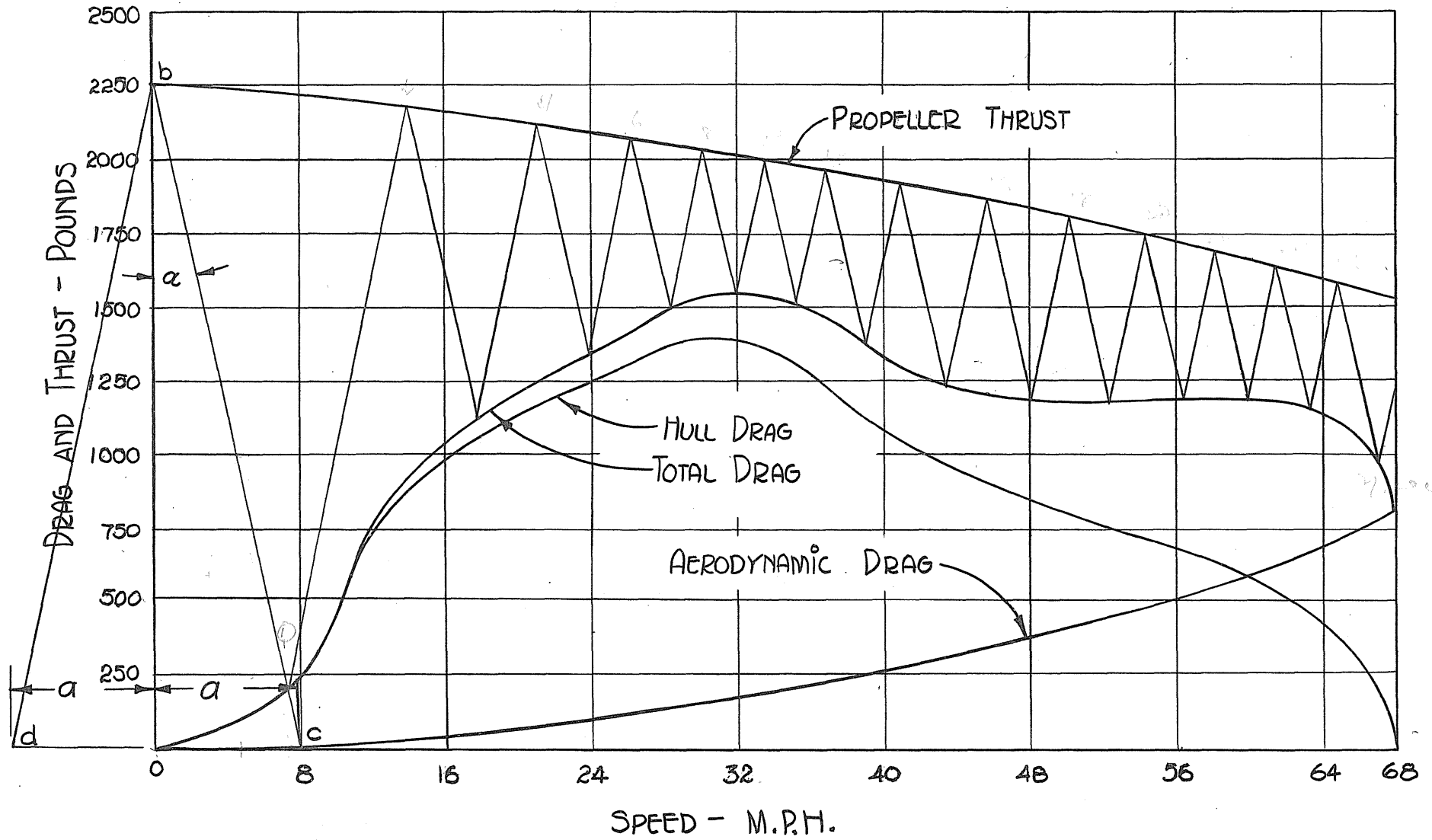
2500
2250
2000
1750
1500
1250
1000
750
500
250
b
a
a
a
d
c
PROPELLER THRUST
HULL DRAG
TOTAL DRAG
AERODYNAMIC DRAG
DRAG AND THRUST - POUNDS
0
8
16
24
32
40
48
56
64
68
SPEED - M.P.H.

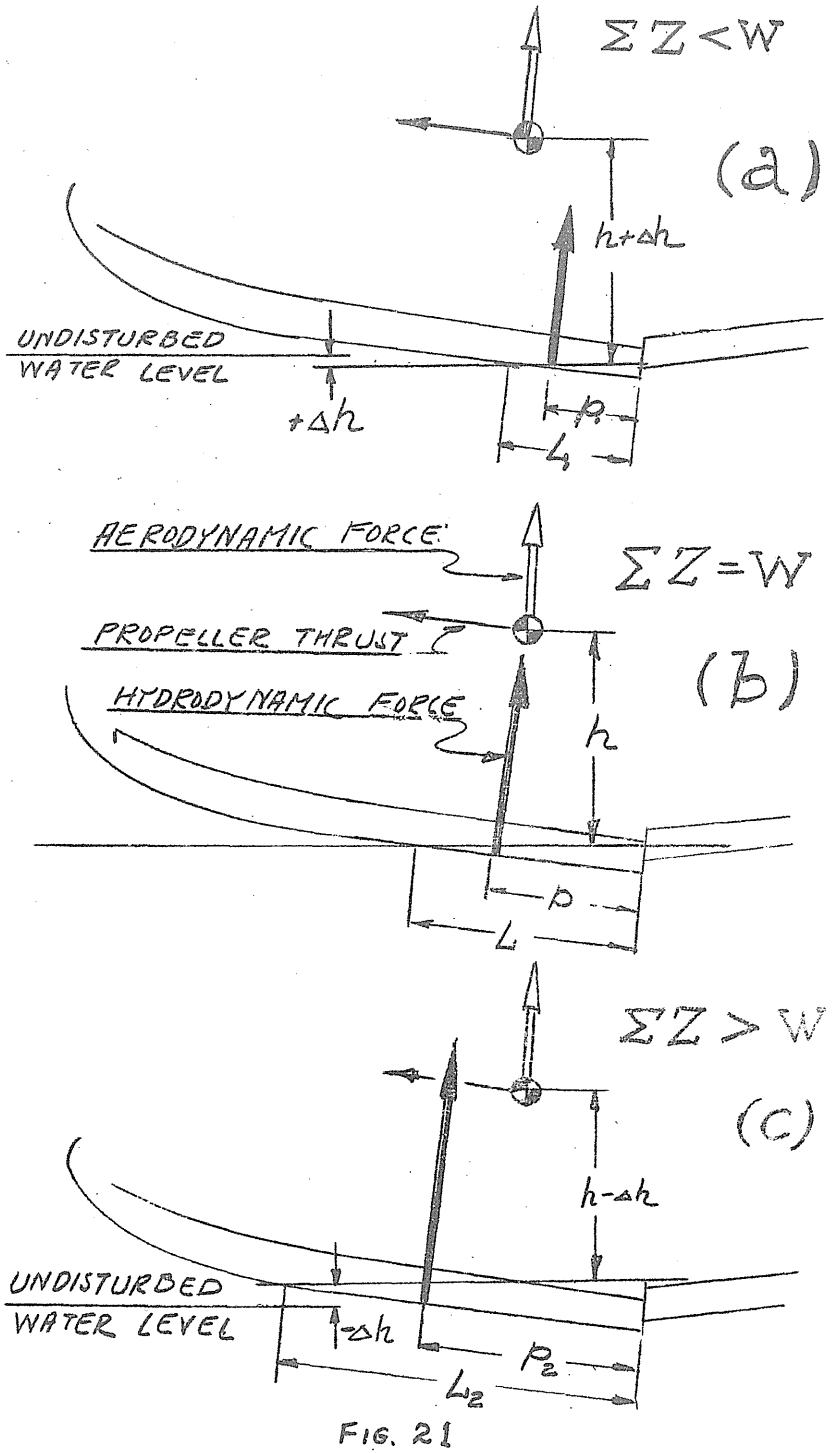
ΣZ<W
(a)
h+Δh
UNDISTURBED
WATER LEVEL
+Δh
p
L
AERODYNAMIC FORCE
ΣZ=W
PROPELLER THRUST
(b)
HYDRODYNAMIC FORCE
h
p
L
ΣZ>W
(c)
h-Δh
UNDISTURBED
WATER LEVEL
-Δh
p2
L2

FIG. 21

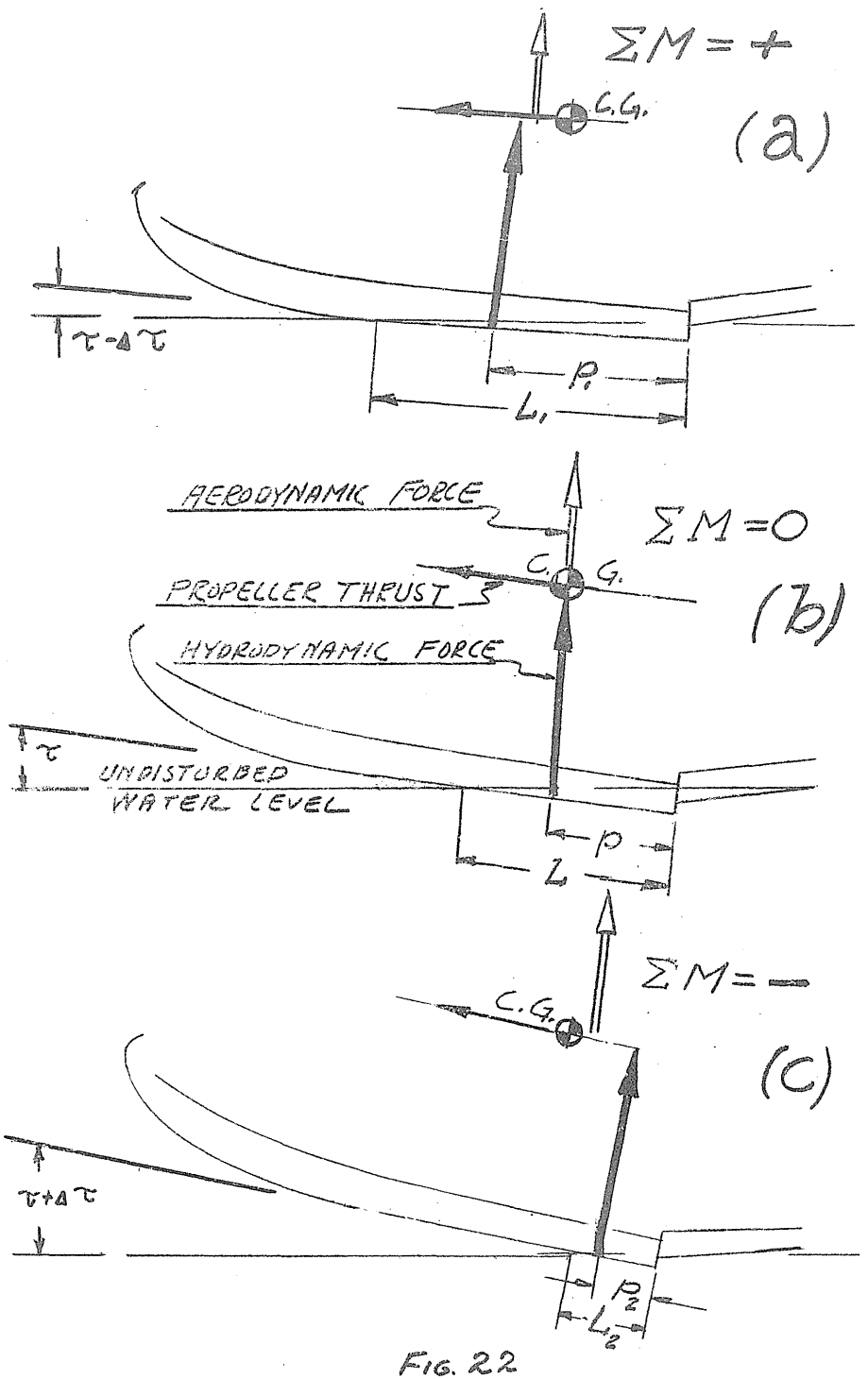
ΣM=+
C.G.
(a)
τ-Δτ
p1
L1
AERODYNAMIC FORCE
ΣM=0
C.G.
PROPELLER THRUST
(b)
HYDRODYNAMIC FORCE
τ
UNDISTURBED
WATER LEVEL
p
L
ΣM=-
C.G.
(c)
τ+Δτ
p2
L2

FIG. 22

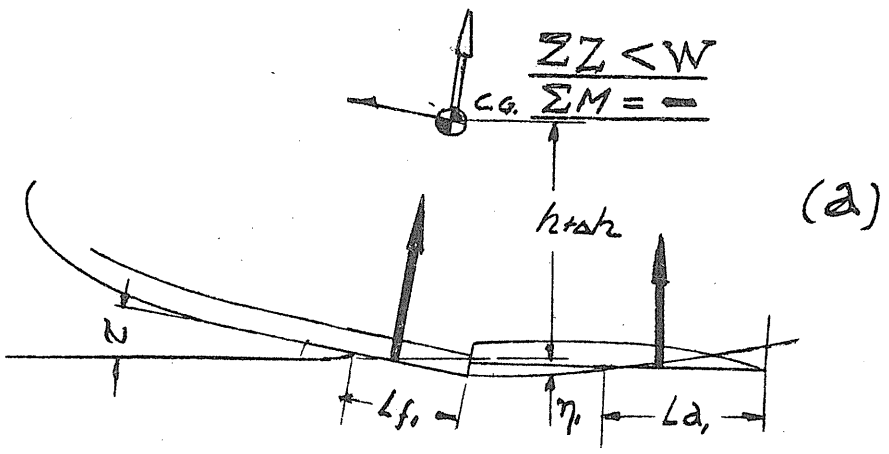
ΣZ < W
C.G. ΣM = −
h+Δh
(a)
Lf1
η1
La1

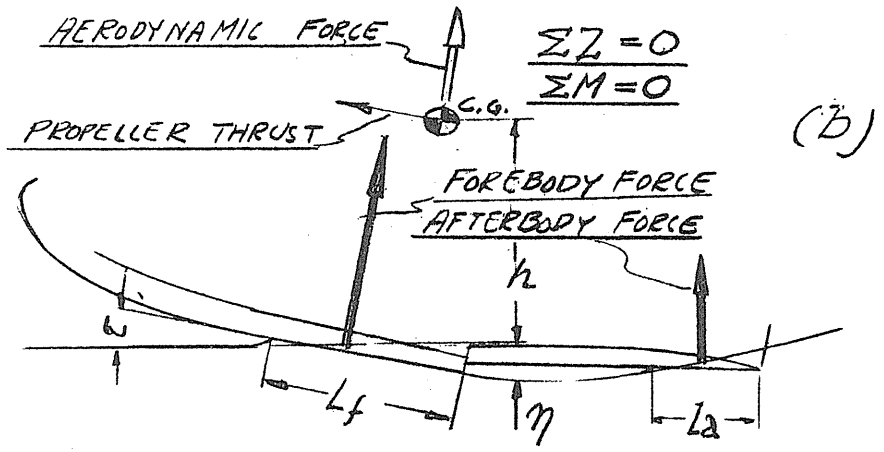
AERODYNAMIC FORCE
ΣZ = 0
ΣM = 0
C.G.
PROPELLER THRUST
FOREBODY FORCE
AFTERBODY FORCE
(b)
h
Lf
η
La

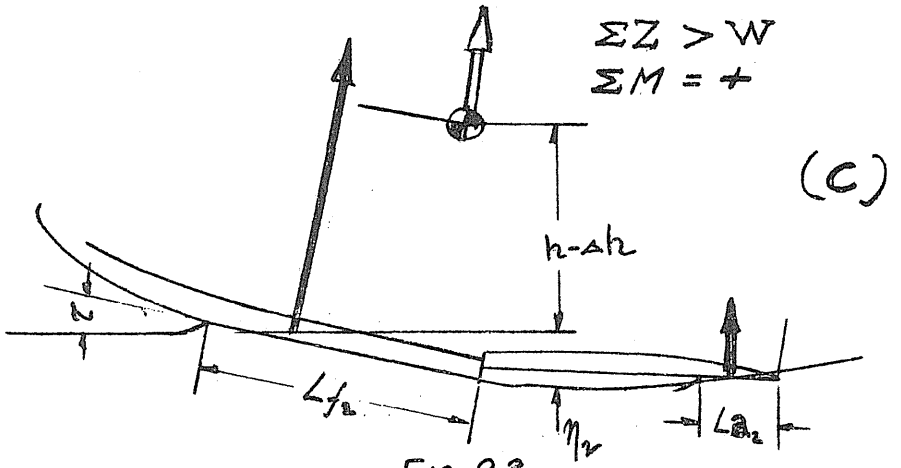
ΣZ > W
ΣM = +
(c)
h-Δh
Lf2
η2
La2

FIG. 23

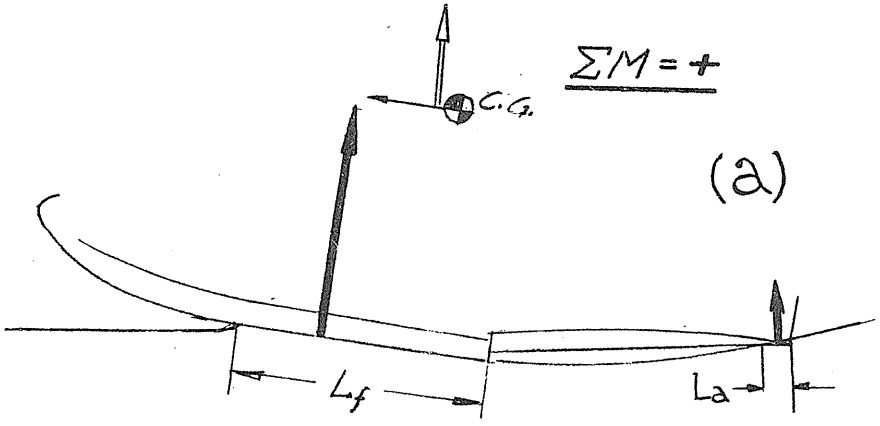
ΣM = +
C.G.
(a)
Lf
La

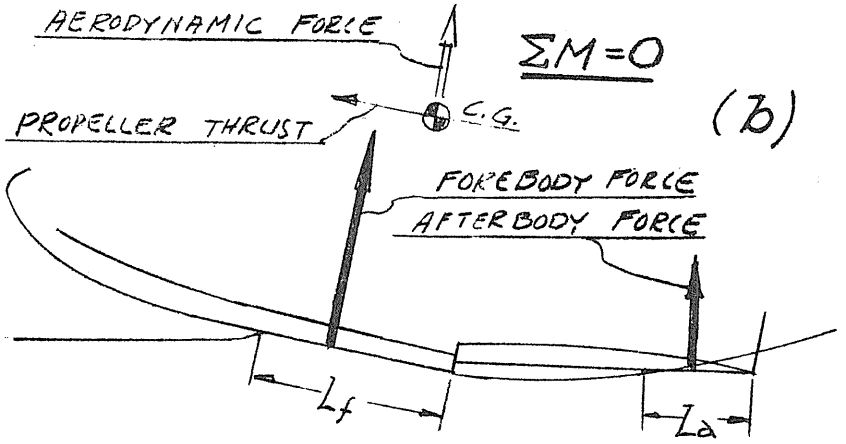
AERODYNAMIC FORCE
ΣM = 0
C.G.
PROPELLER THRUST
(b)
FOREBODY FORCE
AFTERBODY FORCE
Lf
La

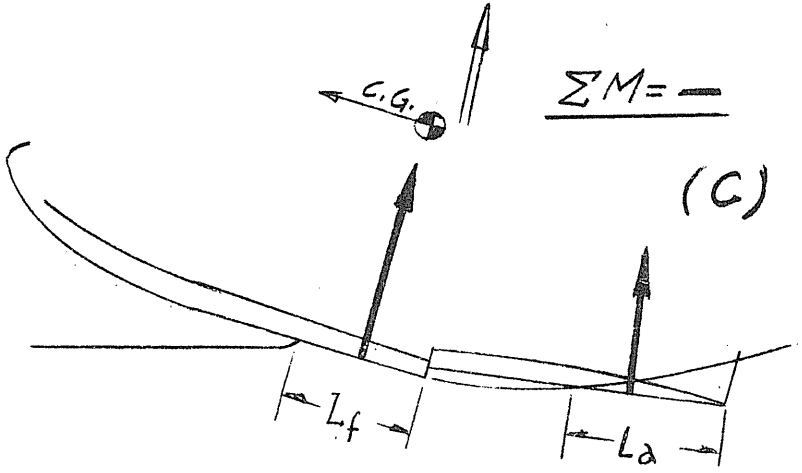
C.G.
ΣM = −
(c)
Lf
La

FIG. 24

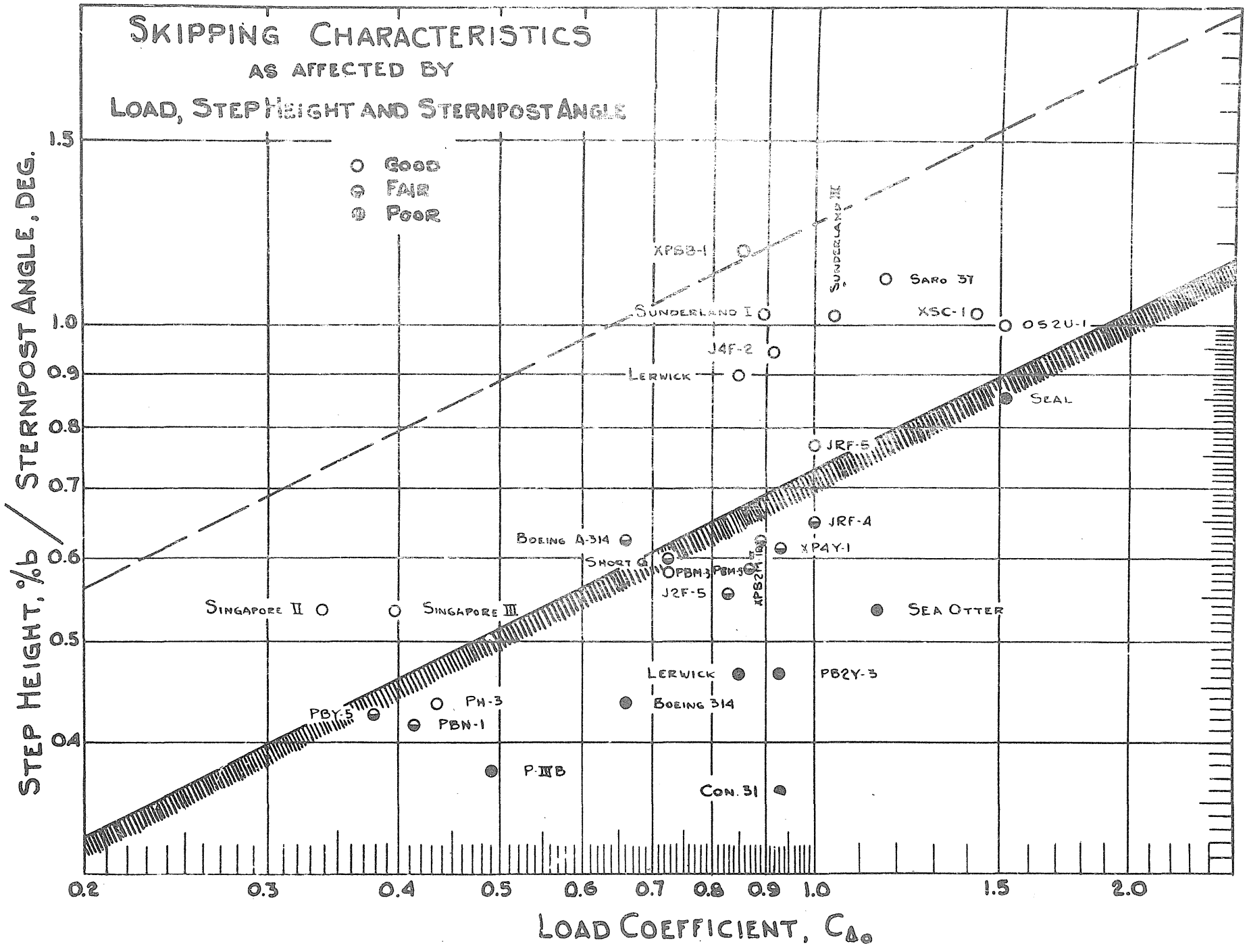
SKIPPING CHARACTERISTICS
AS AFFECTED BY
LOAD, STEP HEIGHT AND STERNPOST ANGLE
Good
Fair
Poor
STEP HEIGHT, %b / STERNPOST ANGLE, DEG.
LOAD COEFFICIENT, C_{Δ_o}
1.5
1.0
0.9
0.8
0.7
0.6
0.5
0.4
0.2
0.3
0.4
0.5
0.6
0.7
0.8
0.9
1.0
1.5
2.0
XPSB-1
SUNDERLAND III
SARO 37
SUNDERLAND I
XSC-10
OS2U-1
J4F-2
LERWICK
SEAL
JRF-5
JRF-4
BOEING A-314
XP4Y-1
SHORT S
OPBM-3
PBM-3
XPB2M (BOEING)
J2F-5
SINGAPORE II
SINGAPORE III
SEA OTTER
LERWICK
PB2Y-3
PBY-5
PH-3
PBN-1
BOEING 314
P-IIIB
CON. 31

FIGURE 25

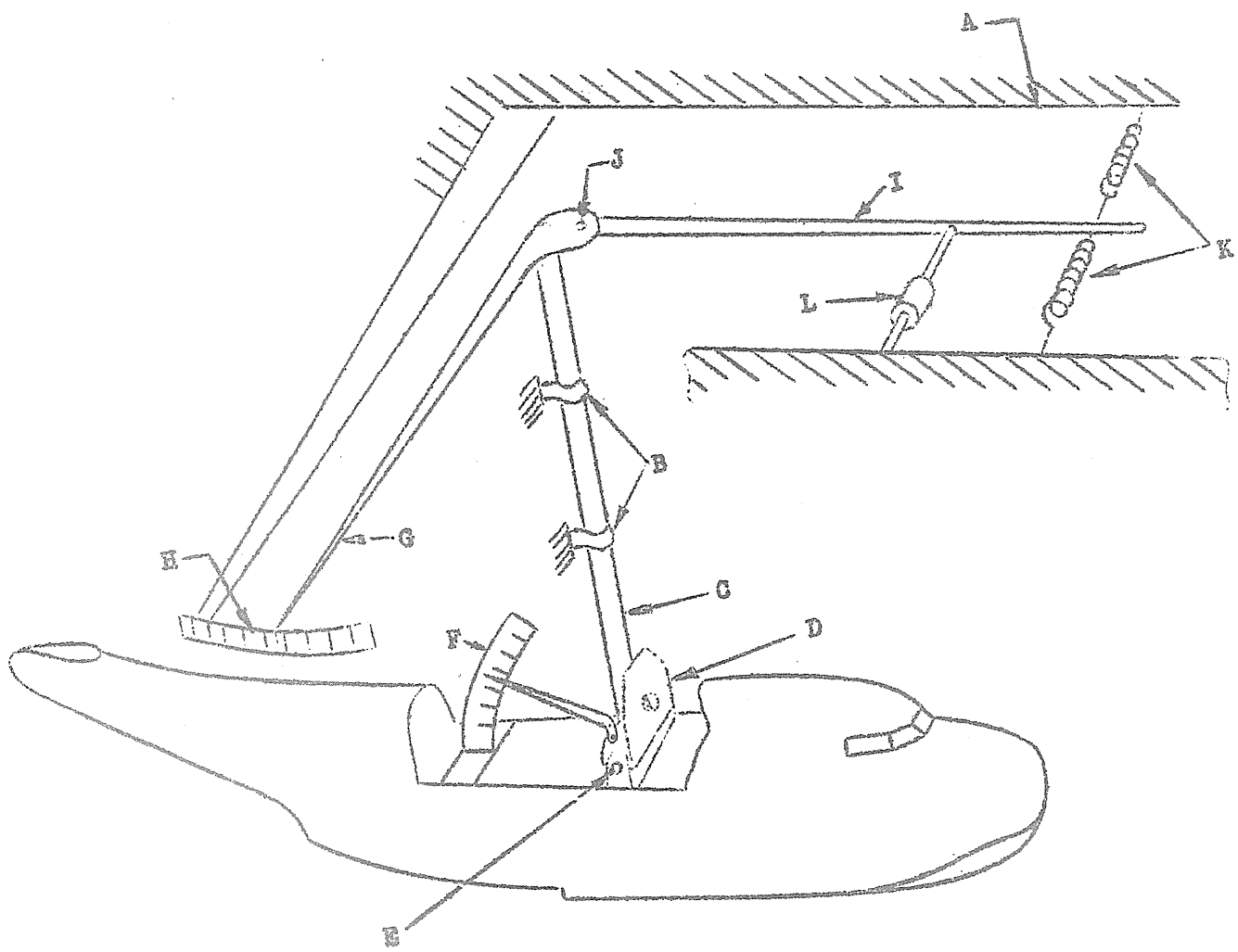

Fig.25A Diagrammatic Sketch of Apparatus for Yaw Tests

A - Main towing gate (free vertically)
B - Strut bearings attached to frame (A)
C - Model support tube (free to rotate about vertical axis
D - Heel angle adjustment
E - Pivot points, model attachment (freedom in pitch)
F - Trim scale on model
G - Yaw angle indicator fastened to tube (C)
H - Yaw angle scale fastened to (A)
I - Torque arm pivoted at axis of (C) clamped to (G)
J - Yaw angle adjustment
K - Spring restraining yaw
L - Dashpot, Yaw Damper

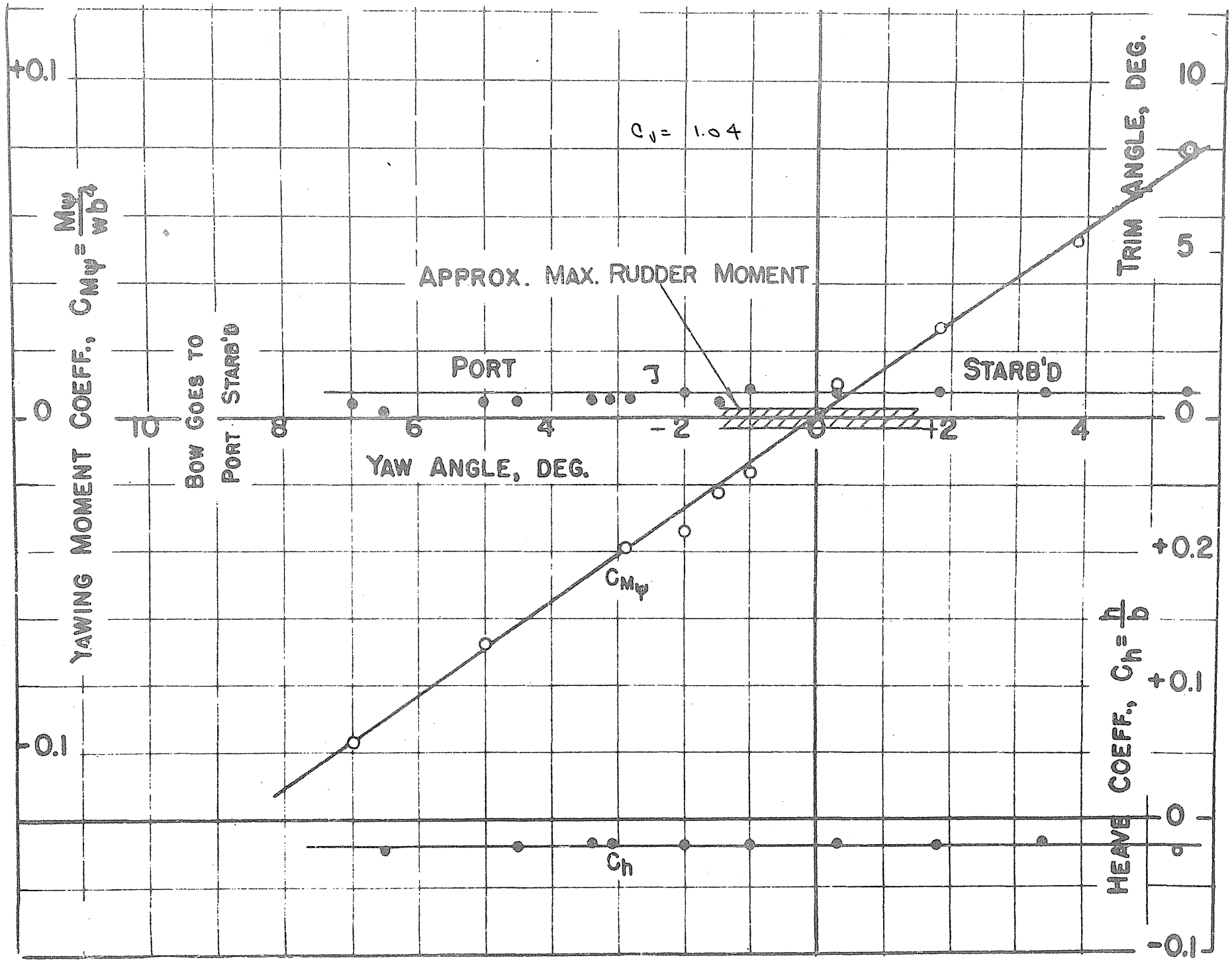
+0.1
0
-0.1
YAWING MOMENT COEFF., $C_{M\psi} = \frac{M\psi}{wb^2}$
$C_V = 1.04$
APPROX. MAX. RUDDER MOMENT
PORT
STARB'D
BOW GOES TO PORT
STARB'D
10
8
6
4
2
0
2
4
YAW ANGLE, DEG.
$C_{M\psi}$
C_h
TRIM ANGLE, DEG.
10
5
0
HEAVE COEFF., $C_h = \frac{h}{b}$
+0.2
+0.1
0
-0.1

FIGURE 26

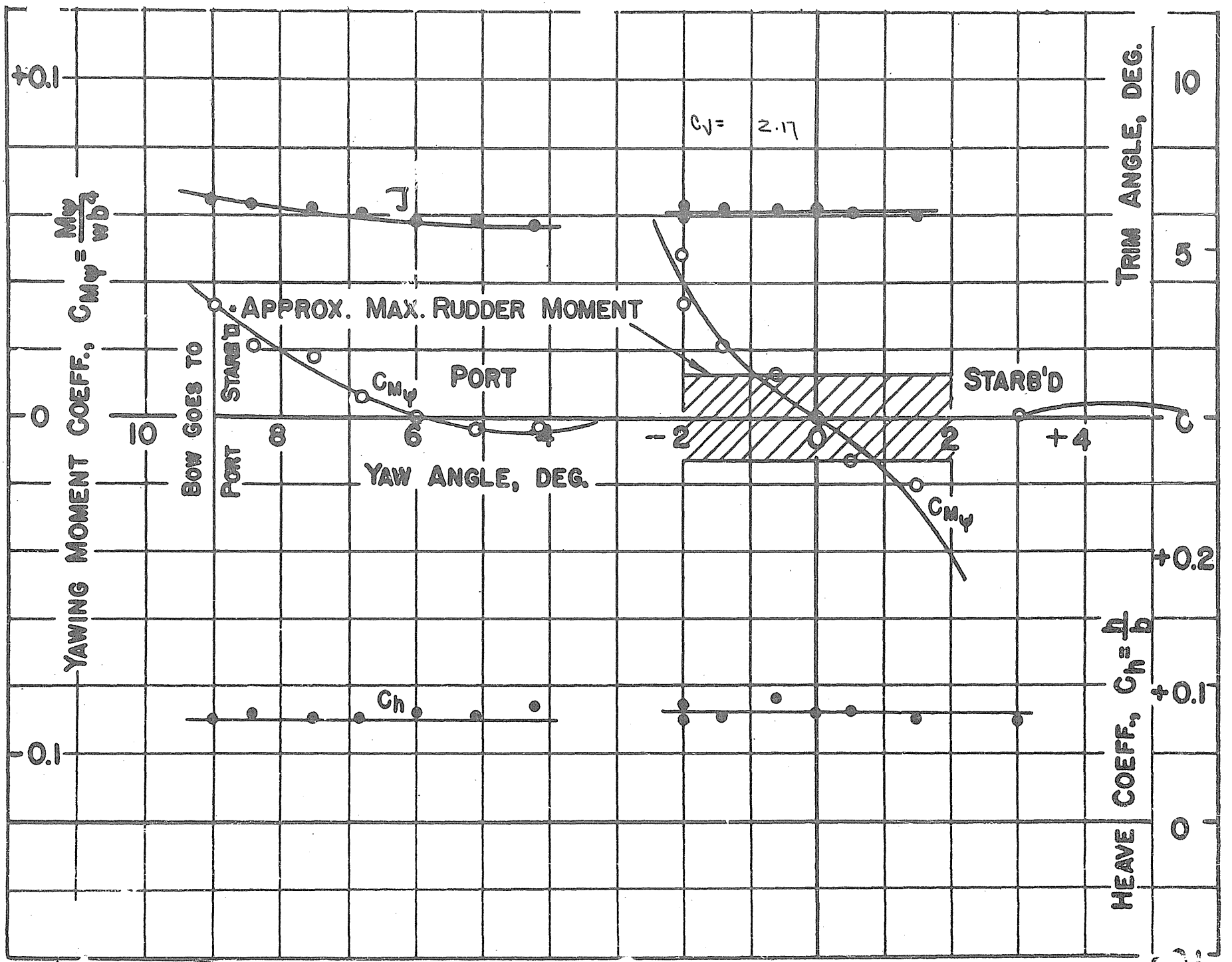
+0.1
0
-0.1
YAWING MOMENT COEFF., $C_{M\psi} = \frac{M_\psi}{wb^3}$
C_V = 2.17
J
APPROX. MAX. RUDDER MOMENT
$C_{M\psi}$
PORT
STARB'D
BOW GOES TO
STARB'D
PORT
10
8
6
4
2
0
2
+4
YAW ANGLE, DEG.
$C_{M\psi}$
C_h
TRIM ANGLE, DEG.
10
5
0
+0.2
+0.1
0
HEAVE COEFF., $C_h = \frac{h}{b}$

FIGURE 27

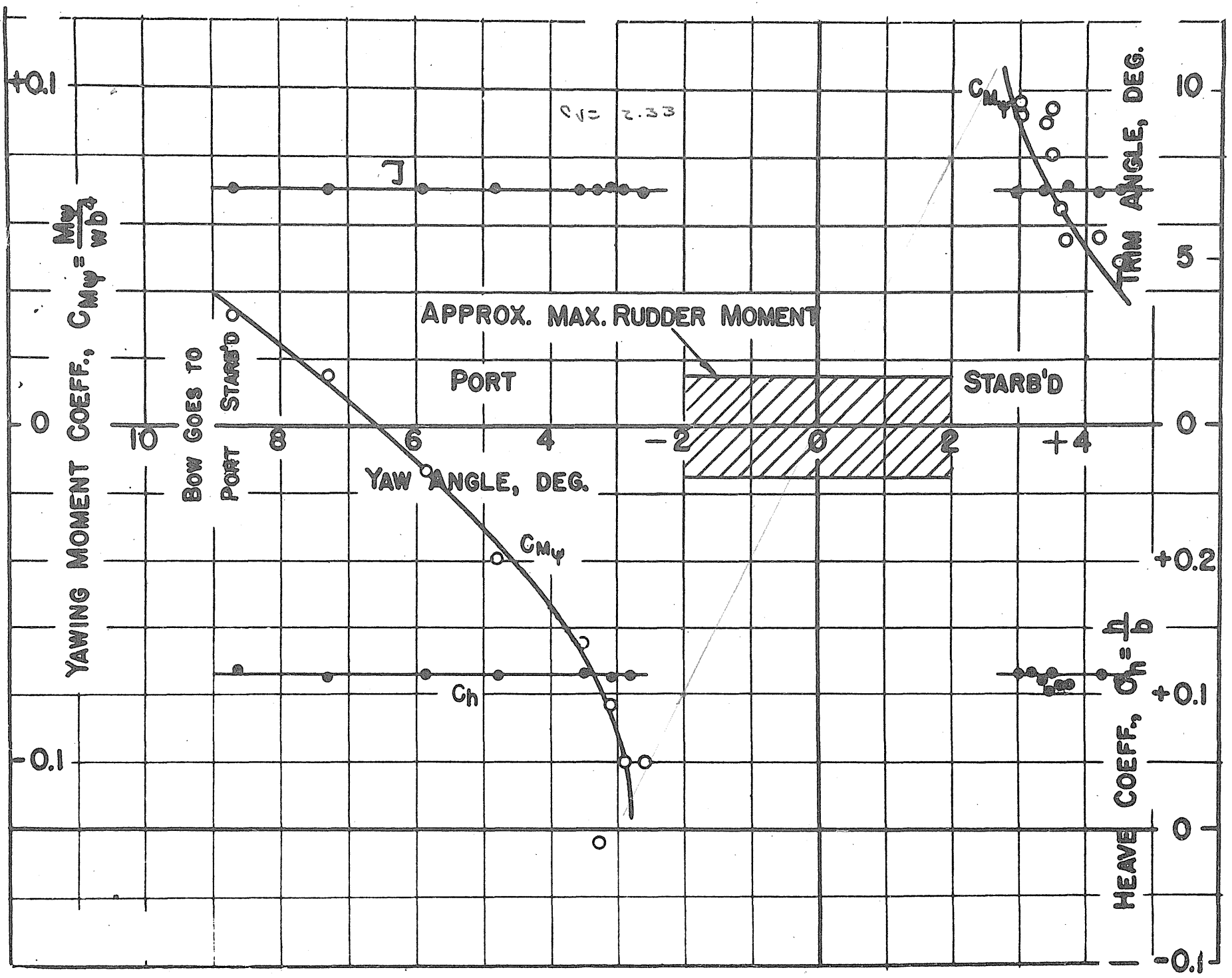
+0.1
0
-0.1
YAWING MOMENT COEFF., $C_{M\psi} = \frac{M_\psi}{wb^4}$
C_{M_ψ}
J
C_h
$V = 2.33$
APPROX. MAX. RUDDER MOMENT
PORT
STARB'D
BOW GOES TO
PORT
STARB'D
10
8
6
4
-2
0
2
+4
YAW ANGLE, DEG.
TRIM ANGLE, DEG.
10
5
0
+0.2
+0.1
0
-0.1
HEAVE COEFF., $C_h = \frac{h}{b}$

FIGURE 28

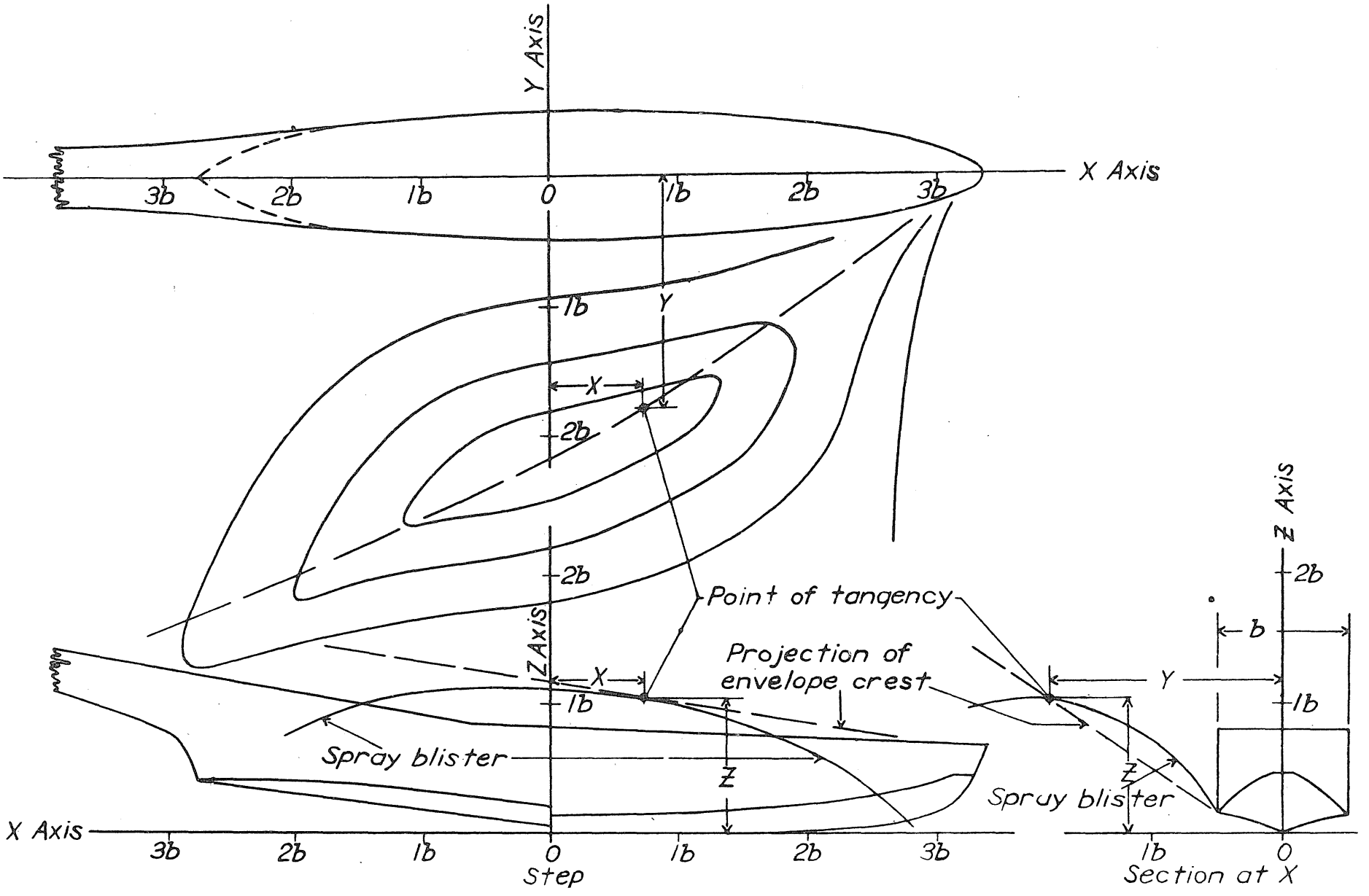
Y Axis
X Axis
3b
2b
1b
0
1b
2b
3b
Y
X
Z Axis
Point of tangency
Projection of envelope crest
Spray blister
Z
Step
Section at X
b

FIGURE 29

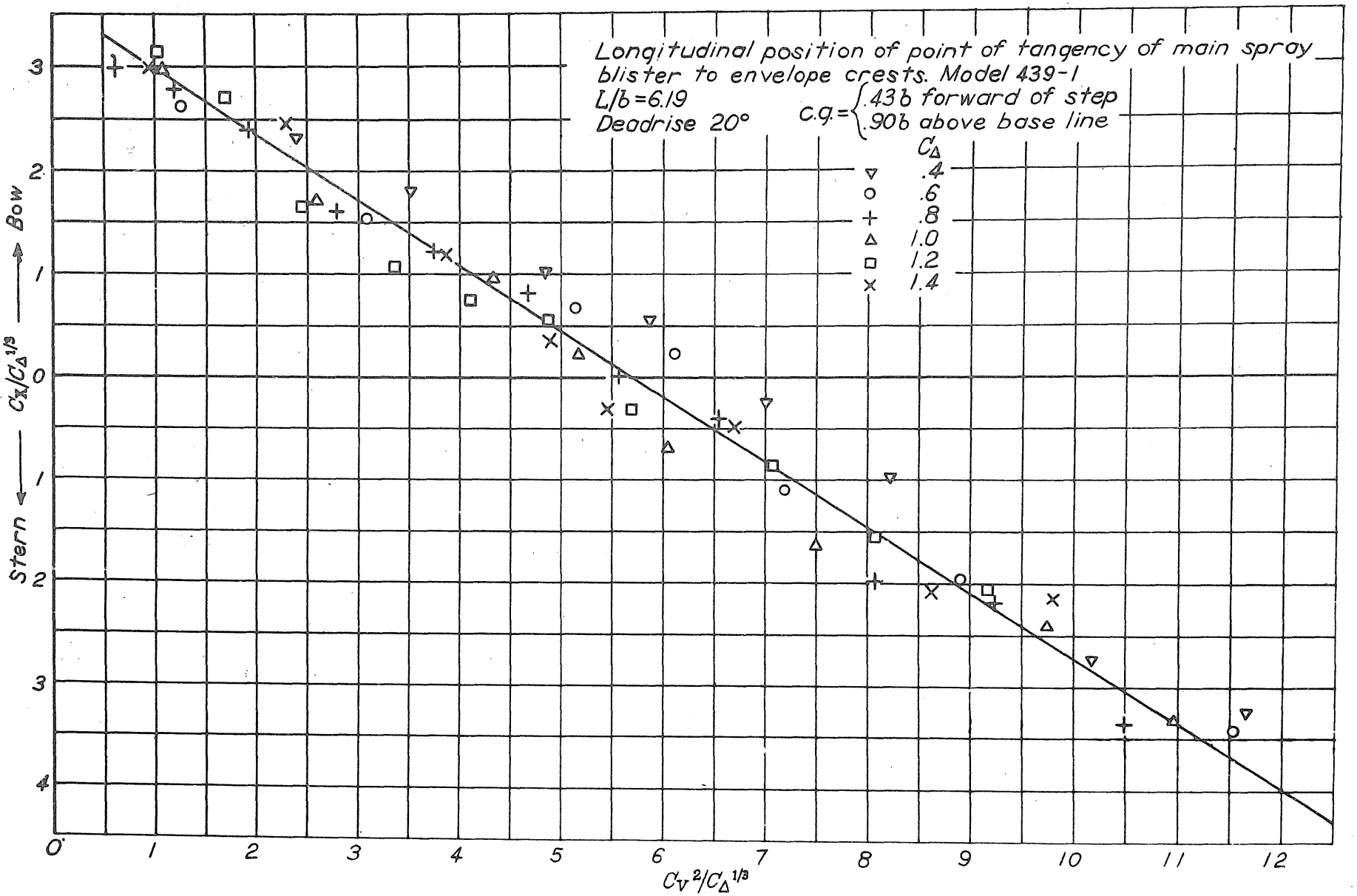
Longitudinal position of point of tangency of main spray blister to envelope crests. Model 439-1
L/b = 6.19
Deadrise 20°
c.g. = .43b forward of step
.90b above base line
C_Δ
.4
.6
.8
1.0
1.2
1.4
Stern ← $C_X/C_\Delta^{1/3}$ → Bow
$C_V^2/C_\Delta^{1/3}$
0
1
2
3
4
5
6
7
8
9
10
11
12

FIGURE 30

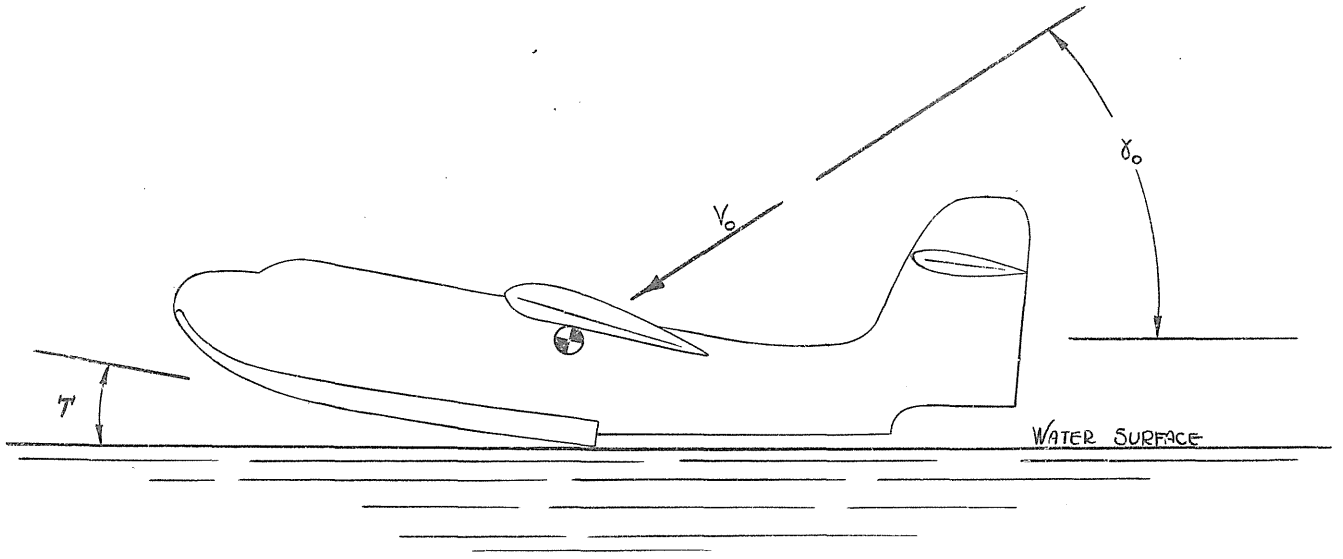

(a)

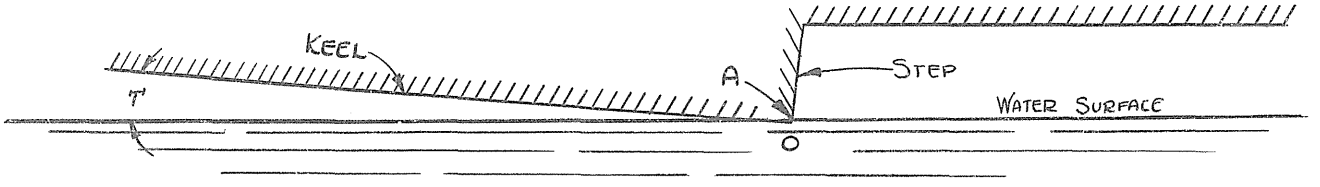

(b)

FIGURE 31

SEAPLANE AT INSTANT OF ENTRY INTO WATER

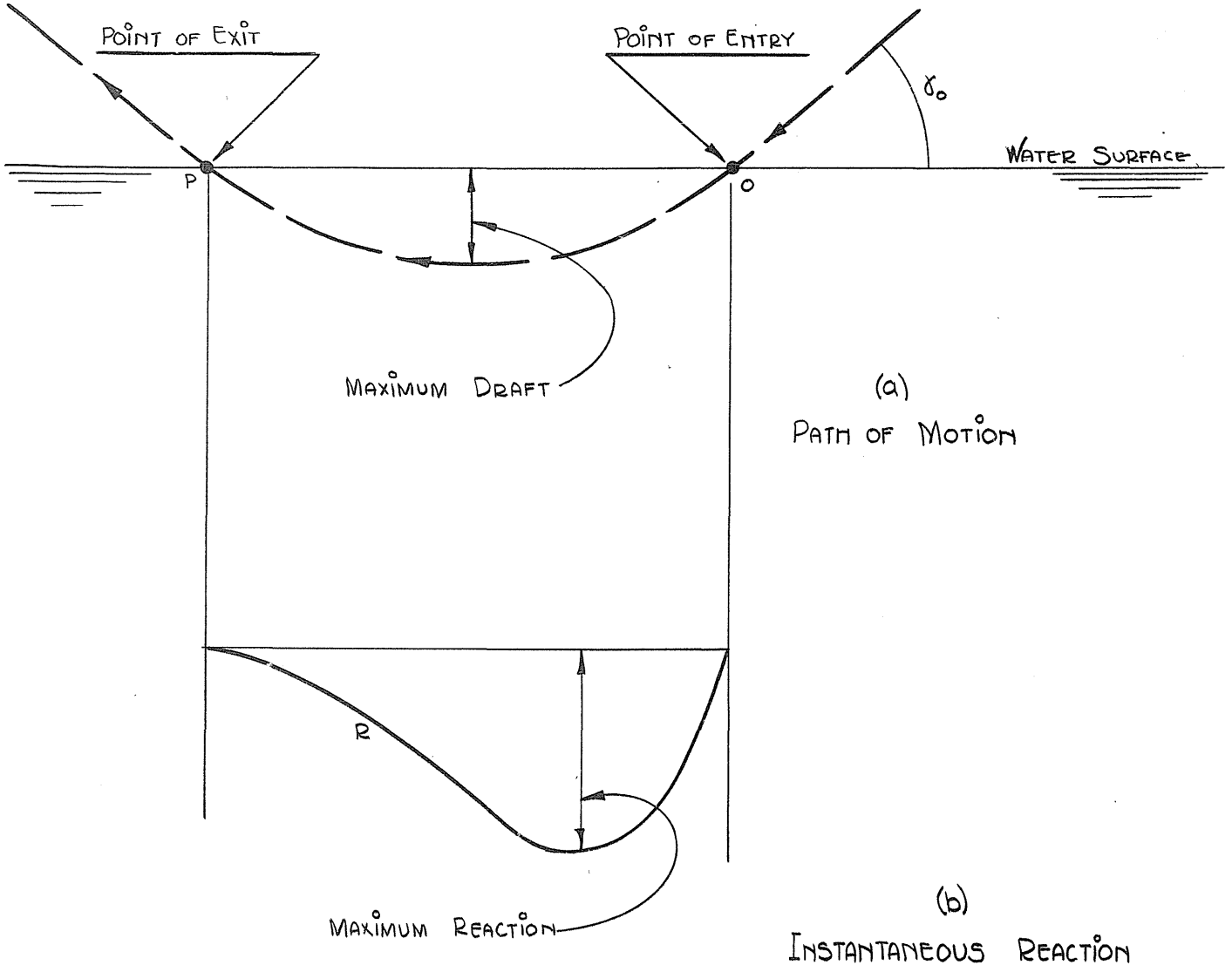

FIGURE 32
TRAJECTORY OF THE STEP POINT AND REACTION DURING IMPACT PERIOD

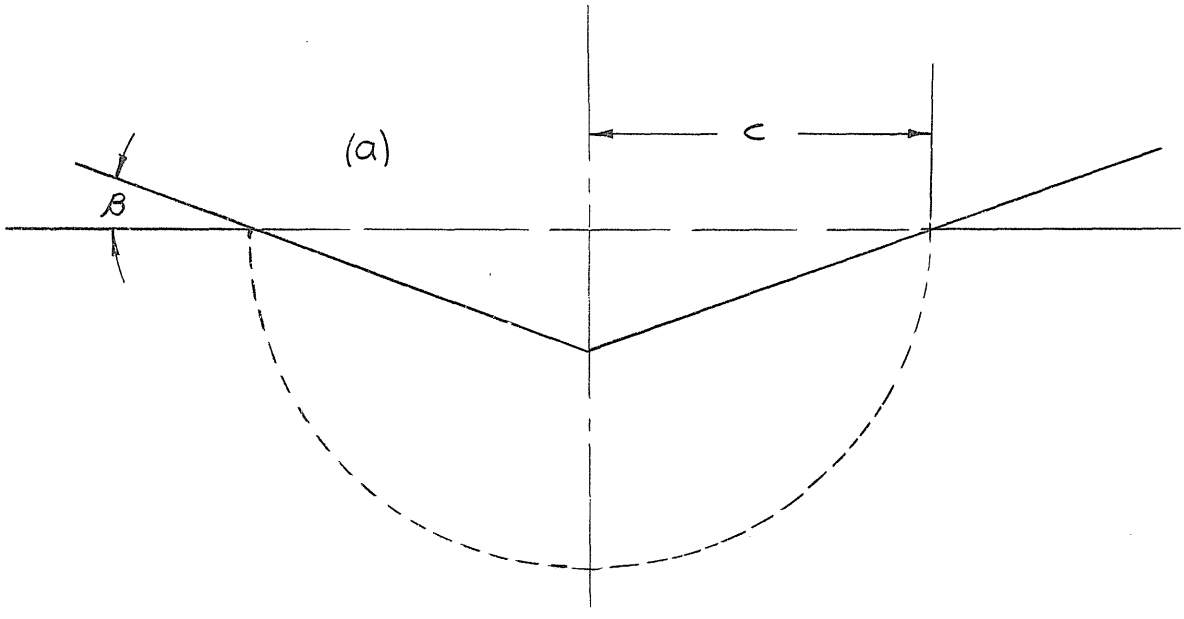

(a) As Originally Visualized By Von Karman

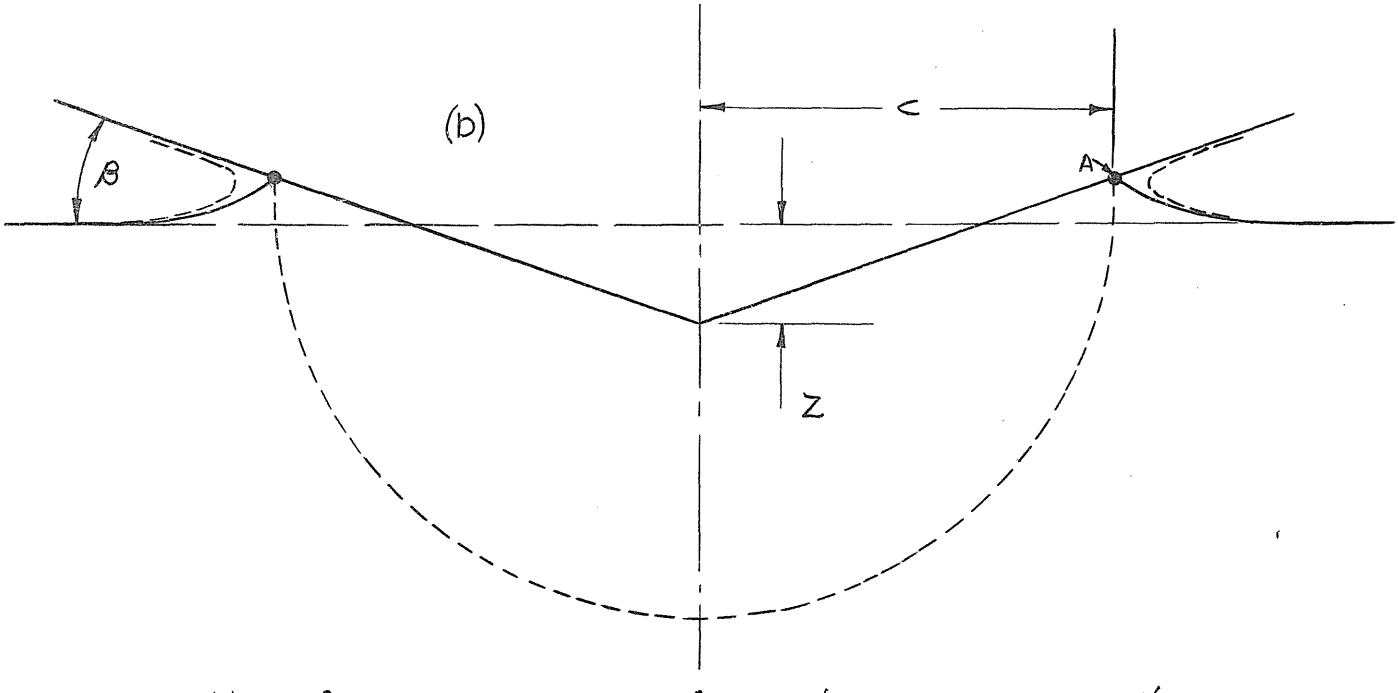

(b) Taking Into Account the Rise of Water as Used By H. Wagner

Figure 33

Half Cylinder of Water the Mass of Which is Added to the Mass of the Wedge in Impact

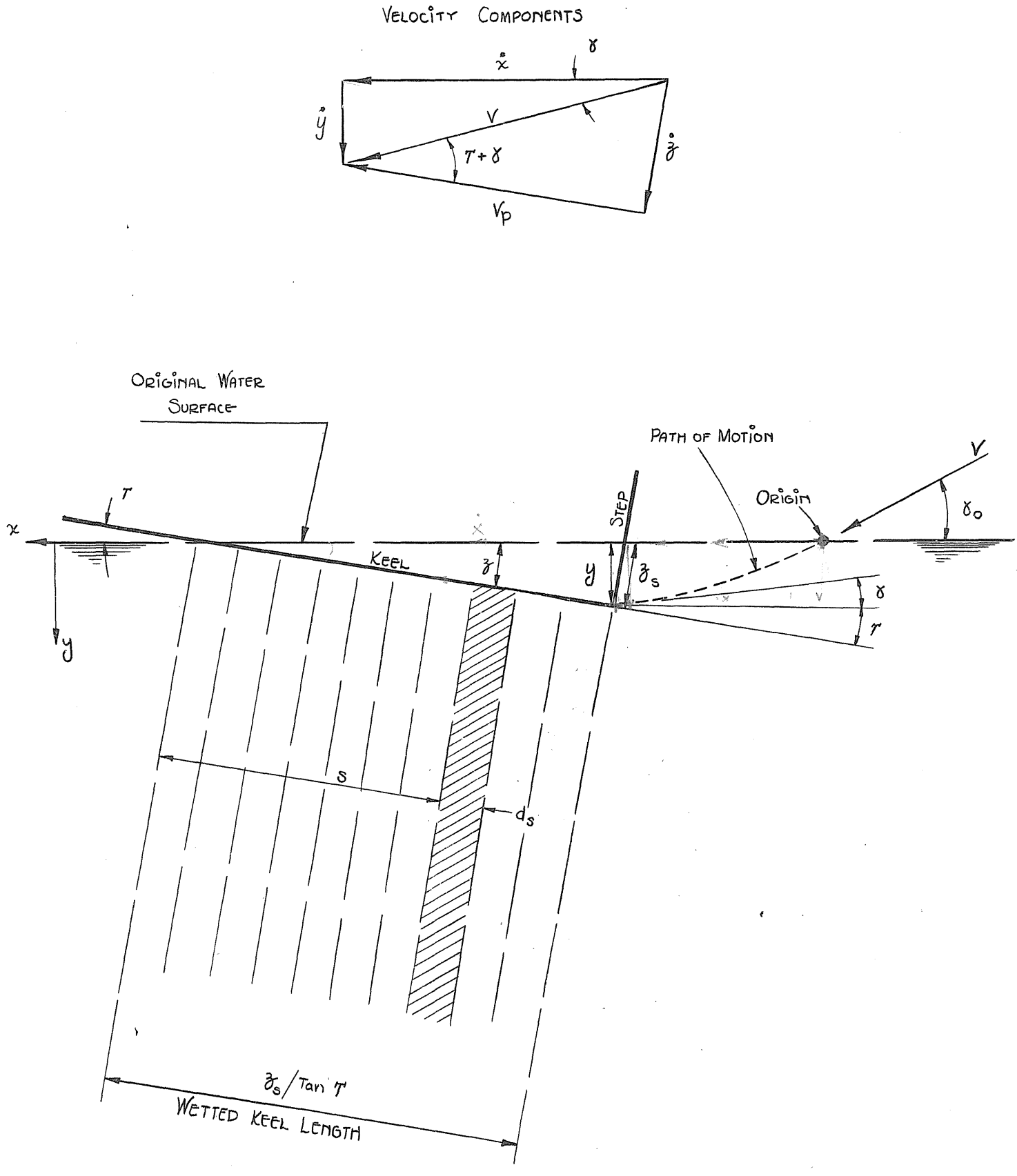

FIGURE 34

INSTANTANEOUS POSITION OF FLOAT IN OBLIQUE IMPACT

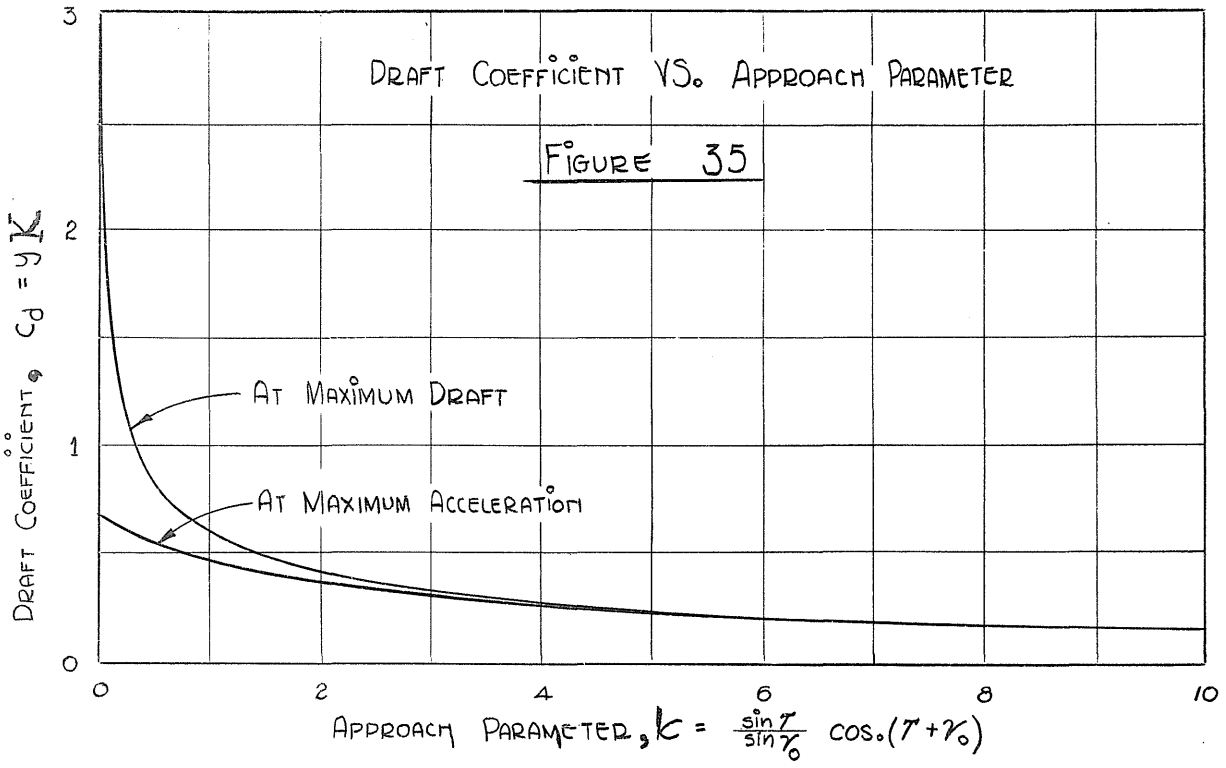
DRAFT COEFFICIENT VS. APPROACH PARAMETER
FIGURE 35
DRAFT COEFFICIENT, $C_d = \gamma K$
AT MAXIMUM DRAFT
AT MAXIMUM ACCELERATION
0
1
2
3
0
2
4
6
8
10
APPROACH PARAMETER, $k = \frac{\sin I}{\sin \gamma_0} \cos.(I + \gamma_0)$

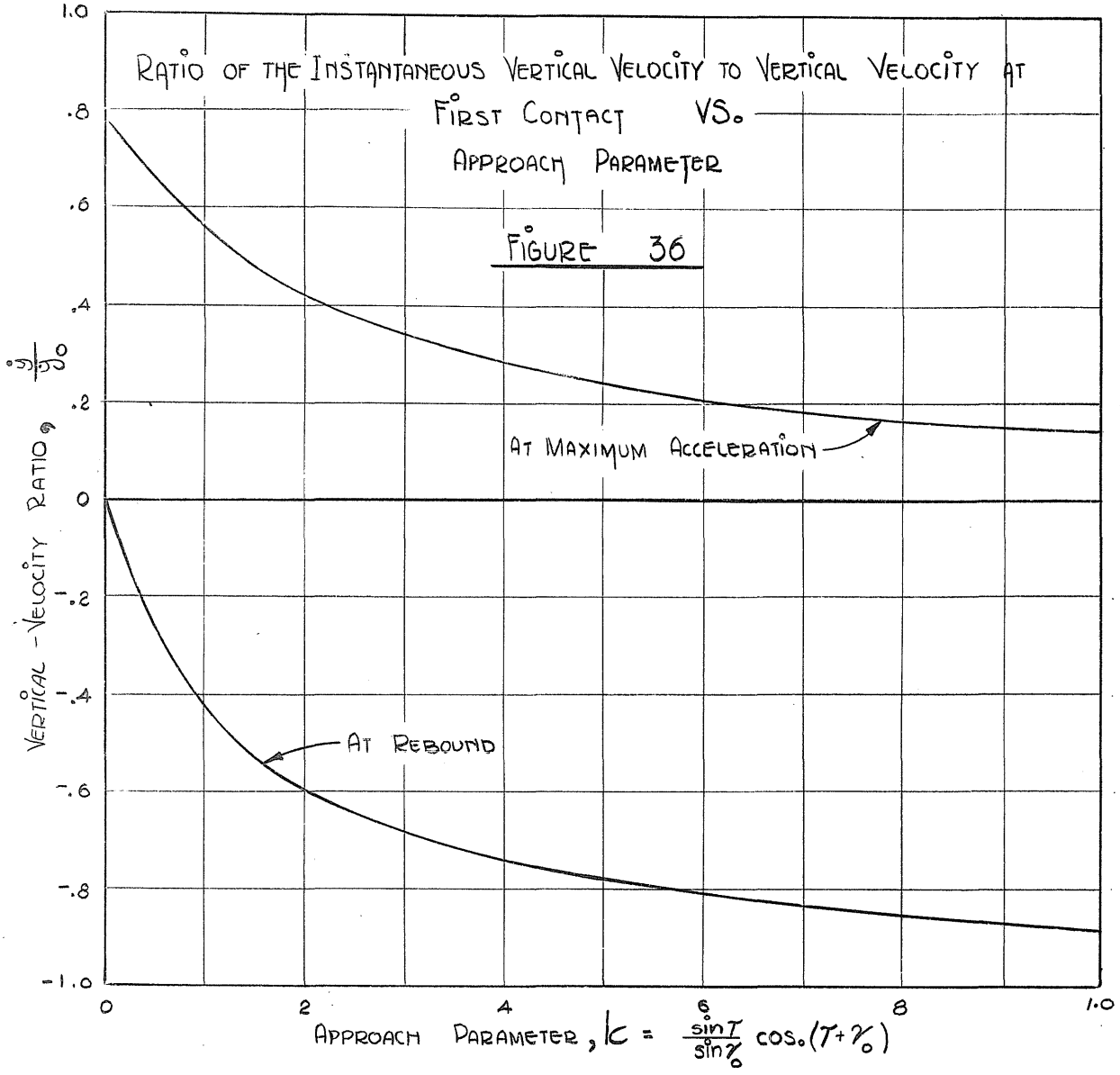
RATIO OF THE INSTANTANEOUS VERTICAL VELOCITY TO VERTICAL VELOCITY AT FIRST CONTACT VS. APPROACH PARAMETER
FIGURE 36
VERTICAL VELOCITY RATIO, $\frac{\dot{y}}{\dot{y}_0}$
AT MAXIMUM ACCELERATION
AT REBOUND
1.0
.8
.6
.4
.2
0
-.2
-.4
-.6
-.8
-1.0
0
2
4
6
8
10
APPROACH PARAMETER, $k = \frac{\sin I}{\sin \gamma_0} \cos.(I + \gamma_0)$

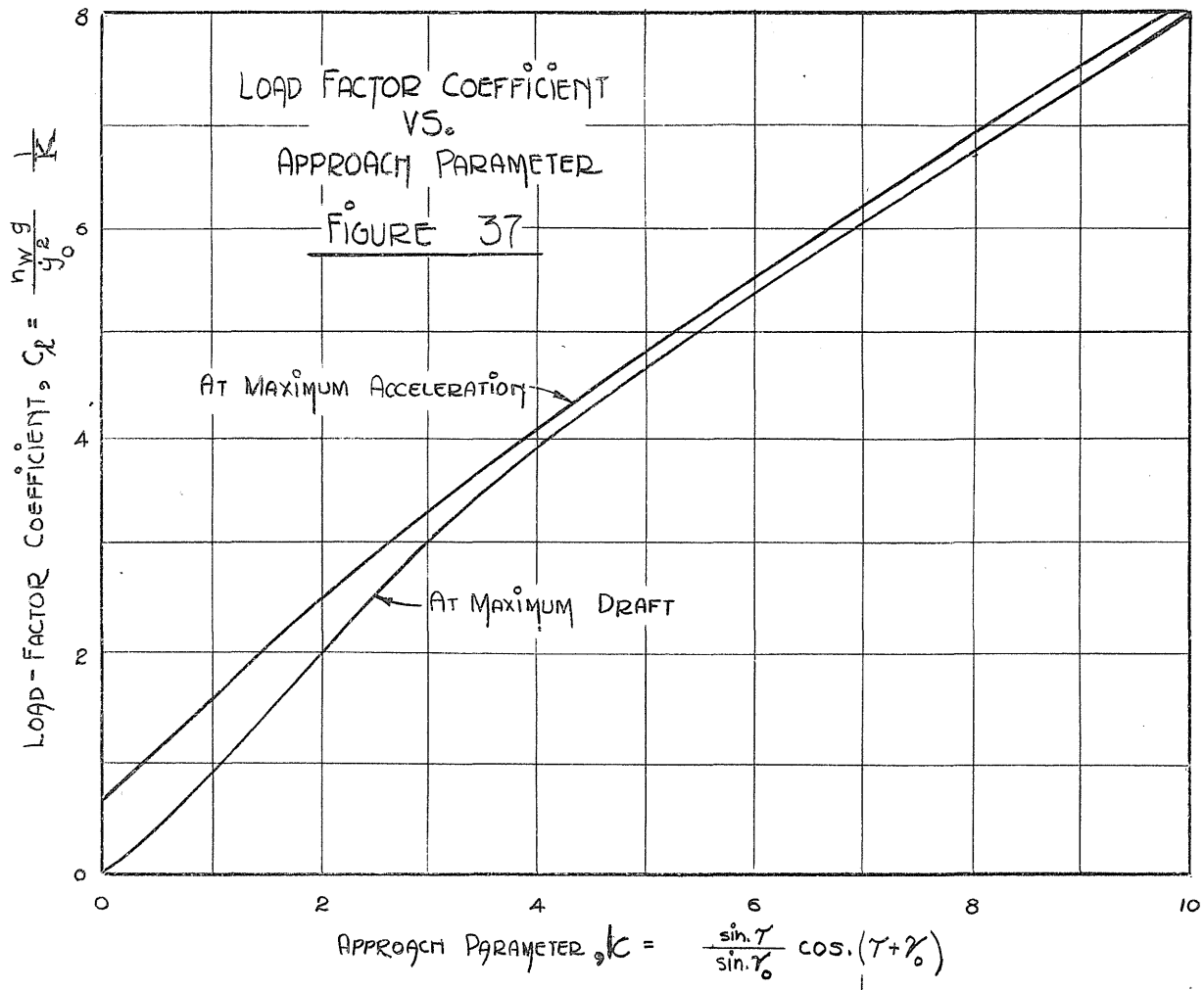
LOAD FACTOR COEFFICIENT
VS.
APPROACH PARAMETER
FIGURE 37
AT MAXIMUM ACCELERATION
AT MAXIMUM DRAFT
LOAD-FACTOR COEFFICIENT, $C_L = \frac{n_w g}{v_o^2} \frac{1}{K}$
APPROACH PARAMETER, $K = \frac{\sin.\tau}{\sin.\gamma_o} \cos.(\tau+\gamma_o)$
0
2
4
6
8
10

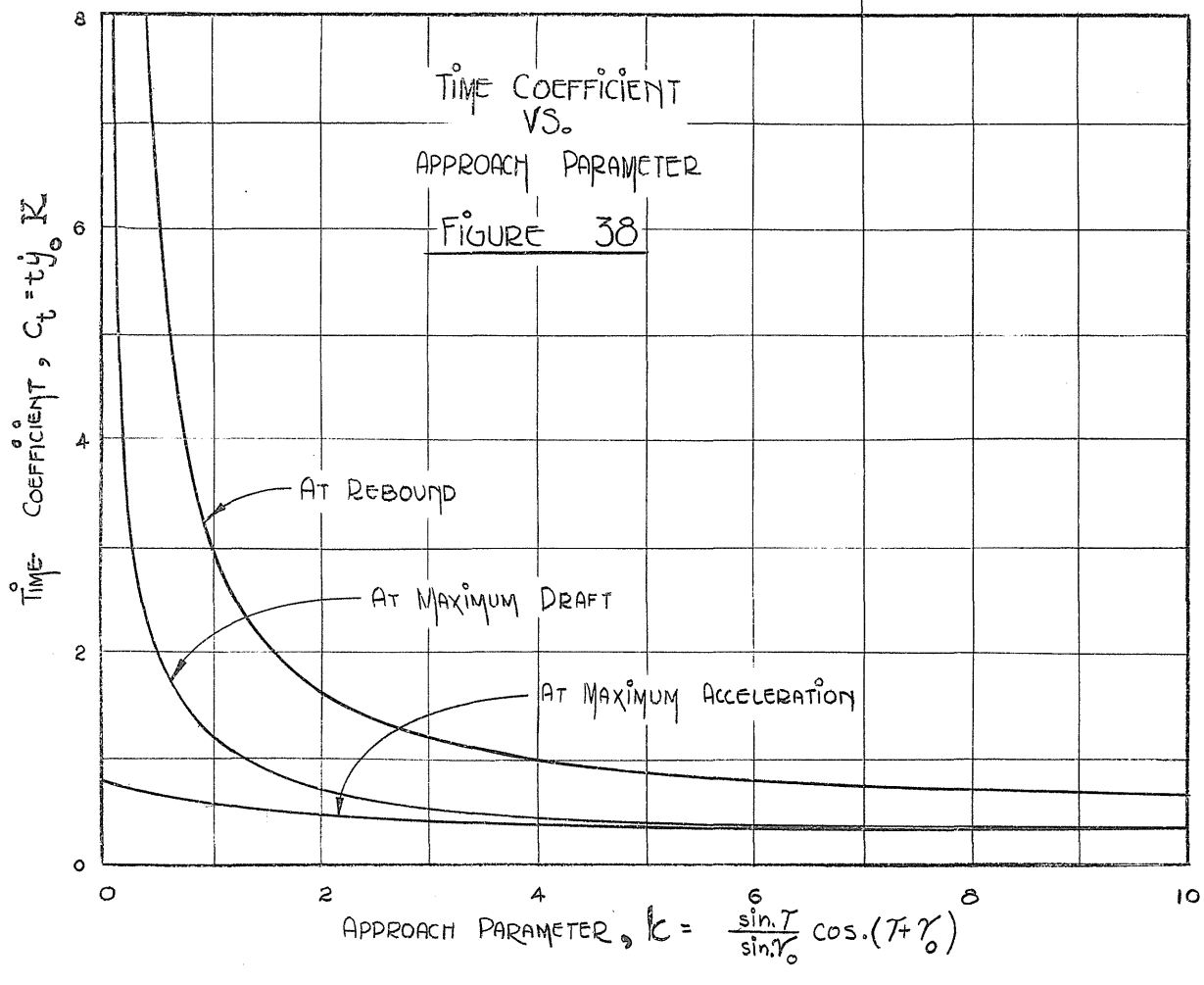
TIME COEFFICIENT
VS.
APPROACH PARAMETER
FIGURE 38
AT REBOUND
AT MAXIMUM DRAFT
AT MAXIMUM ACCELERATION
TIME COEFFICIENT, $C_t = t\frac{v_o}{K}$
APPROACH PARAMETER, $K = \frac{\sin.\tau}{\sin.\gamma_o} \cos.(\tau+\gamma_o)$
0
2
4
6
8
10

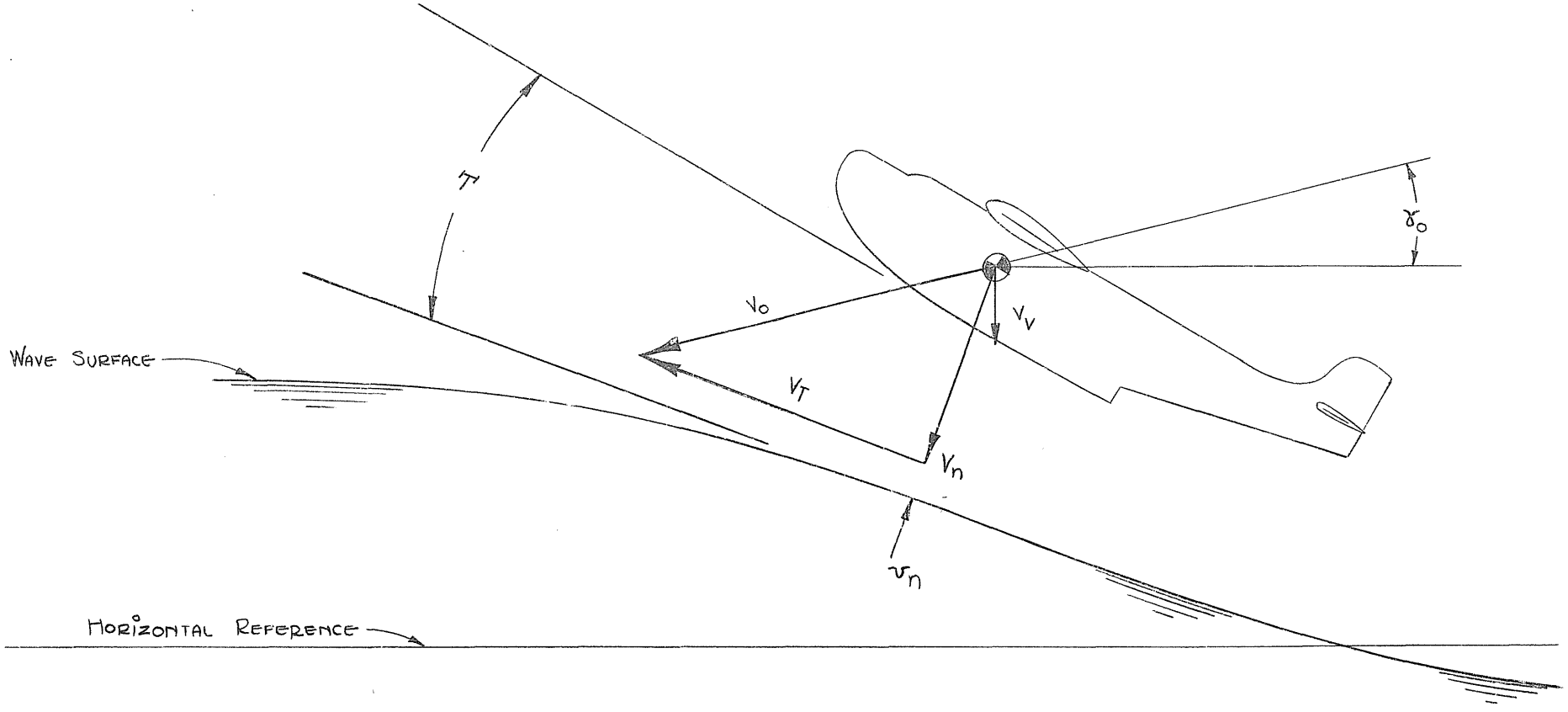

FIGURE 39

LANDING ON THE FLANK OF A WAVE

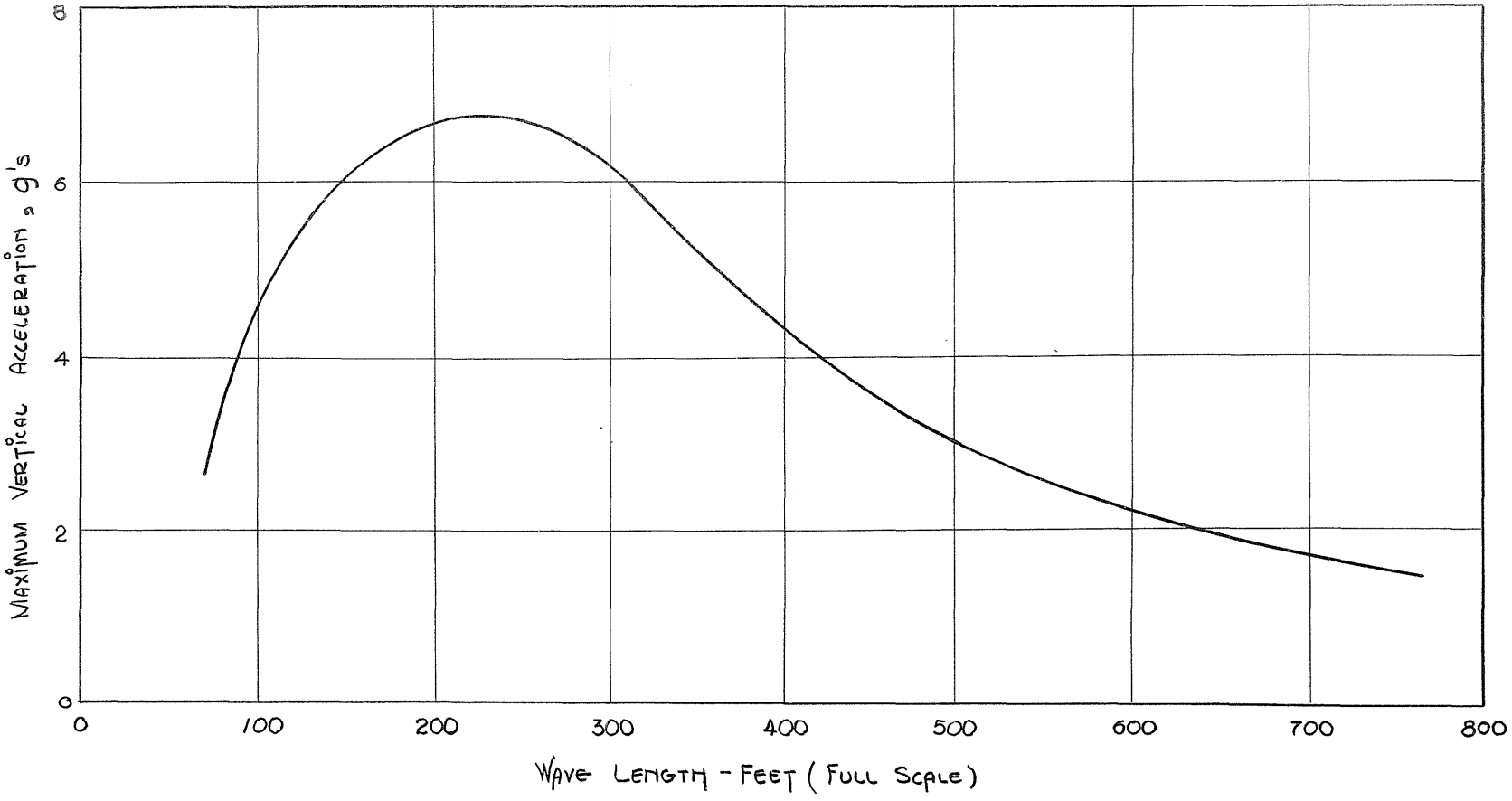

FIGURE 40

ACCELERATION PLOTTED VS.
WAVE LENGTH IN CASE OF A SEAPLANE LANDING IN ONCOMING 4.4 FOOT WAVES.

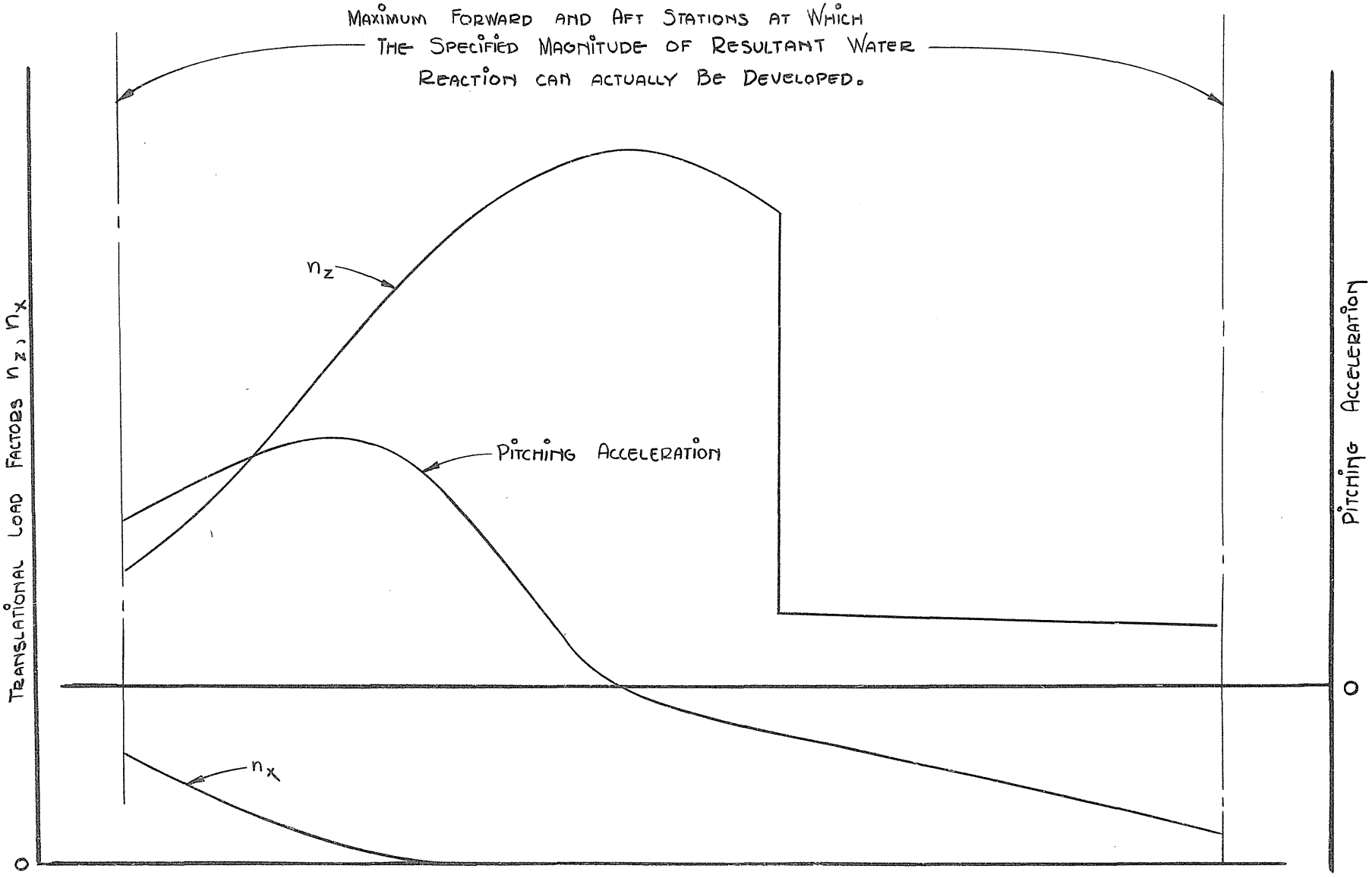

FIGURE 41

THE PLOT SHOWING THE MAGNITUDES OF THE VERTICAL HORIZONTAL AND PITCHING ANGULAR ACCELERATIONS VS. POSITION OF THE RESULTANT FORCE.

$\theta = 9°.5$
$\alpha = 0$
$W = 132$ lb.
$V_0 = 10.7$ Ft./sec.

Fig. 42

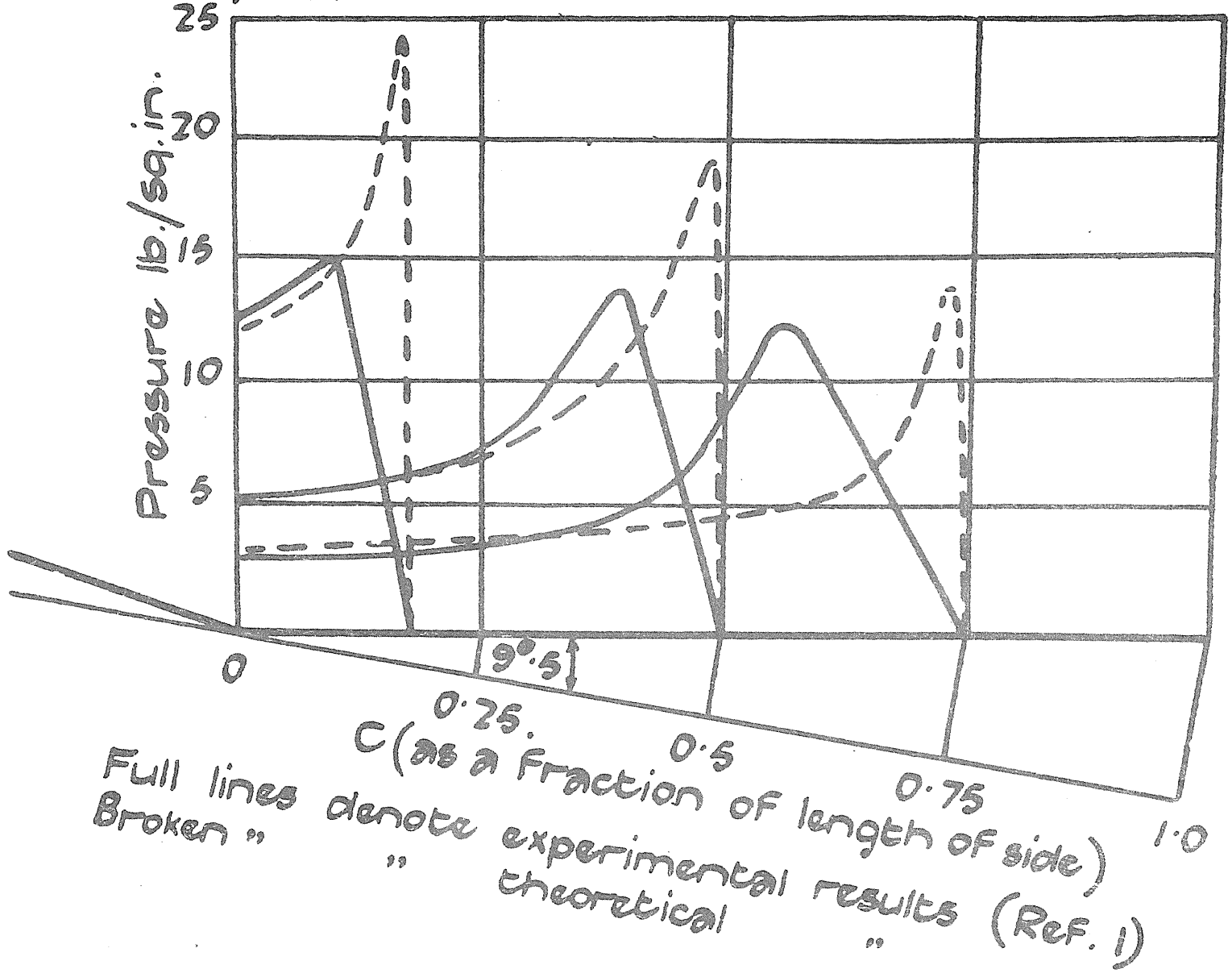

Full lines denote experimental results (Ref. 1)
Broken " " theoretical "

Singapore IIC hull
W = 27,700 lb.
b = 11·0 ft.

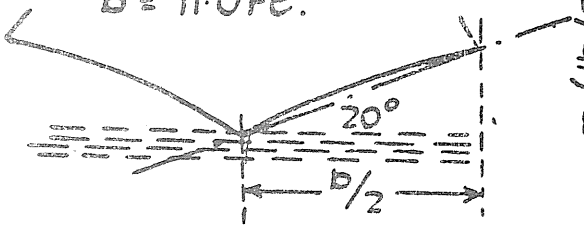

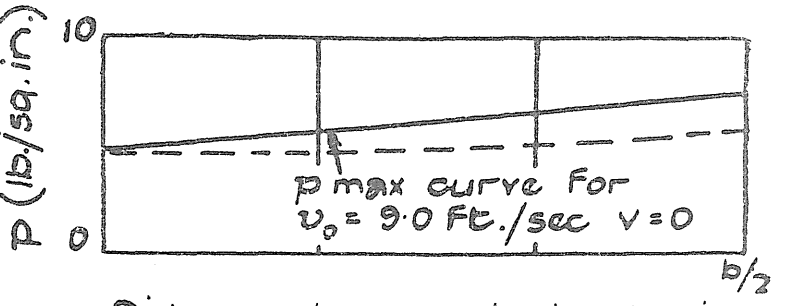

Distance between keel and chine

V shape specimen
W = 176 lb.
b = 22 ins

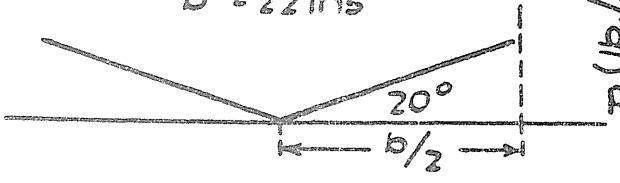

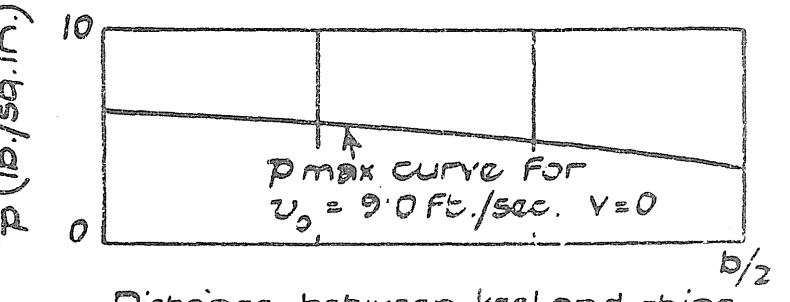

Distance between keel and chine

Southampton hull
W = 15,500 lb.
b = 7·5 ft.

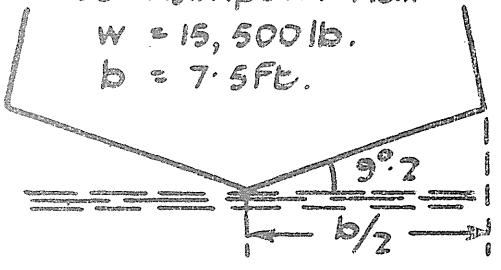

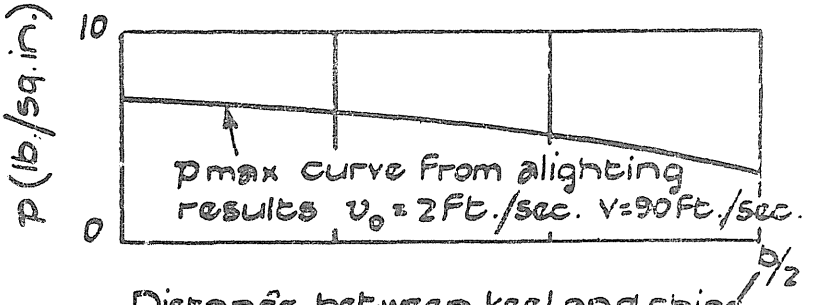

Distance between keel and chine

Perth hull
W = 29,000 lb.
b = 12·5 ft.

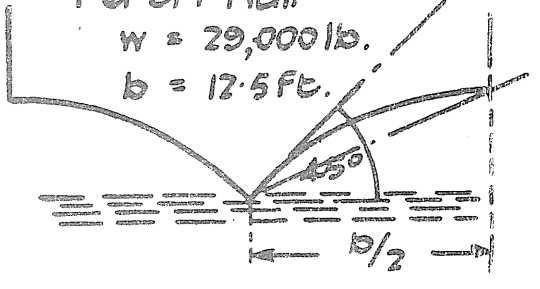

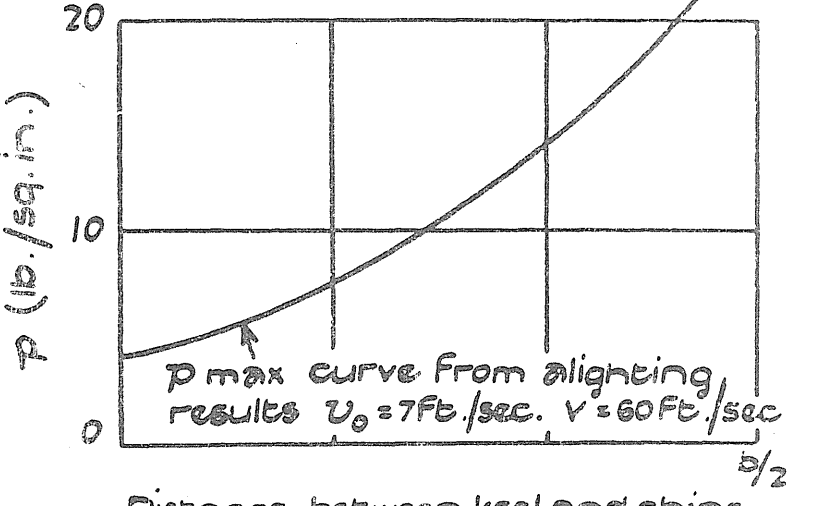

Distance between keel and chine

FIG. 43

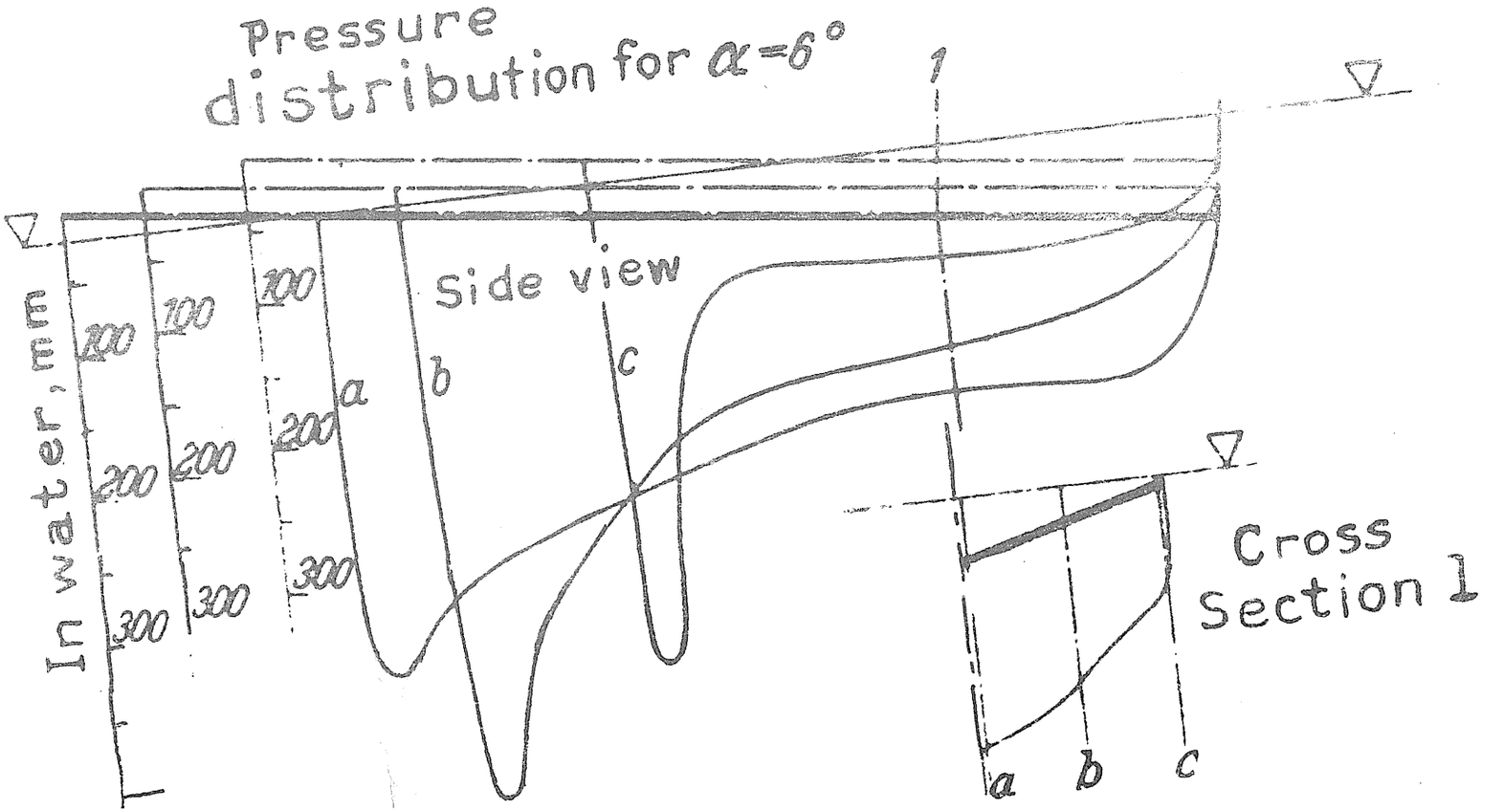
Pressure
distribution for α=6°
1
Side view
In water, mm
100
200
300
a
b
c
Cross
Section 1

Fig. 44

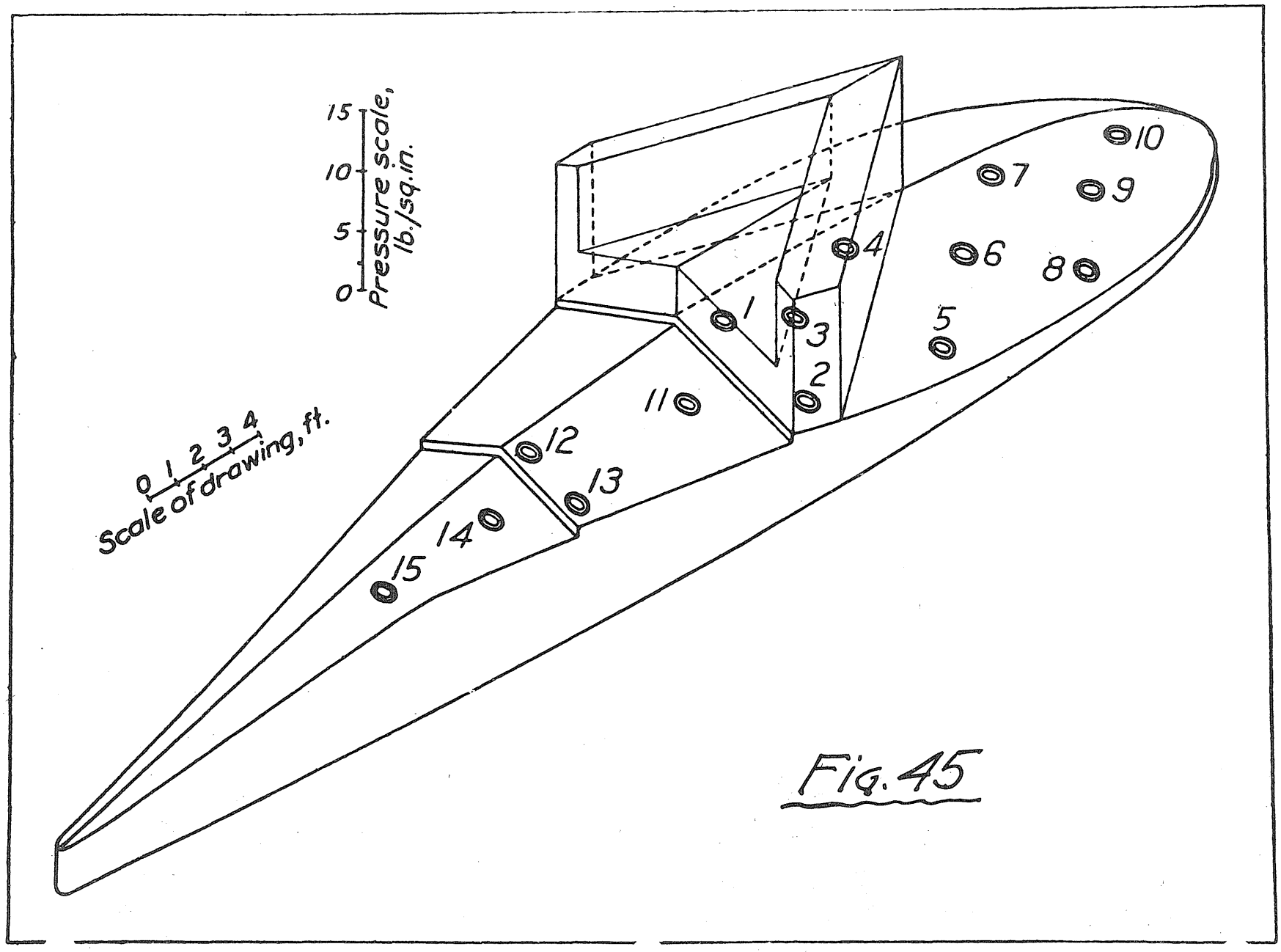
15
10
5
0
Pressure scale, lb./sq.in.
0 1 2 3 4
Scale of drawing, ft.
1
2
3
4
5
6
7
8
9
10
11
12
13
14
15

Fig. 45

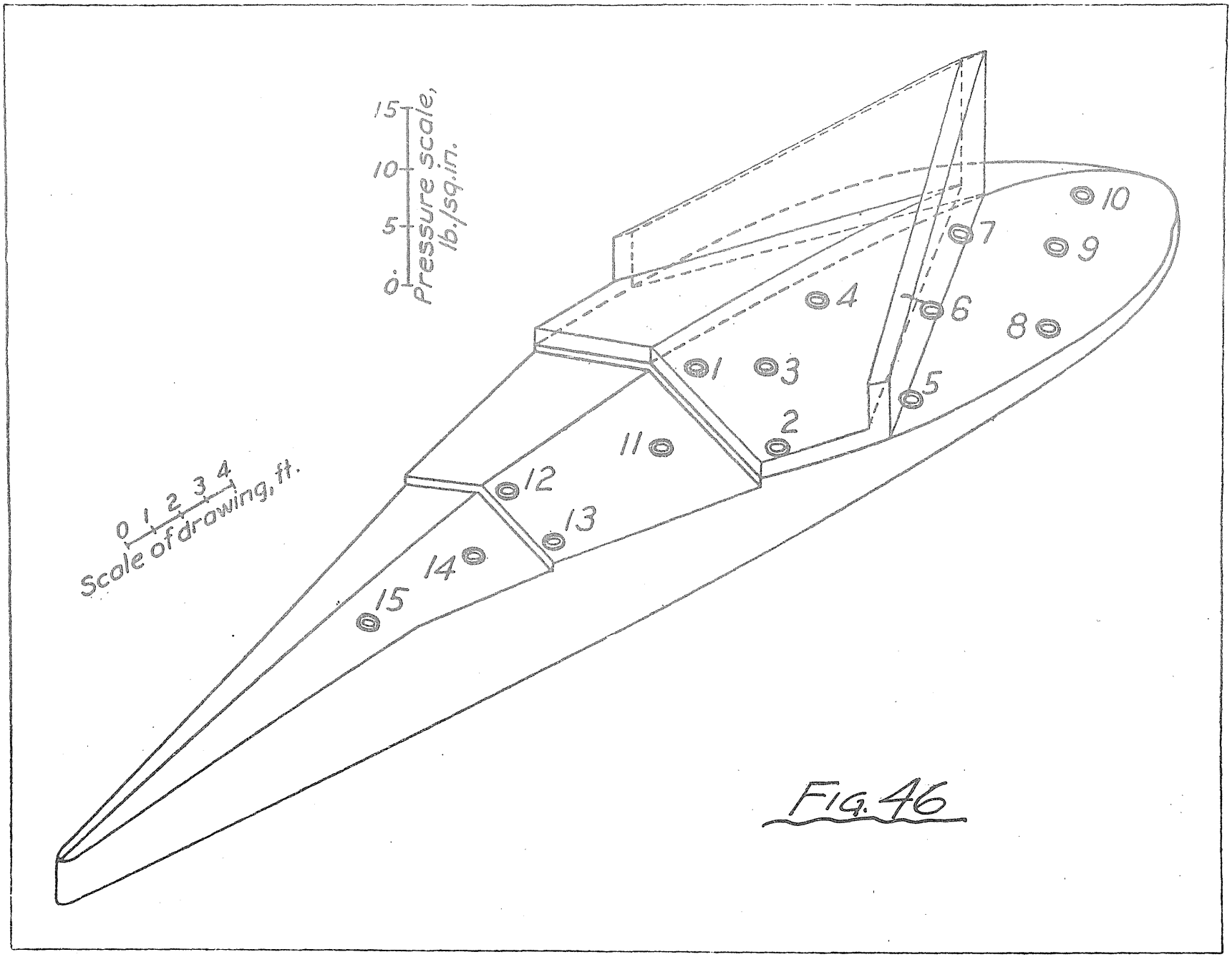
15
10
5
0
pressure scale, lb./sq.in.
0 1 2 3 4
Scale of drawing, ft.
1
2
3
4
5
6
7
8
9
10
11
12
13
14
15

Fig. 46

FIG. 47

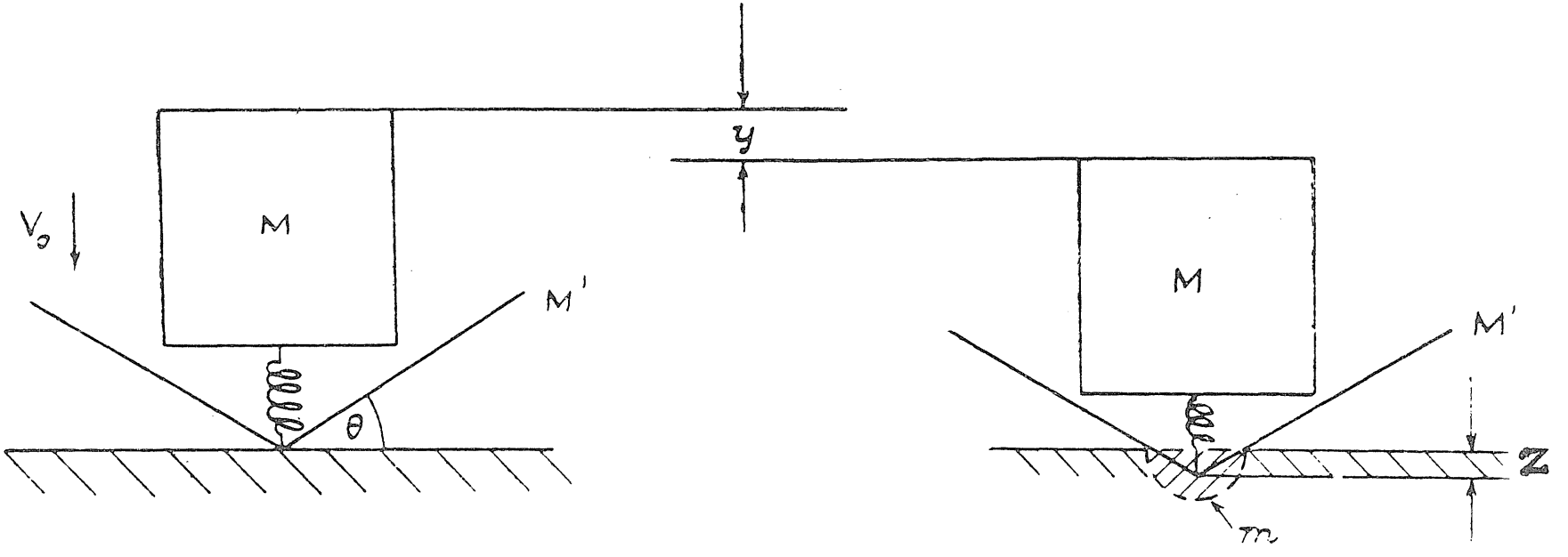

FIG. 48

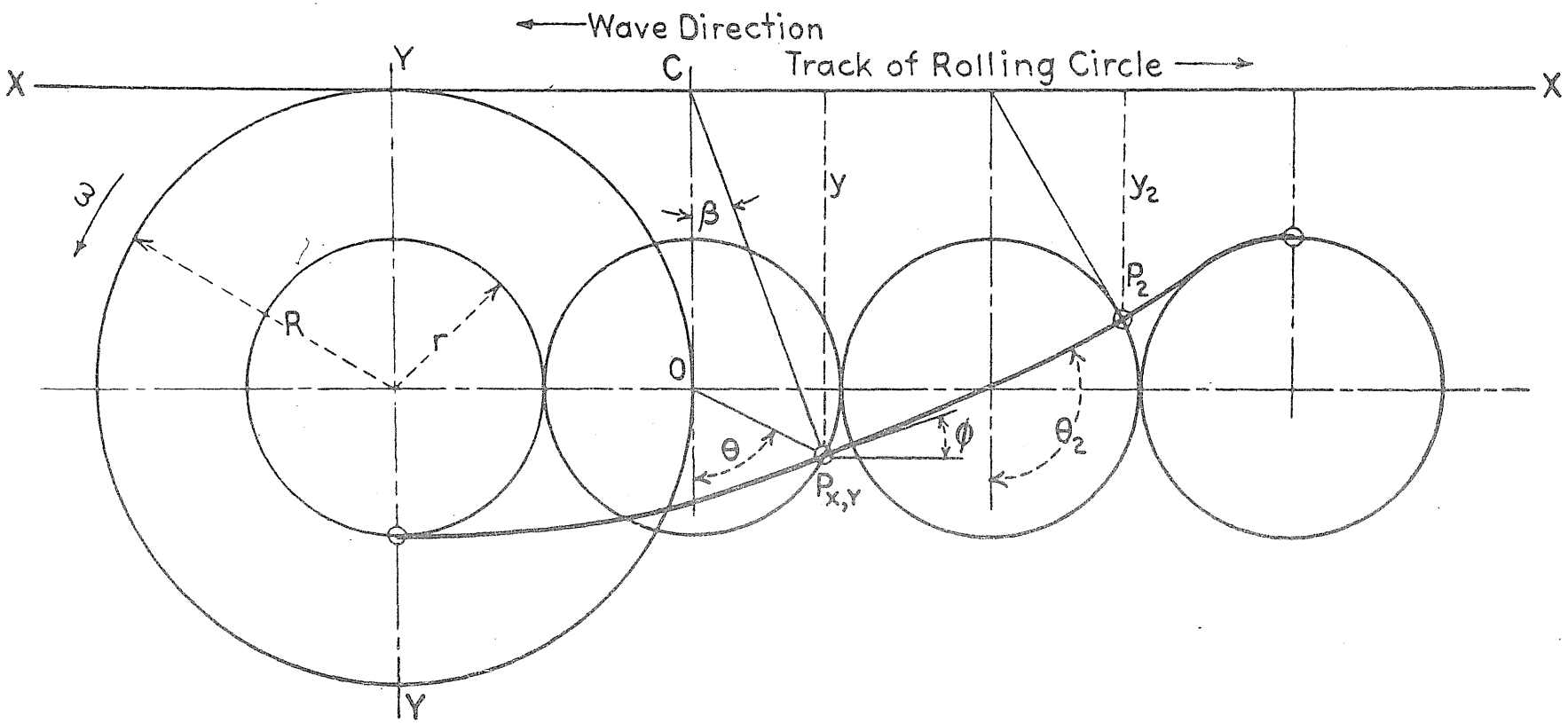
Wave Direction
Track of Rolling Circle
X
X
Y
Y
C
ω
R
r
β
y
y2
P2
0
θ
Px,y
φ
θ2